

Competition between superconductivity and magnetism in ferromagnet/superconductor heterostructures

Yu A Izyumov, Yu N Proshin, M G Khusainov

DOI: 10.1070/PU2002v045n02ABEH001025

Contents

| | |
|---|------------|
| 1. Introduction | 110 |
| 2. The problem of coexistence of superconductivity and ferromagnetism | 110 |
| 2.1 The possibility of coexistence in uniform systems; 2.2 Mechanisms of destruction of superconductivity by localized magnetic moments and the Larkin–Ovchinnikov–Fulde–Ferrel state; 2.3 Proximity effect and superconductivity in layered F/S structures | |
| 3. Theory of FM/S systems consisting of ferromagnetic metal and superconductor layers | 114 |
| 3.1 The boundary-value problem for an FM/S junction; 3.2 The superconducting transition temperature of an FM/S junction; 3.3 3D LOFF state in an FM/S junction; 3.4 π -Phase magnetism and superconductivity in FM/S superlattices; 3.5 Three-layer FM/S/FM system; 3.6 Further development of the theory | |
| 4. FM/S systems: a review of experimental data, a comparison of theory and experiment | 125 |
| 4.1 A brief review of experiments; 4.2 Dependence of the critical temperature on the thickness of FM and S layers and other parameters of the theory; 4.3 Comparison of the theory and experiment | |
| 5. Theory of FI/S systems consisting of layers of a ferromagnetic insulator and a superconductor | 133 |
| 5.1 Indirect exchange of localized spins in a dirty superconductor; 5.2 FI/S multilayers at zero temperature. Ground states; 5.3 FI/S multilayers at finite temperatures. Multicritical points in phase diagrams | |
| 6. FI/S systems with pure superconductors | 139 |
| 6.1 Boundary conditions for a ferromagnetic insulator/pure superconductor junction; 6.2 FI/S/FI system with singlet superconductivity | |
| 7. Transport properties of S/F systems | 142 |
| 7.1 Josephson effect in S/F/S structures; 7.2 Transport of spin-polarized electrons in F/S/F structures; 7.3 Role of the Andreev reflection | |
| 8. Conclusions | 146 |
| References | 147 |

Abstract. The mutual influence of superconductivity and magnetism in F/S systems, i.e. systems of alternating ferromagnetic (F) and superconducting (S) layers, is comprehensively reviewed. For systems with ferromagnetic metal (FM) layers, a theory of the proximity effect in the dirty limit is constructed based on the Usadel equations. For an FM/S bilayer and an

FM/S superlattice, a boundary-value problem involving finite FM/S boundary transparency and the diffusion and wave modes of quasi-particle motion is formulated; and the critical temperature T_c is calculated as a function of FM- and S-layer thicknesses. A detailed analysis of a large amount of experimental data amply confirms the proposed theory. It is shown that the superconducting state of an FM/S system is a superposition of two pairing mechanisms, Bardin–Cooper–Schrieffer’s in S layers and Larkin–Ovchinnikov–Fulde–Ferrell’s in FM ones. The competition between ferromagnetic and antiferromagnetic spontaneous moment orientations in FM layers is explored for the 0- and π -phase superconductivity in FM/S systems. For FI/S structures, where FI is a ferromagnetic insulator, a model for exchange interactions is proposed, which, along with direct exchange inside FI layers, includes indirect Ruderman–Kittel–Kasuya–Yosida exchange between localized spins via S-layer conduction electrons. Within this framework, possible mutual accommodation scenarios for superconducting and magnetic order parameters are found, the corresponding phase diagrams are plotted, and experimental results are explained. The results of the theory of the Josephson effect for S/F/S junctions are presented and the application of the theory of spin-dependent transport to F/S/F junctions is discussed. Application aspects of the subject are examined.

Yu A Izyumov Institute of Metal Physics, Ural Division of Russian Academy of Sciences,

ul. S Kovalevskoi 18, 620219 Ekaterinburg, Russian Federation

Tel. (7-3432) 74 41 93. Fax (7-3432) 74 52 44

E-mail: Yuri.Izyumov@imp.uran.ru

Yu N Proshin Kazan’ State University,

ul. Kremlevskaya 18, 420008 Kazan’, Russian Federation

Tel. (7-8432) 31 51 93. Fax (7-8432) 38 09 94

E-mail: Yurii.Proshin@ksu.ru

M G Khusainov Kazan’ State University,

ul. Kremlevskaya 18, 420008 Kazan’, Russian Federation

Kazan’ State Technical University, “Vostok” Branch,

ul. Engel’sa 127a, 422950 Chistopol’, Russian Federation

Tel. (7-84342) 3 47 58

E-mail: mgkh@vostok-inc.com

Received 18 June 2001

Uspekhi Fizicheskikh Nauk 172 (2) 113–154 (2002)

Translated by S N Gorin; edited by M V Magnitskaya

1. Introduction

Superconductivity and ferromagnetism are antagonistic phenomena and their coexistence in uniform materials requires that special, difficultly realizable conditions be fulfilled. This antagonism manifests itself first in the relation of these phenomena to a magnetic field. A superconductor tends to expel a magnetic field (Meissner effect), whereas a ferromagnet concentrates the force lines of the field inside its volume (effect of magnetic induction). The first explanation of the suppression of superconductivity via ferromagnetic ordering in transition metals was given by Ginzburg [1], who indicated that in these metals magnetic induction exceeds the critical field (see also Zharkov's works mentioned in Ref. [1]).

This antagonism is also understandable from the viewpoint of the microscopic theory: attraction between electrons creates Cooper pairs in a singlet state, whereas exchange interaction, which produces ferromagnetism, tends to arrange electron spins in parallel to one another. Therefore, when the Zeeman energy of the electrons of a pair in an exchange field I exceeds the coupling energy, whose measure is the width of the superconducting gap Δ , the superconducting state is destroyed. The corresponding critical field is $I_c \sim \Delta/\mu_B$, where μ_B is the Bohr magneton. In contrast to the critical field H_c acting on the orbital states of the electrons of a pair, the critical field I_c acts on electron spins (spin degrees of freedom); therefore, the destruction of superconductivity due to this field is called the paramagnetic effect.

For the above reasons, the coexistence of the superconducting and ferromagnetic order parameters (OPs) is unlikely in a uniform system, although it is easily achievable in artificially prepared layered F/S systems consisting of alternating ferromagnetic (F) and superconducting (S) layers. Owing to the proximity effect, a superconducting order parameter can be induced in the F layer; on the other hand, the neighboring pair of F layers can interact with one another via the S layer. Such systems exhibit rich physics, which can be controlled by varying the thicknesses of the F and S layers or by placing the F/S structure in an external magnetic field.

The modern technologies of production of layered structures, such as molecular-beam epitaxy, permit one to apply layers of atomic thicknesses and study the properties of such heterogeneous F/S systems as functions of the thickness of the ferromagnetic (d_f) or superconducting (d_s) layer. Numerous experiments on the F/S structures (junctions and superlattices) revealed nontrivial dependences of the temperature of the superconducting transition T_c on the thickness of the ferromagnetic layer. Of special interest is the study of multilayered F/S structures, in which various types of magnetic order can arise in F layers due to their indirect interaction via S layers. Recently, logical elements of a new type (spin switches) were suggested based on the interrelation between the superconducting and magnetic OPs in three-layer F/S/F and four-layer S/F/S/F structures. Thus, the general theoretical interest in the problem of the mutual influence of superconductivity and magnetism in F/S structures and the rich experimental material and possible engineering applications make the problem discussed quite topical.

2. The problem of coexistence of superconductivity and ferromagnetism

2.1 The possibility of coexistence in uniform systems

The antagonism between the ferromagnetic and superconducting long-range orders in a uniform system can partly be weakened due to a mutual accommodation of the magnetic and superconducting subsystems. This accommodation is reached due to the appearance of a nonuniform modulation of the ferromagnetic OP and/or a state with a nonuniform superconducting OP.

Let us imagine a situation where the magnetic order is uniform in the normal phase of a metal but is nonuniform in the superconducting phase. Consider the case where the superconducting temperature T_c is higher than the temperature of magnetic ordering T_m , i.e., the magnetic phase arises inside the superconducting state. In this situation, it may turn out that the minimum energy corresponds to a superconducting state with a modulated magnetic structure, since the loss in the exchange energy may be smaller than the gain in the energy of condensation due to the retention of the superconducting state. The first who indicated such a possibility were Anderson and Suhl [2] who analyzed the spatially nonuniform spin susceptibility $\chi(\mathbf{q})$ in a superconductor. They supposed that ferromagnetism in a metal is established due to the Ruderman–Kittel–Kasuya–Yosida (RKKY) indirect exchange interaction (see, e.g., Ref. [3]).

In the normal phase, the spin susceptibility of conduction electrons $\chi_n(\mathbf{q})$ has a maximum at $q = 0$, which favors the ferromagnetic state. Upon the transition into the superconducting state, $\chi_s(0)$ becomes zero at $T = 0$, since all the electrons are coupled in singlet pairs. It was found that at $\mathbf{q} \neq 0$, $\chi_s(\mathbf{q})$ passes through a maximum whose position is determined by the wave vector of the magnetic structure modulation

$$Q_0 \sim (a^2 \xi_{s0})^{-1/3}. \quad (2.1)$$

Here, ξ_{s0} is the coherence length of a pure superconductor and a is the magnetic correlation length, which is of the order of interatomic distances. Anderson and Suhl [2] called this state cryptoferromagnetic (CF). It is a result of a mutual adjustment of two competing order parameters, i.e., superconducting and ferromagnetic, and it is realized in the range of $a^{-1} \gg Q_0 \gg \xi_{s0}^{-1}$. The modulated magnetic structure is one of the forms of coexistence of superconductivity and magnetism.

It turned out that in an isotropic superconductor a transverse (helical) magnetic structure can occur [4]. Magnetic anisotropy transforms the spiral structure into a stripe-domain structure with an alternating orientation of magnetizations. The realization of one or other of the coexisting phases depends on the lengths ξ_{s0} and a and, for dirty superconductors, also on the mean free path l_s [5–7].

Such combined phases with modulated magnetic structures were experimentally found in a number of compounds such as ReRh_4B_4 and ReMo_6S_8 . In two representatives of this class, namely, in ErRh_4B_4 and HoMo_6S_8 , which are superconductors with $T_{c1} = 8.7$ K and 1.8 K, respectively, a combined phase with coexisting superconductivity and a modulated magnetic structure was revealed as the temperature decreased to $T_m = 1.0$ K and 0.74 K, respectively. As the temperature decreases to $T_{c2} = 0.8$ K and 0.7 K, respectively,

the superconductivity disappears and the normal (ferromagnetic) phase is restored. A detailed discussion of the properties of these phases and a comparison with theoretical predictions can be found in the comprehensive review by Buzdin et al. [7]. Note here that the theory of coexistence of phases with a magnetic structure of the type of a lattice of domains agrees well with experimental data for the reentrant magnetic superconductor HoMo_6S_8 . Thus, the possibility of coexistence of superconductivity and (crypto) ferromagnetism in a common volume was proved both theoretically and experimentally, although this requires the fulfillment of fairly rigid conditions.

In the last few years, numerous works have appeared, both experimental (initiated by Ref. [8]) and theoretical (see, e.g., Refs [9, 10]), devoted to the coexistence of ferromagnetism and superconductivity in natural layered compounds such as $\text{RuSr}_2\text{GdCu}_2\text{O}_8$. In these compounds, $T_m \simeq 132$ K, $T_c \simeq 46$ K, and the superconducting state arises against the background of already existing magnetic order, in contrast to the above considered case. It was experimentally shown [11, 12] that in this case a kind of antiferromagnetic ordering is established in the system, namely, so-called canted antiferromagnetism arises.

As to the mutual accommodation of superconductivity and magnetism, rare-earth boron-nickel carbides such as $\text{HoNi}_2\text{B}_2\text{C}$ and $\text{TmNi}_2\text{B}_2\text{C}$ should also be noted. Because of the alternation of ferromagnetic planes $\text{Ho}-\text{C}$ or $\text{Tm}-\text{C}$ with superconducting layers Ni_2B_2 , these compounds are natural microscopic analogs of the F/S superlattices, which are considered below. In boron-nickel carbides, interesting phenomena, such as the transformation of a spiral magnetic structure into a layered antiferromagnetic structure, are observed after transition into the superconducting state, as well as a clearly pronounced passage of the upper critical field H_{c2} through a minimum with decreasing temperature [13–15].

2.2 Mechanisms of destruction of superconductivity by localized magnetic moments and the Larkin–Ovchinnikov–Fulde–Ferrel state

Let us consider in more detail how the interaction of electrons with the ferromagnetic OP affects the superconducting state. In a metal in which two (superconducting and ferromagnetic) OPs are competing, two groups of electron states should be distinguished — collective (s) and localized (d) — that form atomic magnetic moments. The interaction between them is described by an sd exchange Hamiltonian

$$H_{sd}(\mathbf{r}) = \sum_j J_{sd}(\mathbf{r} - \mathbf{R}_j) (\mathbf{S}_j \cdot \boldsymbol{\sigma}). \quad (2.2)$$

Here, \mathbf{S}_j is the operator of the localized spin located in a lattice site, J_{sd} is the exchange integral, and $\boldsymbol{\sigma}$ is a vector composed of Pauli matrices. In the paramagnetic phase, the sd interaction leads to electron scattering by localized spins, and in the ferromagnetic phase, it produces magnetic biasing of electrons. The latter can most easily be taken into account by using the mean-field approximation, which reduces to the transition from Eqn (2.2) to the Hamiltonian

$$H_{sd} = I\sigma^z, \quad I = \sum_j J_{sd}(\mathbf{r} - \mathbf{R}_j) \langle S_j^z \rangle. \quad (2.3)$$

Here, I is the effective exchange field acting on the electron spin from localized spins, and $\langle S_j^z \rangle$ is the average (at a given

temperature) value of the spin projection onto the direction of the spontaneous moment.

The effects of exchange scattering and magnetic biasing of electrons are described by two fundamental equations, namely, the Abrikosov–Gor’kov equation [16]

$$\ln \frac{T_c}{T_{cs}} = \Psi\left(\frac{1}{2}\right) - \Psi\left(\frac{1}{2} + \frac{\gamma_s}{2\pi T_c}\right) \quad (2.4)$$

and Baltensperger–Sarma equation [17, 18]

$$\ln \frac{T_c}{T_{cs}} = \Psi\left(\frac{1}{2}\right) - \Psi\left(\frac{1}{2} + i \frac{I}{2\pi T_c}\right). \quad (2.5)$$

Here, T_c and T_{cs} are the temperatures of the superconducting transitions of the metal in the presence and in the absence of an sd interaction, respectively, and $\Psi(x)$ is the digamma function. Equation (2.4), which is valid for the paramagnetic phase of the metal, describes the effects of scattering by localized spins; the parameter γ_s specifies the damping of the electron wave function due to this scattering. Equation (2.5), which is valid for the ferromagnetic phase of the metal, takes into account the effect of exchange splitting of the electron energy level on the T_c temperature. These equations determine the implicit dependence of T_c on the parameters γ_s or I . In both cases, T_c falls off rapidly and vanishes at $\gamma_s \sim T_{cs}$ or $I \sim T_{cs}$.

The numerical solution to Eqn (2.5) is shown in Fig. 1 by a solid line in the interval between T_{cs} and T_t corresponding to second-order phase transitions. In the interval of fields from $I = \Delta_0/2$ to $I_t \simeq 0.62\Delta_0$, where $dT_c/dI = \infty$, curve (2.5) is two-valued, which indicates the instability of the system and the possibility of a first-order phase transition.

In this case, we should consider a more general equation as compared to (2.5). An analysis [18] shows that, beginning from the field I_t corresponding to the tricritical point $T_t = 0.56T_{cs}$, the phase transition is first-order. The corresponding (dashed) line terminates at the point $I_p = \Delta_0/\sqrt{2}$, which is called the Chandrasekhar–Clogston paramagnetic limit [19, 20]. Above this field, a ferromagnetic metal at $T = 0$ cannot remain a superconductor with a uniform OP. A further analysis [21, 22] showed that in a narrow range of fields (from I_t to $I_c \simeq 0.76\Delta_0$) exceeding the paramagnetic limit, a new, Larkin–Ovchinnikov–Fulde–Ferrel (LOFF)

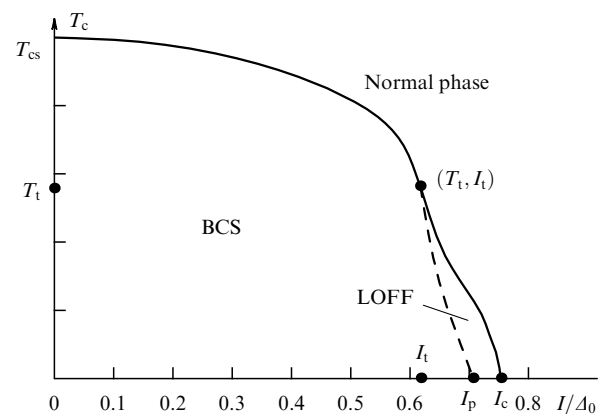


Figure 1. T_c as a function of the exchange field I in the ferromagnetic metal. Solid lines — curves of second-order phase transitions; dashed line — curve of first-order phase transitions.

state arises. In this state, pairing of electrons that belong to the exchange-split Fermi surface occurs; therefore, pairs are formed from the $|\mathbf{p}\uparrow\rangle, |-\mathbf{p}+\mathbf{k}\downarrow\rangle$ states, where $k \sim I/\hbar v_F$.

Thus, in the LOFF state, the superconducting OP is spatially nonuniform and, in the simplest case, depends on the coordinate as follows:

$$A(\mathbf{r}) = A_0 \exp(i\mathbf{k}\mathbf{r}). \quad (2.6)$$

Since the LOFF state is formed at $I \sim A_0$, the wave vector of the OP modulation

$$k \sim \frac{I}{\hbar v_F} \sim \frac{A_0}{\hbar v_F} \sim \frac{1}{\xi_{s0}} \quad (2.7)$$

is determined by the inverse correlation length of the superconductor. The spin density in the LOFF state is modulated with the same wave vector.

The electron scattering by nonmagnetic impurities prevents the formation of pairs with a nonzero total momentum [23–25] and makes the superconducting state of the Bardeen–Cooper–Schrieffer (BCS) type to be energetically favorable. For this reason, the LOFF state apparently can form only in sufficiently pure superconductors. In the phase diagram shown in Fig. 1, the LOFF state is separated from the superconducting state with the BCS type of pairing by the line of first-order phase transitions, whereas the transition from the LOFF phase into the normal phase occurs along the line of second-order phase transitions [23]. The LOFF state in a pure bulk superconductor, which can be realized in the above-mentioned narrow region of exchange fields I , has not been observed experimentally; however, the range of its existence widens for the case of nonuniform structures such as F/S junctions and F/S superlattices. We will see below that this state plays a key role in the formation of the superconducting state in these structures.

2.3 Proximity effect and superconductivity in layered F/S structures

The proximity effect [26] usually refers to a partial transfer of superconducting properties to a normal metal (N) that is in electrical contact with a superconductor (S). The origin of the phenomenon is in the large spatial extension of the wave function of Cooper pairs, which penetrates (to the extent of the S/N boundary transparency) from the S into the N layer at the distances comparable with coherence length. For this reason, sharing of electron interactions responsible for the superconducting transition in a nonuniform N/S system occurs. Thus, the layered N/S structure on the whole becomes superconducting, with a critical temperature T_c that is smaller than the T_{cs} temperature of the superconductor. The magnitude of T_c depends to a significant extent on the transparency of the N/S interface [27, 28], on the relation between the thicknesses of the metal layers and the coherence length, and on the relation between the parameters of the electron structure and electron interaction of the contacting metals [26–28]. The experimental and theoretical investigations concerning the proximity effect in various N/S systems have been comprehensively reflected in the review by Jin and Ketterson [29].

We will consider layered systems with metallic ferromagnetic layers (FM/S) and insulating ferromagnetic layers (FI/S) (Fig. 2). The majority of experiments were performed using FM/S systems [30–60].

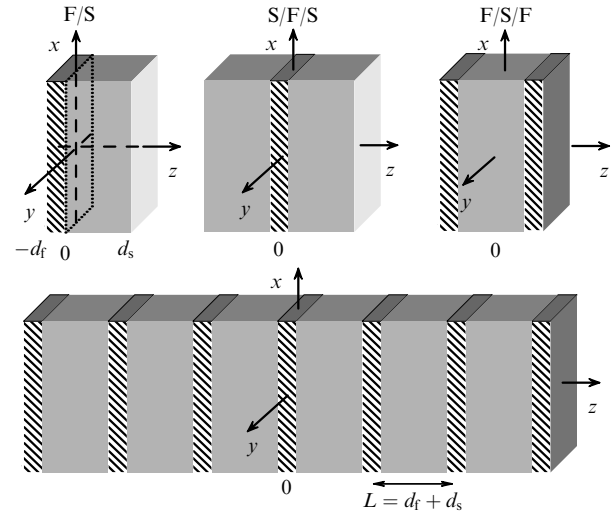


Figure 2. Multilayered F/S systems that have been studied in experiments: bilayers, trilayers, and superlattices.

It may seem that the greater the thickness of the ferromagnetic metallic layer d_f , the greater should be the effect of suppression of superconductivity in such a system. However, in experiments, a nonmonotonic and even oscillating dependence of T_c on d_f was frequently observed. Moreover, an analysis of experiments with FM/S systems indicates a qualitatively different behavior of the dependence of the critical temperature T_c on the thickness of ferromagnetic interlayers d_f for the same FM/S structures. In particular, in some experiments on Fe/V system [36] and Gd/Nb system [37] the rapid initial decrease in T_c with increasing d_f is replaced by the subsequent passage onto a plateau, but in other experiments with the same systems [31, 40] the plateau is preceded by an oscillating behavior of $T_c(d_f)$.

In the first theoretical works on FM/S systems [61, 62], the possible oscillations of T_c occurring with increasing d_f were ascribed to the appearance of π -phase superconductivity [63]. In the presence of several S layers separated by F layers, a change in the phase of the OP can occur on going from layer to layer. If the phase of the superconducting OP changes by π , a change occurs in the sign of the OP; this type of superconductivity in multilayers is called π -phase superconductivity [63]. As was shown in Ref. [61], as the d_f changes, a transition from 0-phase to π -phase superconductivity can occur; in this case, a nonmonotonic variation of T_c depending on d_f (oscillations) takes place. However, oscillations were also observed in three-layer structures such as Fe/Nb/Fe [42, 45] and Fe/Pb/Fe [56], in which the π -phase superconductivity is impossible in principle. To explain this fact, a further development of the theory was required.

For the FM/S superlattice, the authors of the pioneering works [61, 62] formulated a boundary-value problem for the pair amplitude (wave function of a Cooper pair) in a dirty superconductor and calculated T_c as a function of d_f . Both a monotonic fall-off of T_c and an oscillating dependence were obtained. However, the boundary conditions used in Refs [61, 62] are valid only in the limit of a high transparency of the ferromagnet–superconductor interface. In subsequent works [64–69], the boundary conditions for the boundary-value problem were derived from the microscopic theory; they are valid for any degree of transparency of the boundary. Based on the solution of the more general equations of the

boundary-value problem with allowance for the complex nature of the diffusion coefficient, other types of the $T_c(d_f)$ behavior were also predicted, namely, reentrant and periodically reentrant superconductivity [64–66, 68, 69]. The theory of FM/S systems that was developed in Refs [61, 62] and in subsequent works [64–66, 68, 69] leads to a conclusion that the superconductivity in FM/S systems is a combination of BCS pairing in S layers and LOFF pairing in F layers. As was shown, such a state leads to an oscillating $T_c(d_f)$ dependence in the case of the high transparency of the junction, whereas at a low or moderate transparency, the $T_c(d_f)$ dependence may take on a smoothed monotonic form.

Let us now consider the problem of parameters that characterize an FM/S heterostructure. The S layer is characterized by two parameters with a dimensionality of length: the coherence length ξ_s and the mean free path l_s . For an FM layer, along with two analogous parameters ξ_f and l_f , we should also introduce the spin-stiffness length $a_f = v_f/2I$ (which determines the characteristic length of modulation of the electron spin density in the ferromagnetic metal due to a relative shift of the Fermi surface for electrons with different spin orientations). To these parameters, two more geometric lengths should also be added, namely, the thicknesses of the superconducting (d_s) and ferromagnetic (d_f) layers.

Because of the strong depairing effect of the exchange field ($I \gg T_{cs}$), the superconductivity in such nonuniform systems as FM/S structures can be retained if the condition $d_s \gg d_f$ is fulfilled. The superconducting metal is considered in the dirty limit

$$l_s < \xi_s, \quad (2.8)$$

which corresponds to the conditions of the preparation of the FM/S junction or the FM/S superlattice and facilitates the theoretical description of the system, permitting one to use the Usadel equations [70] instead of the more exact equations by Gor'kov or Eilenberger [71].

In the FM layer, two cases should be considered depending on the relationship between the a_f and l_f lengths, namely,

$$a_f < l_f < \xi_f \quad (2I\tau_f > 1), \quad (2.9)$$

$$l_f < a_f < \xi_f \quad (2I\tau_f < 1). \quad (2.10)$$

Both cases correspond to the dirty limit, in the sense of the character of the superconducting state, but differ in the degree of atomic disorder leading to the wave ($2I\tau_f > 1$) or diffusion ($2I\tau_f < 1$) types of motion of quasi-particles in the ferromagnetic metal. Here, τ_f is the free-path time, so that $l_f = v_f\tau_f$, where v_f is the velocity of electrons at the Fermi surface in the FM layer.

The interface in the FM/S junction is characterized by a coefficient of transparency, which in the theory that is described below [64–66, 68, 69] can have an arbitrary value, unlike the first works [61, 62] where the limit of high transparency was considered. The introduced parameters l_s , ξ_s , l_f , ξ_f , a_f , and the coefficient of transparency admit several qualitatively different variants of the $T_c(d_f)$ dependence, which is the principal subject of experimental and theoretical investigations.

Other interesting aspects of the problem of coexistence and mutual adjustment of superconductivity and ferromagnetism arise in ferromagnetic insulator–superconductor (FI/S) structures (see, e.g., review [72]). In particular, no

clarity exists so far as to the nature of internal fields that lead to splitting of the BCS peak in the density of states of aluminum quasi-particles in tunnel junctions such as EuO/Al/Al₂O₃/Al [73], EuS/Al/Al₂O₃/Ag [74], and Au/EuS/Al [75], where EuO and EuS are ferromagnetic insulators. This splitting is observed as an excessive (as compared to the Zeeman one) effect in the presence of an external magnetic field and saturates as the field grows; in the case of junctions with EuS [74, 75], the splitting of the BCS peak takes place even in the zero field. As the magnetic field increases further, a first-order phase transition to the normal state occurs in the FI/S junctions [73–75], although the existing theory [76] predicts a second-order transition for this range of fields.

A specific feature of the FI/S systems (as compared to the above-discussed FM/S structures) is that the FI layers are nontransparent for the conduction electrons of the S layers. Therefore, the superconducting layers are subjected to the action of only the exchange field of localized spins located at the FI/S interfaces. From physical considerations, the presence of an internal field that provides the splitting of the BCS peak in the density of states of FI/S junctions and its saturation in a magnetic field can be described by a nonuniform magnetic ordering which is induced in the ferromagnetic film by the superconducting substrate. In addition, the anomalously weak suppression of superconductivity found in Eu/V superlattices [77] can also be interpreted in terms of the mutual adjustment of the superconductivity and magnetism. Therefore, the problem of the mechanisms of intralayer and interlayer exchange coupling in FI/S superlattices and multilayers is a key point for the understanding of effects related to the coexistence and mutual accommodation of two competing types of long-range order. Such a mechanism which ensures the long-range interaction between localized spins belonging to the same FI/S boundary, as well as between localized spins of neighboring FI/S boundaries in superlattices, may serve the RKKY indirect exchange via the conduction electrons of superconducting interlayers [78, 79]. The dependence of the RKKY exchange integral on the distance between localized spins $\mathbf{S}(\mathbf{r})$ and $\mathbf{S}(\mathbf{r}')$ is known [3] to be determined by the spatial dispersion of spin susceptibility $\chi(\mathbf{r}, \mathbf{r}')$ of conduction electrons. The singlet Cooper pairing of electrons in a superconductor leads to the appearance of a long-range antiferromagnetic contribution to the RKKY indirect exchange [2, 78–80]. As a result, the purely ferromagnetic ordering of localized spins of the FI/S boundary related to the direct exchange over the FI film becomes unstable with respect to the long-wavelength modulation of the magnetic order. This leads, on the one hand, to the retention of the short-range ferromagnetic order in the arrangement of localized spins and to a not too large loss in the exchange energy and, on the other hand, to an effective averaging of spin polarization of conduction electrons and the retention of superconducting pairing. In addition, the appearance of the antiferromagnetic coupling between neighboring FI layers through the superconducting interlayers will shift the phases of these cryptoferrromagnetic structures by π , thereby establishing a three-dimensional π -phase spin order over the entire FI/S superlattice.

The expected magnetically ordered phases that are incommensurate with the period of the crystal lattice of the FI and S layers originate from the competition between the short-range direct ferromagnetic exchange of the localized spins of the FI/S boundary and the long-range antiferromag-

netic RKKY exchange between them through Cooper pairs of the S layers. The phase diagrams of substances possessing incommensurate phases are characterized by the existence of a triple point, i.e., the Lifshitz point [81] at which all three phases meet: initial, commensurate, and incommensurate. The lattice parameter of the incommensurate phase increases on approaching the Lifshitz point and becomes infinite at it. The presence of an incommensurate phase in layered FI/S structures may indicate the existence of such an interesting feature as the Lifshitz point in their phase diagram.

The construction of a theory that would describe the expected mutual adjustment of superconductivity and ferromagnetism in FI/S systems implies, first of all, the development of the theory of indirect RKKY exchange in low-dimensional superconductors. In particular, it is necessary to know the dependence of the RKKY exchange integral on not only the distances between localized spins $\mathbf{S}(\mathbf{r})$ and $\mathbf{S}(\mathbf{r}')$, but also on their mutual arrangement with respect to the boundaries of the superconducting layers. The antiferromagnetic correlations between localized spins may be expected to become stronger on approaching the surface of the superconductor or on decreasing its dimensionality. This is due to the increase in the effective time of pair correlations of quasi-particles near the reflecting boundary.

The structure of this review is as follows. In Section 3, we describe the theory of FM/S junctions and superlattices for the case of an arbitrary transparency of the boundaries, and in Section 4, we analyze in detail the experiments based on the theory developed. In Sections 5 and 6, we consider layered systems consisting of superconducting and ferromagnetic insulating layers (FI/S systems). There, the key point is the study of the mutual accommodation of the superconducting and magnetic order parameters, in particular, the appearance of cryptoferromagnetism and antiferromagnetism in FI/S superlattices. Separately, a F/S/F trilayer is considered and the behavior of T_c depending on the mutual orientation of the magnetizations of the layers is analyzed. In view of its large practical importance, this problem is considered for two cases: when the ferromagnet is a metal (Section 3) and an insulator (Section 6). In Section 7, we consider other properties of F/S systems, e.g., Josephson and tunnel currents through F/S junctions.

Thus, the aim of this review is to report the state of the art of the theory of F/S systems with metallic and insulating ferromagnetic layers, in which the effects of the mutual adjustment of the superconducting and magnetic OPs are considered from a common viewpoint. Many predictions of the theory are confirmed in experiments, the number of which is growing rapidly.

3. Theory of FM/S systems consisting of ferromagnetic metal and superconductor layers

3.1 The boundary-value problem for an FM/S junction

Consider a planar junction between a ferromagnetic metal (FM) occupying the half-space $z < 0$ and a superconductor (S) lying at $z > 0$. To determine the temperature of the superconducting transition of such a nonuniform system, we should use the Gor'kov equation [82] for the OP $\Delta(\mathbf{r})$,

$$\Delta(\mathbf{r}) = V(\mathbf{r}) T \text{Re} \sum_{\omega}' \int H(\mathbf{r}, \mathbf{r}', \omega) \Delta(\mathbf{r}') d\mathbf{r}'. \quad (3.1)$$

Here, $V(\mathbf{r})$ is the potential of the pairing interaction; summing is performed over the Matsubara frequencies $\omega_n = (2n+1)\pi T$, where T is the temperature, and $n = 0, \pm 1, \pm 2, \dots$ (the prime at the sum sign denotes restriction to the Debye frequency ω_D). In addition, here and below, $\hbar = k_B = \mu_B = 1$.

The kernel of integral equation (3.1) is determined by the expression

$$H(\mathbf{r}, \mathbf{r}', \omega) = \langle G_{\uparrow}(\mathbf{r}, \mathbf{r}', \omega) G_{\downarrow}(\mathbf{r}, \mathbf{r}', -\omega) \rangle_{\text{imp}}, \quad (3.2)$$

where $G_{\alpha} = G_{\alpha}(\mathbf{r}, \mathbf{r}', \omega)$ is the Green's function of an electron with spin $\alpha = \uparrow, \downarrow$ in the normal phase of metal, and the angular brackets denote averaging over impurities, since below we consider the contacting metals in the dirty limit.

First, we consider the simplest variant of the theory, where the OP Δ depends only on z and Eqn (3.1) takes the form

$$\Delta(z) = V(z) T \text{Re} \sum_{\omega}' \int_{-\infty}^{\infty} H(z, z', \omega) \Delta(z') dz', \quad (3.3)$$

where $V(z > 0) = V_s$, $V(z < 0) = V_f$,

$$H(z, z', \omega) = \int d^2\mathbf{p} H(\mathbf{r}, \mathbf{r}', \omega),$$

and $\mathbf{p} = (\mathbf{r} - \mathbf{r}')_{\perp}$ is the two-dimensional radius vector in the plane of junction.

Averaging over nonmagnetic impurities in Eqn (3.2) is performed using the Abrikosov–Gor'kov diagrammatic technique [82, 83]. It turns out that for an FM/S junction, the two-particle correlator H is a solution to the integral equation of the form

$$H(z, z', \omega) = K(z, z', \omega) + \int \frac{K(z, z_1, \omega) H(z_1, z', \omega)}{2\pi N(z_1) \tau(z_1)} dz_1. \quad (3.4)$$

The kernel of this equation is expressed through the product of averaged (over impurities) Green's functions for the normal phase,

$$K(z, z', \omega) = \int \frac{d^2\mathbf{p}}{(2\pi)^2} G_{\uparrow}(\mathbf{p}, z, z', \omega) G_{\downarrow}(\mathbf{p}, z, z', -\omega). \quad (3.5)$$

Here, $G_{\alpha}(\mathbf{p}, z, z', \omega)$ is the Fourier transform of the Green's function $G_{\alpha}(\mathbf{r}, \mathbf{r}', \omega)$ with respect to the variable \mathbf{p} .

Integral equation (3.4) contains full information both on the parameters of the electron structure and kinetic characteristics of the metals being in contact and on the jumplike variation of their magnitudes upon the passage through the sharp FM/S interface. However, in the case where the contacting FM and S metals are sufficiently dirty, it is convenient to reduce the problem of solving integral equation (3.4) for the correlator $H(z, z', \omega)$ to the solution of an equivalent differential boundary-value problem. It is important to note that the concept of a dirty limit, which for a superconductor traditionally corresponds to the smallness of the mean free path $l_s = v_s \tau_s$ as compared to the coherence length ξ_s , is substantially modified for the case of a ferromagnetic metal. The thing is that, as we have already mentioned, there is a third characteristic scale in the FM region, apart from l_f and ξ_f , namely the length of spin stiffness $a_f = v_f/2I$, which is responsible for the wave mode of

motion of quasi-particles. Therefore, in an impurity ferromagnetic metal at $l_f, a_f < \xi_f$ we should separately consider the cases (2.9) $l_f < a_f$ ($2I\tau_f < 1$) and (2.10) $l_f > a_f$ ($2I\tau_f > 1$) (see Refs [64–66]).

The boundary-value problem obtained includes the equation

$$\left[|\omega| + iI(z) \operatorname{sgn} \omega - \frac{1}{2} D(z) \frac{\partial^2}{\partial z^2} \right] H(z, z', \omega) = \pi N(z) \delta(z - z'), \quad (3.6)$$

in which the magnitude of the exchange field $I(z)$ and the diffusion coefficient $D(z)$ have a step character: $I(z < 0) = I$, $I(z > 0) = 0$, $D(z < 0) = D_f(I)$, and $D(z > 0) = D_s$. Here, I is the exchange field acting on the electron spins in the ferromagnetic metal; D_s and $D_f(I)$ are the diffusion coefficients in the superconducting and ferromagnetic metals, respectively; and $D_s = v_s l_s / 3$. The coefficient of diffusion in the ferromagnet depends on the exchange field and is a complex quantity [64–66]:

$$\begin{aligned} D_f(I) &\simeq \frac{D_f}{1 + i2I\tau_f}, & \text{at } 2I\tau_f \ll 1, \\ D_f(I) &\simeq \frac{3D_f}{1 + i2I\tau_f}, & \text{at } 2I\tau_f \gg 1, \end{aligned} \quad (3.7)$$

where $D_f = v_f l_f / 3$ is the usual coefficient of diffusion in the FM layer. The complex diffusion coefficient $D_f(I)$ takes into account the competition between the diffusion and wave motions of the electron in the ferromagnetic metal. Finally, $N(z)$ in Eqn (3.6) is the density of states at the Fermi surface.

The differential equation (3.6) should be completed by boundary conditions [64–66] following from the same integral equation (3.4):

$$\begin{aligned} D_s \frac{\partial H(z, z', \omega)}{\partial z} \Big|_{z=+0} &= D_f(I) \frac{\partial H(z, z', \omega)}{\partial z} \Big|_{z=-0} \\ &= \frac{\sigma_s v_s H(+0, z', \omega) - \sigma_f v_f H(-0, z', \omega)}{4}, \end{aligned} \quad (3.8)$$

where $\sigma_{s,f}$ are the parameters of the transparency of the junction on the S and F side, respectively. These parameters are expressed through the quantum-mechanical transparency σ of the barrier as follows:

$$\sigma_{s,f} = \left\langle \frac{\sigma(x_{s,f})}{1 - \sigma(x_{s,f})} x_{s,f} \right\rangle, \quad (3.9)$$

where $x_{s,f}$ is the cosine of the angle between the direction of the electron velocity and the normal to the boundary. The parameters of the transparency $\sigma_{s,f}$ thus defined can vary within wide limits: $0 < \sigma_{s,f} < \infty$.

The reduction of the integral boundary-value problem to the differential problem in the dirty limit $l_{f,s} \ll \xi_{f,s}$ proves to be possible because the order parameter $\Delta(z)$ and the correlator $H(z, z', \omega)$ have a characteristic scale of spatial changes $\xi_{f,s}$ that is much greater than $l_{f,s}$, i.e., the range of the kernel $K(z, z', \omega)$. It is for this reason that the asymptotically smoothed (on scales of about $\xi_{f,s}$) expressions lose terms that rapidly oscillate at distances of atomic order or fall off exponentially at distances of the order of the mean free path.

After solving the boundary-value problem (3.6), (3.8), we find the kernel of the Gor'kov equation (3.3) that determines

the T_c temperature of the nonuniform FM/S system. Now, it is suitable to introduce a function

$$F(z, \omega) = \frac{1}{\pi N(z)} \int H(z, z', \omega) \Delta(z') dz', \quad (3.10)$$

through which we express the superconducting OP

$$\Delta(z) = 2\lambda(z) \pi T \operatorname{Re} \sum_{\omega > 0}' F(z, \omega). \quad (3.11)$$

Here, we introduced a dimensionless coupling constant $\lambda(z) = V(z)N(z)$. The $F(z, \omega)$ function is known in the literature as the anomalous Usadel function [70]. For this function, the Usadel equation [70] was formulated, which is a quasi-classical approximation of the Gor'kov equation (3.1) for a dirty superconductor. Given the Usadel function, we find the temperature of the transition from Eqn (3.11).

Using definition (3.10) and Eqns (3.6) and (3.8), we can easily obtain equations for the Usadel function at $\omega > 0$ in the superconducting and ferromagnetic regions of space [64–66]

$$\begin{cases} \left[\omega - \frac{1}{2} D_s \frac{\partial^2}{\partial z^2} \right] F_s(z, \omega) = \Delta_s(z), \\ \left[\omega + iI - \frac{1}{2} D_f(I) \frac{\partial^2}{\partial z^2} \right] F_f(z, \omega) = \Delta_f(z) \end{cases} \quad (3.12)$$

with boundary conditions

$$\begin{cases} \left. \frac{4D_s}{\sigma_s v_s} \frac{\partial F_f(z, \omega)}{\partial z} \right|_{z=+0} = F_s(+0, \omega) - F_f(-0, \omega), \\ \left. \frac{4D_f(I)}{\sigma_f v_f} \frac{\partial F_f(z, \omega)}{\partial z} \right|_{z=-0} = F_s(+0, \omega) - F_f(-0, \omega). \end{cases} \quad (3.13)$$

When deriving boundary conditions (3.13) from Eqn (3.8), we took into account the condition of detailed balancing [27]

$$\sigma_s v_s N_s = \sigma_f v_f N_f, \quad (3.14)$$

which indicates the equal number of transitions from the S layer into the FM layer and *vice versa*. The boundary conditions (3.13), which relate the flux of the Usadel function through the boundary with its jump at the FM/S interface, generalize the corresponding conditions that were obtained earlier [84] for dirty N/S contacts.

3.2 The superconducting transition temperature of an FM/S junction

Now, we apply the above-formulated boundary-value problem (3.12), (3.13) to the calculation of the T_c temperature of a planar FM/S junction between a ferromagnetic metal occupying the region $-d_f < z < 0$ and a superconductor occupying the region $0 < z < d_s$. In addition to conditions (3.13) for the FM/S boundary of the junction, we should also write boundary conditions at free boundaries of the FM and S layers in a form excluding any flux of the Usadel function through these boundaries:

$$\left. \frac{\partial F_s(z, \omega)}{\partial z} \right|_{z=d_s} = 0, \quad \left. \frac{\partial F_f(z, \omega)}{\partial z} \right|_{z=-d_f} = 0. \quad (3.15)$$

We search for a solution to Eqn (3.12) in the single-mode approximation, whose validity for $d_s \gtrsim \xi_s$ was shown in

Refs [66, 67, 85]:

$$F_s(z, \omega) = A_s \cos k_s(z - d_s), \quad F_f(z, \omega) = A_f \cos k_f(z + d_f). \quad (3.16)$$

This form of the solution takes into account conditions (3.15) at free boundaries; the relation between the parameters k_s and k_f is determined from boundary conditions. For simplicity, we assume that $\lambda_f = 0$, so that in the FM region the OP $\Delta_f = 0$. Then, from the set of equations (3.12), (3.13), and (3.11) with allowance for (3.14) we obtain the following closed set of equations in k_s , k_f and $t = T_c/T_{cs}$ (T_{cs} is the temperature of the superconducting transition for an isolated S layer):

$$\ln t = \Psi\left(\frac{1}{2}\right) - \operatorname{Re} \Psi\left(\frac{1}{2} + \frac{D_s k_s^2}{4\pi T_{cs} t}\right), \quad (3.17)$$

$$D_s k_s \tan k_s d_s = \frac{\sigma_s v_s}{4 - [\sigma_s v_f n_{sf}/D_f(I) k_f] \cot k_f d_f}, \quad (3.18)$$

$$k_f^2 = -\frac{2iI}{D_f(I)} = -\frac{2iI(1 + 2iI\tau_f)}{D_f}. \quad (3.19)$$

Equations (3.18) and (3.19) were obtained at $2I\tau_f \lesssim 1$. At $2I\tau_f \gtrsim 1$, $D_f(I)$ is replaced by $3D_f(I)$ in Eqns (3.18) and (3.19).

The first of these equations is an equation of the Abrikosov–Gor'kov type (2.4) for a superconductor with magnetic impurities. The quantity $D_s k_s^2$ plays the role of the parameter of depairing due to the breaking of Cooper pairs by the exchange field in the FM layer. The wave number k_s , which describes spatial changes in the pair amplitude across the S layer, is determined from the transcendental equation (3.18). Its right-hand side is a periodic function of the thickness of the ferromagnetic layer d_f , which leads to an oscillatory $T_c(d_f)$ dependence. For convenience, we introduced here the dimensionless quantity $n_{sf} = v_s N_s / v_f N_f$ [see Eqn (3.14)]. The third equation defines the complex wave number k_f . Its real part specifies spatial oscillations of the Usadel function in the FM layer; the imaginary part defines their damping on moving from the boundary of the junction deeper into the FM layer.

In the limit of the infinite transparency of the FM/S boundary ($\sigma_s, \sigma_f \rightarrow \infty$), Eqn (3.18) is simplified to

$$N_s D_s k_s \tan k_s d_s = -N_f D_f k_f \tan k_f d_f. \quad (3.20)$$

This equation for k_s was obtained in Ref. [85] in the single-mode approximation. The authors of Ref. [85] used the boundary condition ($z = 0$)

$$F_s(z, \omega) = F_f(z, \omega), \quad (3.21)$$

which, as is seen from the general equations (3.13), is valid only in the limit of infinite transparency of the junction. This theory [85] also used the relation $k_f^2 = -2iI/D_f$ instead of Eqn (3.19), i.e., the complex nature of the diffusion coefficient in the FM layer was ignored.

The various types of the $T_c(d_f)$ dependences calculated by formulas (3.17)–(3.19) at various values of the parameters of the theory are given in Fig. 3. It follows from this figure that at small values of σ_s and $2I\tau_f < 1$, the critical temperature first rapidly falls off with increasing d_f , then passes onto a plateau (Fig. 3a). With increasing transparency of the FM/S boundary, a deep minimum is developed in the $T_c(d_f)$ dependence, which may lead to reentrant superconductivity (Fig. 3b). At $2I\tau_f > 1$, the Usadel function and the $T_c(d_f)$ dependence oscillate with a period of the order of the spin-

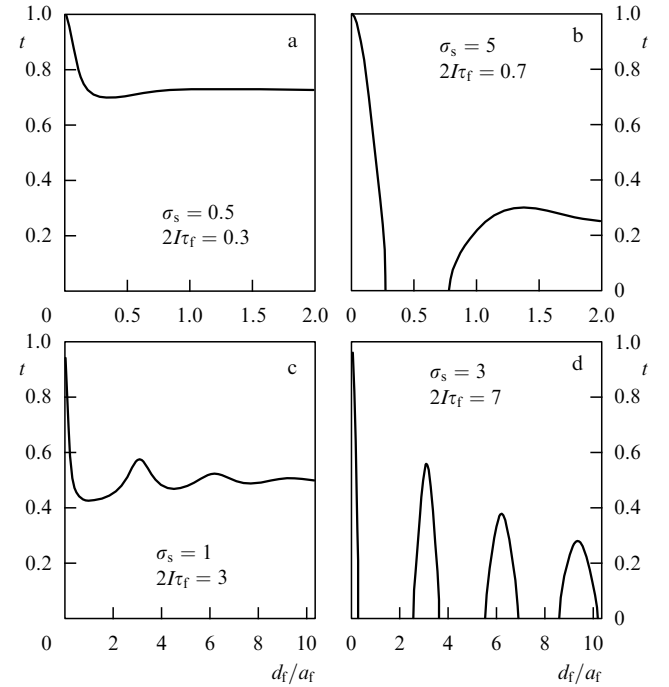


Figure 3. Reduced transition temperature $t = T_c/T_{cs}$ as a function of the reduced thickness of the FM layer d_f/a_f for two-layer FM/S systems in terms of the 1D theory ($q_f = 0$). Here, $l_s = 0.25\xi_{s0}$, $d_s = 0.625\xi_{s0}$, and $n_{sf} = N_s v_s / N_f v_f = 1$; the values of the parameters σ_s and $2I\tau_f$ are given in the figure taken from Ref. [65]: (a) passage onto a plateau; (b) reentrant superconductivity; (c) oscillations; and (d) periodically reentrant superconductivity.

stiffness length a_f . The oscillations damp at $d_f > l_f$; $F_f(z, \omega)$ becomes zero on moving away from the FM/S boundary and T_c becomes constant, as is shown in Fig. 3c. Note that at sufficiently large values of the parameters σ_s and $2I\tau_f$ the superconductivity of the FM/S junction has a periodically reentrant character (Fig. 3d).

Physically, the nature of the $T_c(d_f)$ oscillations in the case of an FM/S junction at $2I\tau_f > 1$ can easily be understood (Fig. 4). The condition of the absence of a flux of LOFF pairs through the external boundary (ferromagnet–vacuum) leads to the fixation of an antinode of the pair amplitude at this boundary, which, in turn, leads, with increasing thickness of the FM layer, to oscillations of the jump of the pair amplitude at the FM/S boundary. Each time when a node of the pair amplitude of LOFF turns out at the FM/S boundary (Fig. 4a), the jump and the related flux of Cooper pairs from the S into the FM layer become maximum. Since the Cooper pairs, when penetrating into the FM layer, are immediately destroyed by the strong exchange field, minima appear in the $T_c(d_f)$ dependence at these thicknesses of the FM layer or even complete suppression of superconductivity occurs. If an antinode of the LOFF amplitude occurs at the FM/S boundary (Fig. 4b), the flux of Cooper pairs through the S/FM boundary becomes minimum. With such thicknesses of the FM layer, maxima will arise in the $T_c(d_f)$ dependence. When the thickness of the ferromagnetic layer becomes greater than the depth of penetration of paired quasiparticles, the quantum coupling between its boundaries becomes destroyed, the flux of pairs through the S/FM boundary becomes constant, and the $T_c(d_f)$ function passes onto a plateau (Fig. 4c). As the concentration of nonmagnetic impurities in the FM layers increases, the wave mode motion

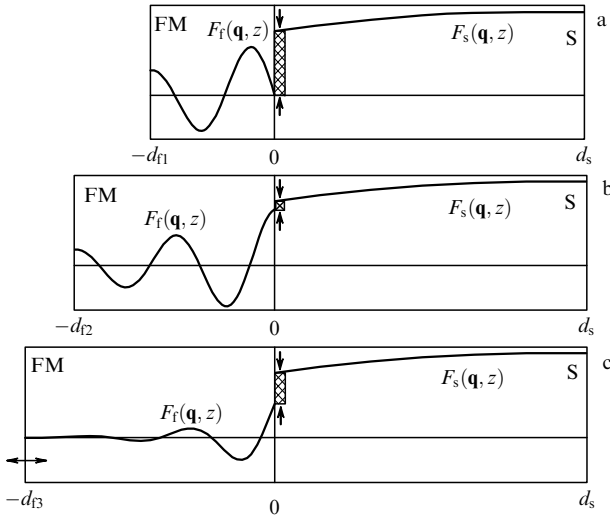


Figure 4. Mechanism of oscillations of T_c of the two-layer FM/S junction as a function of the thickness of the FM layer d_f (schematic). Solid lines show the variation of pair amplitude $F(\mathbf{q}, z)$. The absence of a flux of pairs through the external boundaries leads to the fixation of antinodes of $F(\mathbf{q}, z)$ at them. Vertical arrows show the magnitude of the jump of pair amplitude at the boundary (3.13): (a) maximum jump in $F(\mathbf{q}, z)$, maximum flux of BCS pairs from the S layer into the FM layer, and minimum T_c (strong pair-breaking effect); (b) minimum jump in $F(\mathbf{q}, z)$, minimum flux of BCS pairs from the S layer into the FM layer, maximum T_c (weak pair-breaking effect); and (c) constant flux of BCS pairs from the S layer into the FM layer (passage of T_c onto a plateau).

of quasi-particles, which is inherent in pure ferromagnet with $2I\tau_f > 1$ will be replaced by diffusion mode at $2I\tau_f < 1$. The momentum k of the pairs becomes a bad quantum number in this case, and the oscillations of the LOFF pair amplitude become strongly damped and cease to ensure the coherent coupling between the two boundaries of the FM layer (Fig. 4c). In this case, the $T_c(d_f)$ dependence takes on a smooth monotonic character.

On the other hand, in experiment, both for two-layered and multilayered FM/S structures, frequently only one local minimum in the $T_c(d_f)$ dependence is observed. The reason, in our opinion, is the fact that the above theory [61, 62, 64–66] is, strictly speaking, applicable only to such FM/S systems where the FM layers are quasi-one-dimensional ferromagnets. In this case, the spatial variations of the pair amplitude along the FM/S boundaries can be neglected. However, the realistic FM/S systems, such as Fe/V or Gd/Nb that were analyzed in the above-mentioned experiments, are three-dimensional (3D). Therefore, the pair correlations induced by the S layers in the FM layers (to the extent of the transparency of the interfaces) should also have a 3D character and should be described by a three-dimensional coherent momentum \mathbf{k} of pairs in correspondence with the LOFF theory [21, 22] for isotropic ferromagnetic superconductors. Therefore, below, we give a generalization of the above-described approach allowing for spatial variations of the pair amplitude in three dimensions.

3.3 3D LOFF state in an FM/S junction

Indeed, in order that a theory of the proximity effect be adequate to the layered nature of FM/S structures, it should take into account spatial changes in the pair amplitude not only across the FM and S layers, but also along the plane of the FM/S interfaces. This requires, in contrast to the

approaches used in Refs [61, 62] and [64–66], the solution of the three-dimensional (3D) rather than one-dimensional (1D) boundary-value problem for the pair amplitude $F(\mathbf{r})$. The specific feature of the LOFF state with a nonzero coherent 3D momentum of pairs \mathbf{k} is such that the pair amplitude in the FM layer is a periodic function of coordinates. This means [21, 22] that the LOFF pairs form a lattice with dimensions of the unit cell of about $a_f = v_f/2I$, and their wave function satisfies the Bloch theorem. Therefore, the pair momentum \mathbf{k} in reality is a quasi-momentum defined to an accuracy of the reciprocal lattice vector \mathbf{K} , whose absolute value is of the order of $2\pi/a_f$. Thus, the allowance for the competition between the 1D and 3D LOFF states is equivalent to the choice of the type (1D or 3D) of the lattice of LOFF pairs at a given thickness of the FM layer by the minimization of the free energy of the FM/S system. In turn, this procedure is equivalent to the allowance, along with normal processes retaining the transverse pair momentum \mathbf{q} ($q_s = q_f = 0$, 1D case), also for the Umklapp processes ($q_s = 0$, $q_f = K \neq 0$, 3D case), in which the transverse quasi-momentum of the LOFF pairs is not conserved upon crossing the FM/S interface. This resembles the situation with the reflection of an electron from the surface of a crystal, which can be multichannel in view of the nonconservation of the transverse component of the quasi-momentum [86].

It may be expected that the appearance, along with the known 1D states, of new, 3D LOFF states with an $F(\mathbf{r})$ function sinusoidally modulated in the plane of the FM/S interface will lead to an increase in the period of its oscillations across the FM layers. When the period is greater than the penetration depth of Cooper pairs into the FM layer, the coherent coupling between its boundaries will be broken, and the oscillations of the $T_c(d_f)$ function will be hardly discernible. Therefore, we believe that the competition between the old (1D) and new (3D) LOFF states should substantially modify the above-considered picture of the nonmonotonic behavior of the critical temperature in FM/S structures.

Taking into account the translational invariance of the FM/S system in the plane of the interface xy , Eqns (3.12) and (3.13) can be generalized, by writing them for the two-dimensional Fourier transform of the Usadel function $F(\mathbf{q}, z, \omega)$, where \mathbf{q} is the two-dimensional wave vector describing spatial changes along the FM/S boundary [68, 69]:

$$\begin{cases} \left[\omega + iI + \frac{1}{2} D_f(I) \left(q_f^2 - \frac{\partial^2}{\partial z^2} \right) \right] F_f(\mathbf{q}_f, z, \omega) = A_f(\mathbf{q}_f, z), \\ \left[\omega + \frac{1}{2} D_s \left(q_s^2 - \frac{\partial^2}{\partial z^2} \right) \right] F_s(\mathbf{q}_s, z, \omega) = A_s(\mathbf{q}_s, z). \end{cases} \quad (3.22)$$

The boundary conditions at the interface $z = 0$ corresponding to Eqn (3.22) then have the form

$$\begin{aligned} \frac{4D_s}{\sigma_s v_s} \frac{\partial F_s(\mathbf{q}_s, z, \omega)}{\partial z} \Big|_{z=+0} &= \frac{4D_f(I)}{\sigma_f v_f} \frac{\partial F_f(\mathbf{q}_f, z, \omega)}{\partial z} \Big|_{z=-0} \\ &= F_s(\mathbf{q}_s, z, \omega) - F_f(\mathbf{q}_f, z, \omega). \end{aligned} \quad (3.23)$$

These equations should be solved simultaneously with the self-consistency equations

$$\begin{cases} A_s(\mathbf{q}_s, z) = 2\lambda_s \pi T \text{Re} \sum_{\omega>0}' F_s(\mathbf{q}_s, z, \omega), \\ A_f(\mathbf{q}_f, z) = 2\lambda_f \pi T \text{Re} \sum_{\omega>0}' F_f(\mathbf{q}_f, z, \omega). \end{cases} \quad (3.24)$$

Thus, we obtain the following set of equations for determining the reduced temperature of the superconducting transition t [68, 69]:

$$\ln t = \Psi\left(\frac{1}{2}\right) - \operatorname{Re} \Psi\left(\frac{1}{2} + D_s \frac{k_s^2 + q_s^2}{4\pi T_{cs} t}\right), \quad (3.25)$$

$$D_s k_s \tan k_s d_s = \frac{\sigma_s v_s}{4 - [\sigma_s v_f n_{sf}/D_f(I)k_f] \cot k_f d_f}, \quad (3.26)$$

$$k_f^2 + q_f^2 = -\frac{2iI}{D_f(I)} = -\frac{2iI(1 + 2iI\tau_f)}{D_f}. \quad (3.27)$$

We see that it is only the equation for k_s that remained unaltered, whereas in the equations for t and k_f , the substitutions $k_s^2 \rightarrow k_s^2 + q_s^2$ and $k_f^2 \rightarrow k_f^2 + q_f^2$ have been made. The possible noncoincidence of q_s and q_f is due to the fact that the quasi-momentum \mathbf{q}_f is defined to an accuracy of the vector \mathbf{K} of the reciprocal lattice of LOFF states, as was noted above. From the condition of the minimum of free energy [maximum of $T_c(d_f)$], it follows that q_s is strictly equal to zero. This is not surprising, since in the case of the BCS pairing with a zero total momentum in the S layer the pair amplitude $F_s(\mathbf{r}, \omega)$ should have a constant sign. At the same time, in the FM layer pairing occurs according to the LOFF mechanism, with a nonzero three-dimensional coherent momentum of pairs $\mathbf{k} = (\mathbf{q}_f, k_f)$ and oscillating pair amplitude $F_f(\mathbf{r}, \omega)$. It follows from Eqns (3.25)–(3.27) that the magnitude of the 2D component of the momentum of the LOFF pairs q_f (remaining arbitrary) should be determined by optimization, i.e., from the condition of the maximum of T_c . It follows from boundary conditions (3.23) that the left-hand side of Eqn (3.26), which defines the pair-breaking parameter $D_s k_s^2$ in Eqn (3.25) for T_c , is proportional to the flux of Cooper pairs from the S layer into the FM layer. In this case, the resonance denominator of the right-hand side of Eqn (3.26), which is inversely proportional to the jump of the pair amplitude at the FM/S boundary, periodically changes the magnitude of this flux of pairs with increasing thickness of the FM layer at the expense of the function $\cot k_f d_f$. However, in contrast to the previously obtained (in Section 3.2 [64–66]) 1D solutions with $q_f = 0$, the appearance of 3D solutions with real $q_f \neq 0$ strongly decreases $\operatorname{Re} k_f$, according to Eqn (3.27). This leads to an increase in the period of oscillations of the pair amplitude $F(\mathbf{q}, z, \omega)$ along the z axis, which can become greater than the depth of penetration of pairs into the FM layer ($\operatorname{Im} k_f > \operatorname{Re} k_f$), and the coherent coupling between the two boundaries of the FM layer will break. As a result, the observability of oscillations in $T_c(d_f)$ (except for, maybe, the first peak) will strongly decrease.

Figure 5 displays the $T_c(d_f)$ dependences optimized with respect to the magnitude of q_f with allowance for the competition between the 1D and 3D LOFF states for different values of the main parameters of the theory. In principle, all qualitatively different variants of the behavior of $T_c(d_f)$ are possible, from the monotonic fall-off (up to zero) to the reentrant superconductivity and subsequent passing onto a plateau, both nonmonotonic (through a single spike) [42] and gradual [37]. The periodically reentrant superconductivity (Fig. 5c) predicted by the 1D theory [64–66] [see Eqns (3.17)–(3.19)] shown by dashed lines is almost completely overlapped by the monotonically falling 3D curve. The only spike in $T_c(d_f)$, as in the experiment [42] on the Fe/Nb/Fe trilayer, is due to the cascade of alternating phase transitions 3D–1D–3D. The top panels of Fig. 5a–d

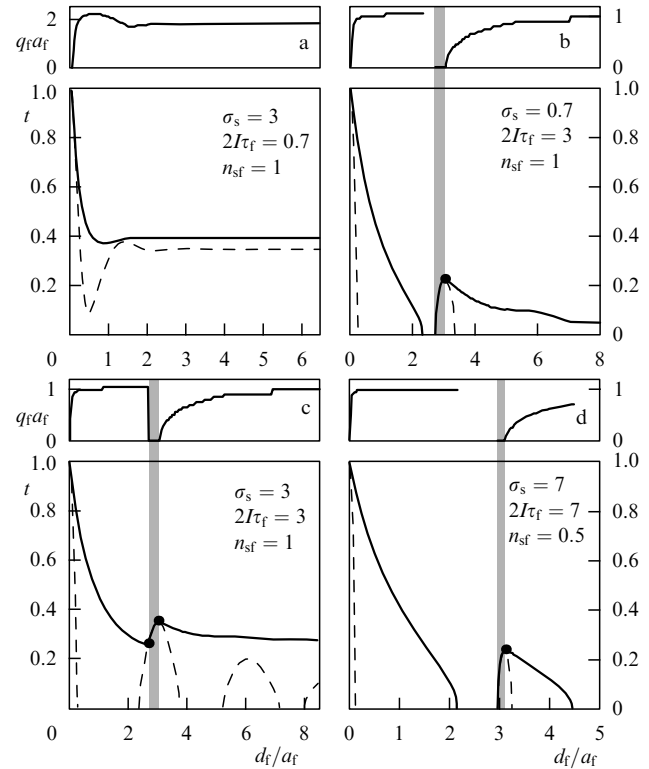


Figure 5. Reduced transition temperature $t = T_c/T_{cs}$ and the magnitude $q_f a_f$ as functions of the reduced thickness of the FM layer d_f/a_f for two-layered FM/S systems at $l_s = 0.25\xi_{s0}$ and $d_s = 0.625\xi_{s0}$ for various values of the parameters σ_s , $2I\tau_f$, and $n_{sf} = N_s v_s/N_f v_f$. Thick solid lines correspond to optimized solutions with allowance for the competition between the 1D and 3D LOFF states; thin dashed lines correspond to pure 1D solutions with $q_f = 0$ considered in Section 3.2. Here, these lines separate regions of the 1D and 3D phases. Regions of the dominant 1D LOFF states ($q_f = 0$) are hatched. The regions where 3D LOFF phases are predominant ($q_f \neq 0$) are unshaded.

show the dependence of the magnitude of the two-dimensional wave vector q_f on d_f . The phase diagram $T_c(d_f)$ displayed possesses an interesting feature in the form of triple Lifshitz points (intersections of solid and dashed lines), where three phases meet, i.e., two superconducting (a commensurate 1D phase with $\mathbf{q}_f = 0$ and an incommensurate 3D phase with $\mathbf{q}_f \neq 0$) and a normal phase. Note that the regions of existence of reentrant superconductivity predicted earlier [64–66] for the 1D case are restricted in the 3D case to a very narrow range of parameter values. This explains why this phenomenon up to now has not been revealed experimentally in realistic FM/S systems. (Recently, a preliminary communication appeared on the observation of this effect in Fe/V/Fe trilayers [60].)

3.4 π -Phase magnetism and superconductivity in FM/S superlattices

It should be noted that the theories of the proximity effect [61, 62, 64–66] for FM/S superlattices absolutely do not take into account the back influence of superconductivity on the ferromagnetism of the FM layers. At the same time, it was shown by one of us [78, 79] (see also Section 5) that in the case of analogous FI/S structures the long-range RKKY exchange between neighboring FI layers through S interlayers leads to a layered antiferromagnetic superconducting state (AFS). In the AFS state, the phases of the magnetic OP in

neighboring FI layers are shifted by π , which substantially weakens the depairing action of the paramagnetic effect of the exchange field for S layers and increases T_c . It should be expected that such a mutual adjustment of the superconducting and magnetic order parameters leading to a quantum coupling between the interfaces and to the realization of π -phase magnetism should also take place in FM/S superlattices.

Consider an FM/S superlattice formed by alternating (along the z axis) FM layers of thickness d_f and S layers of thickness d_s . To study the mutual adjustment of the competing BCS and LOFF types of pairing, on the one hand, and magnetism, on the other hand, it is convenient to choose the unit cell of the FM/S superlattice in the form of an S/FM/S/FM sequence of layers. This choice permits one to take into account the possible change of the phases of the superconducting and magnetic OPs upon the passage through the FM or S layers, respectively. For simplicity, we will consider the 1D case, where the OP and the pair amplitude depend only on z . A generalization on the 3D case is performed in the same manner as was made in Section 3.3. The boundary-value problem for the Usadel function $F(z, \omega, I)$ will be described by differential equations (3.12), respectively, in the S layers occupying the regions $-(d_f + d_s) < z < -d_f$ and $0 < z < d_s$, and in FM layers located in the regions $-d_f < z < 0$ and $d_s < z < (d_f + d_s)$. The boundary conditions at the central interface $z = 0$ of the unit cell have the form (3.13). At other boundaries of the unit cell, i.e., $z = d_s, -d_f, (d_f + d_s), -(d_f + d_s)$, relationships analogous to (3.13) completed by periodicity conditions

$$F(z + L, \omega, I) = \exp(i\phi) F(z, \omega, \exp(i\chi) I) \quad (3.28)$$

will be satisfied. Here $L = d_f + d_s$ is the superlattice parameter, and ϕ and χ are the phases of the superconducting and magnetic OPs, respectively. The periodicity conditions (3.28) permit us to take into account two important effects. First, they allow for the competition between 0-phase and π -phase types of superconductivity, which also was considered in the previous proximity theories [61, 62, 64–66]. Second, they include the interaction of localized moments of neighboring FM layers through the superconducting S interlayers. Below, we show that, apart from the known competition between the 0-phase and π -phase superconductivity, competition between the 0-phase and π -phase types of magnetism also exists in FM/S superlattices. This leads to a new classification of states of such an FM/S system. We will seek solutions to the boundary-value problem (3.12), (3.13) for the central FM/S junction of the unit cell in the form

$$\begin{cases} F_s(z, \omega) = A(\omega) \cos \left[k_s \left(z - \frac{d_s}{2} \right) \right] + C(\omega) \sin \left[k_s \left(z - \frac{d_s}{2} \right) \right], \\ 0 < z < d_s, \\ F_f(z, \omega) = B \cos \left[k_f \left(z + \frac{d_f}{2} \right) \right] + D \sin \left[k_f \left(z + \frac{d_f}{2} \right) \right], \\ -d_f < z < 0, \end{cases} \quad (3.29)$$

where the coefficients $A(\omega)$, B , $C(\omega)$, and D are independent of z . The solutions for two outer S and FM layers entering into the S/FM/S/FM unit cell are analogous to (3.29) with allowance for the condition of periodicity (3.28). The minimization of the free energy of the unit cell with respect to the phases of the superconducting (ϕ) and magnetic (χ)

OPs leads to the possible realization of four different states (Fig. 6)

- (1) 00-phase ($\phi = 0, \chi = 0$);
 - (2) $\pi 0$ -phase ($\phi = \pi, \chi = 0$);
 - (3) 0π -phase ($\phi = 0, \chi = \pi$);
 - (4) $\pi\pi$ -phase ($\phi = \pi, \chi = \pi$).
- (3.30)

In the 00 state, we have $C(\omega) = D = 0$, i.e., the pair amplitudes are even functions with respect to the centers of the S and FM layers; in the $\pi 0$ phase, the pair amplitude in the FM layer becomes odd. In the two new states, i.e., 0π , where $D = 0$ and $B \neq 0$, and $\pi\pi$, where, on the contrary, $B = 0$ and $D \neq 0$, the coefficients $A(\omega)$ and $C(\omega)$ are nonzero, i.e., the pair amplitude in the S layer does not possess evenness. An admixture of sine solutions to the cosine ones in the first of the expressions (3.29) reflects the partial compensation of the paramagnetic effect of the exchange field I for the S layers in the AFS state with an antiparallel orientation of the magnetizations in the neighboring FM layers.

The first two states 00 and $\pi 0$ were studied in Refs [61, 62, 64–66] (see below), where it was implicitly assumed that $\chi = 0$, which corresponded to the ferromagnetic state (FS) of the superlattice with a parallel orientation of the magnetizations of all FM layers. In the limit of large thicknesses of S layers ($d_s \gg \xi_s$), this assumption is correct, since the mutual

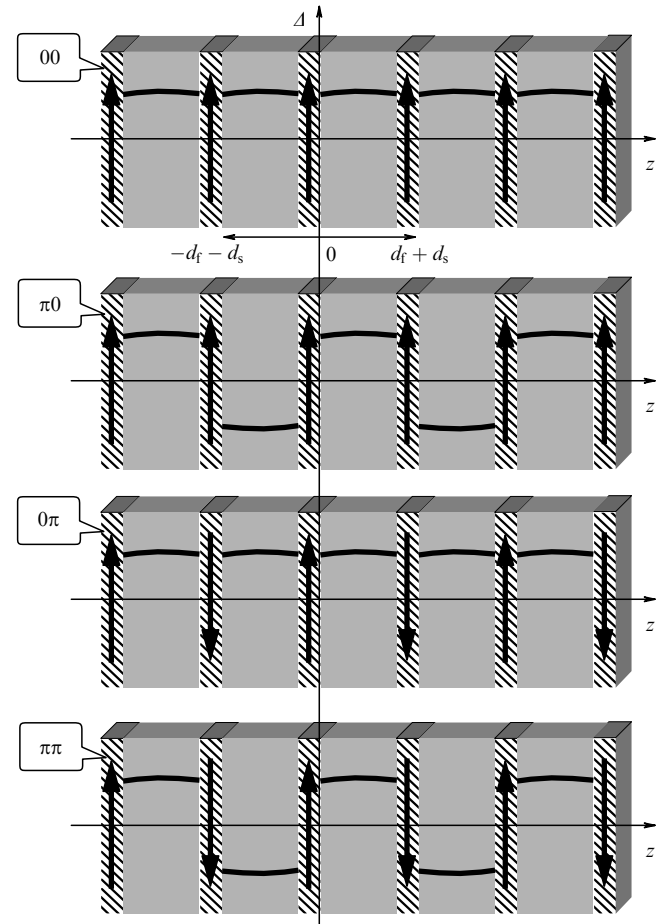


Figure 6. Four possible states of the FM/S superlattice. Horizontal arrows show the unit cell of the superlattice. Solid lines show the behavior of the superconducting order parameter ($A(z)$) in the S layers. In the FM layers, thick solid arrows show the direction of magnetizations, which plays the role of the magnetic OP.

orientation of the magnetizations of the neighboring FM layers is unimportant until the indirect RKKY exchange through the S layers is exponentially small. However, for superlattices with thicknesses d_s close to critical ($d_s^c \sim \xi_s$), greater T_c appear to be characteristic of the π -phase (with respect to magnetism) 0π and $\pi\pi$ LOFF states rather than 0 -phase 00 and $\pi 0$ states, respectively. Below, we will show that the superconducting state of the superlattice is a result of competition of four different LOFF states: 00 , 0π , $\pi 0$, and $\pi\pi$.

Calculations for the reduced temperature of the superconducting transition of the superlattice t yield the conventional equation (3.17). The pair-breaking parameter $D_s k_s^2$ is a solution to other transcendental equations [its own for each of the four phases (3.30)]. For the 00 phase, this equation has the form

$$D_s k_s^{00} \tan \frac{k_s^{00} d_s}{2} = \frac{\sigma_s v_s}{4 - [\sigma_s v_f n_{sf} / D_f(I) k_f] \cot(k_f d_f / 2)}. \quad (3.31)$$

This equation differs from the analogous equation (3.18) for the FM/S junction only in the natural substitutions $d_f \rightarrow d_f/2$, $d_s \rightarrow d_s/2$ following from the symmetry of the problem. The complex wave number k_f , as before, is defined by Eqn (3.19). To calculate T_c in the 0π state, Eqn (3.31) should be supplemented by an expression that relates $k_s^{0\pi}$ to k_s^{00} :

$$(k_s^{0\pi})^2 - 2 \operatorname{Re} \left[k_s^{00} \tan \frac{k_s^{00} d_s}{2} \right] k_s^{0\pi} \cot(k_s^{0\pi} d_s) = \left| k_s^{00} \tan \frac{k_s^{00} d_s}{2} \right|^2. \quad (3.32)$$

The pair-breaking factor in the $\pi 0$ state can be found from Eqn (3.31) by substituting $k_s^{\pi 0}$ for k_s^{00} in the left-hand side and $-\tan(k_f d_f / 2)$ for $\cot(k_f d_f / 2)$ in its right-hand side. The equation that relates $k_s^{\pi\pi}$ with $k_s^{\pi 0}$ is obtained from (3.32) if we substitute $k_s^{\pi 0}$ for k_s^{00} and $k_s^{\pi\pi}$ for $k_s^{0\pi}$ in it.

The set of phase diagrams $t(d_s)$ for the superlattices at various values of d_f and a reasonable choice of the other parameters of the theory is given in Fig. 7. As was expected, in the region of thicknesses d_s smaller than a certain threshold value d_s^π , the AFS states 0π and $\pi\pi$ (curves B and D) with an antiparallel orientation of the magnetizations of neighboring FM layers are energetically more favorable compared to the known FS states 00 and $\pi 0$ (curves A and C). For the FM/S superlattices, the threshold thickness d_s^π below which π -phase (in magnetism) states are realized depends on the magnitude of the other parameters of the theory and changes between $0.6\xi_{s0}$ and $0.85\xi_{s0}$. It is important that the critical thickness of superconducting layers d_s^c at which T_c becomes zero is always smaller for the AFS states than for the FS states, i.e., $d_s^c(\text{AFS}) < d_s^c(\text{FS})$, where $d_s^c(\text{AFS}) = \min\{d_s^c(0\pi), d_s^c(\pi\pi)\}$, and $d_s^c(\text{FS}) = \min\{d_s^c(00), d_s^c(\pi 0)\}$. Thus, for the superlattices with $d_s^c(\text{AFS}) < d_s < d_s^\pi$, the superconductivity will have a purely AFS nature. It is seen from Fig. 7 that, with the indicated set of the parameters of the theory, this range of thicknesses is sufficiently wide and can exceed $0.3\xi_{s0}$. In addition, for certain thicknesses d_s from this range, the difference between the critical temperatures $T_c(\text{AFS}) - T_c(\text{FS})$ may be quite substantial. Note also the competition between the AFS 0π and $\pi\pi$ states themselves (curves B and D in Fig. 7) at different thicknesses of the

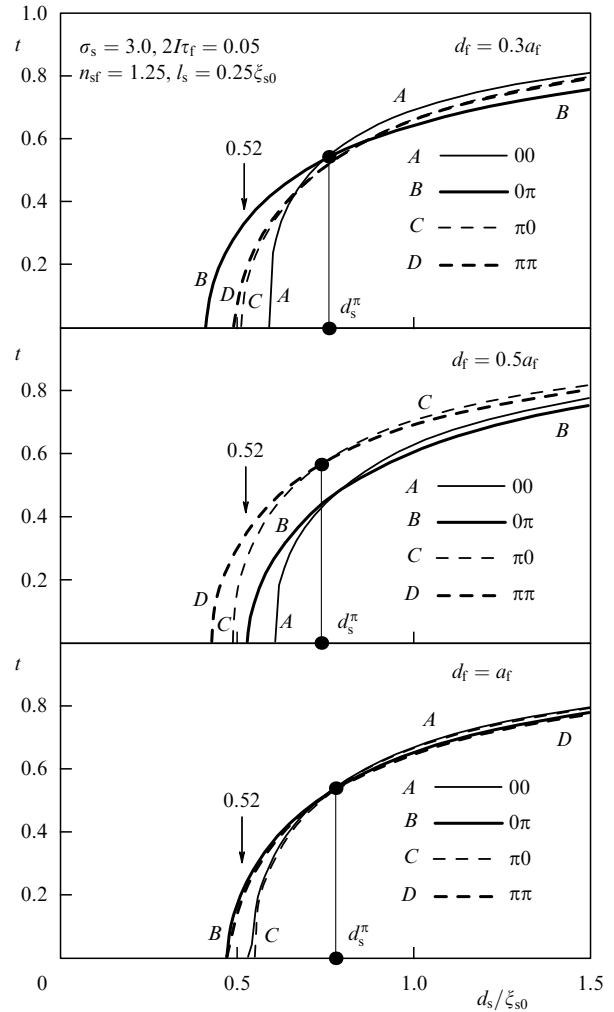


Figure 7. Reduced critical temperature $t = T_c/T_{cs}$ of the FM/S superlattice as a function of the reduced thickness of the S layer d_s/ξ_{s0} at various values of the FM-layer thickness [88]. The values of the main parameters of the theory are given in the top panel (left). The value $d_s = 0.52\xi_{s0}$ shown by vertical downward arrows corresponds to the curves $t(d_f)$ in Fig. 8.

FM layers d_f . This competition indicates that the nature of oscillations in $T_c(d_f)$ at $d_s < d_s^\pi$ is related to a cascade of phase transition $0\pi - \pi\pi - 0\pi$ between the new AFS LOFF states (see Fig. 8).

As the thickness of the S layers increases, the gain due to the partial compensation of the paramagnetic effect of the exchange field in the AFS state decreases, and at $d_s > d_s^\pi$ becomes negligible. In this case, the symmetric FS solutions 00 and $\pi 0$, which lead to smaller fluxes of Cooper pairs through the S/FM interfaces, possess a slightly greater critical temperature than the 0π and $\pi\pi$ LOFF states. However, the difference between $T_c(\text{AFS})$ and $T_c(\text{FS})$ in the range of thicknesses $d_s > d_s^\pi$ is quite insignificant and can hardly be observed experimentally. Most probably, the FM/S superlattice in the range of thicknesses $d_s > d_s^\pi$ is effectively quasi-two-dimensional in the magnetic aspect, i.e., it breaks up into a system of S/FM/S sandwiches, in which no correlation between the phases of the magnetic OP in neighboring FM layers exists. At the same time, the 0 - or π -type matching between the phases of the superconducting OP in neighboring S layers is retained in this case. This should lead to a nonmonotonic behavior of $T_c(d_f)$ at $d_s > d_s^\pi$ due to

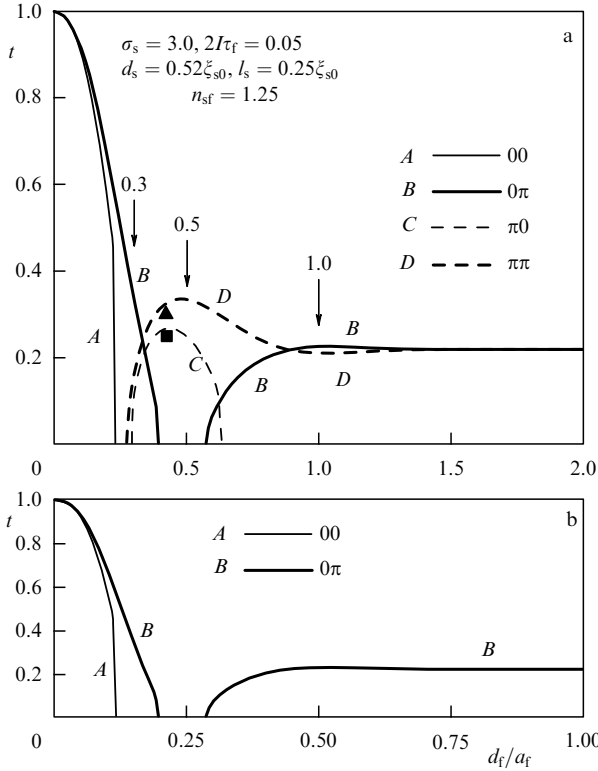


Figure 8. (a) Reduced critical temperature t of the FM/S superlattice as a function of the reduced thickness of the FM layer d_f/a_f at $d_s = 0.52\xi_{s0}$ and values of the other parameters of the theory corresponding to Fig. 7. Vertical arrows correspond to thicknesses d_f at which the phase diagrams shown in Fig. 7 were constructed. (b) Phase diagram for a three-layer FM/S/FM system. (After Ref. [88].)

the transitions between the 00 and $\pi 0$ states, as was shown in Refs [61, 62, 64–66] for FM/S superlattices.

Thus, an analysis of Fig. 7 shows that, at $d_s < d_s^\pi$, it is the AFS states 0π and $\pi\pi$ that are dominating, whereas at $d_s > d_s^\pi$, 00 and $\pi 0$ FS states are realized. Let us consider these cases separately.

As was noted above, of most physical interest in Fig. 7 is the range of thicknesses d_s where the critical temperatures of all four LOFF states differ most strongly. Therefore, to analyze the $t(d_f)$ dependences, we chose superlattices with the same parameters as in Fig. 7, with a thickness of the S layer $d_s = 0.52\xi_{s0}$ corresponding to this range. Figure 8a displays curves corresponding to all four possible LOFF states. It is seen from this figure that the curves B and D corresponding to the AFS states 0π and $\pi\pi$ go much higher than the 00 and $\pi 0$ FS states (curves A and C) with the reentrant superconductivity. Consequently, the appearance of new AFS LOFF states prevents the premature suppression of superconductivity and substantially increases the area of superconducting regions in the phase diagrams in Figs 7 and 8. Note that at a given choice of the parameters of the theory ($2I\tau_f \ll 1$, $d_s < \xi_{s0}$), the appearance of 3D states virtually does not affect the $t(d_s)$ and $t(d_f)$ phase diagrams.

The simplest structure admitting competition of the 0-phase and π -phase magnetism and of the 0-phase and π -phase superconductivity in the same sample is a four-layer structure S/FM/S/FM whose phase diagrams are analogous to those shown in Figs 7 and 8a for superlattices. The simultaneous study of the $T_c(d_s)$ phase diagrams given in Fig. 7 and of the

$T_c(d_f)$ diagrams shown in Fig. 8a permits one to optimize the choice of the parameters of this four-layer system, making it possible to control its superconducting and magnetic properties, e.g., using a weak external magnetic field. In order to reorient the magnetizations of the FM layers from the antiferromagnetic into the ferromagnetic arrangement, magnetic fields H are required which are greater than their coercive field H_{coer} . Such fields ($H_{\text{coer}} \sim 10\text{--}100$ Oe, see, e.g., Ref. [89]) are too weak to substantially change the phase diagrams of S/FM/S/FM structures, which possess simultaneously two channels of recording information, namely, on the superconducting current and on the magnetic order. In particular, as follows from Fig. 8a, if we select the working point of the system immediately below the curve D [e.g., $t \approx 0.3$, $d_f \approx 0.45a_f$ (solid triangle)], the effect of a field $H > H_{\text{coer}}$ will transform the system from the AFS($\pi\pi$) state directly into the ferromagnetic normal (FN) state, making the superconducting current resistive. Switching off of this field restores the system into the initial AFS state. In this regime, the four-layer S/FM/S/FM system works as a device with a 100% negative magnetoresistance. This resembles the model of a ‘spin switch’ based on FM/S/FM trilayers suggested in Refs [90, 91] (see the next section of this paper).

In particular, if we fix the orientation of the magnetization of the outer layer FM', e.g., due to pinning in the junction with a magnetic insulator, then by the application of a field H (which is greater than the upper critical field H_{c2}) of the opposite orientation, we can obtain the transition of the four-layer structure from the AFS into the antiferromagnetic normal (AFN) state. In this case, we have a change in only information recorded in the superconducting current, whereas the information recorded in the mutual orientation of the magnetizations of the FM layers is retained. Note that, choosing the position of the working point with respect to the curve of the superconducting transition $T_c(d_f)$ in Fig. 8, we can always achieve the necessary magnitude of the H_{c2} field by making it smaller than the field H_p required to lift pinning. An additional transition AFN \rightarrow FN in the S/FM/S/FM system arises under the effect of a field $H > H_p$. A system prepared in this way can have three different states — AFS, FN, and AFN — differing in the information recorded in the magnetic order and in the superconducting current.

On the other hand, in accordance with the theory of second-order phase transitions, that state is realized under given conditions that possesses a lower free energy (a greater critical temperature). Therefore, if we chose the working point below the curve C ($t \approx 0.25$, $d_f \approx 0.45a_f$, solid square in Fig. 8a), then the action of a field H of a proper magnitude and direction leads to a transition AFS($\pi\pi$) \rightarrow FS($\pi 0$), which changes magnetic information and, at the same time, retains information recorded in the superconducting current. As the field strength increases to a value exceeding H_{c2} in the FS($\pi 0$) state, the S/FM/S/FM structure passes into the FN state. By applying fields of opposite orientations and exceeding H_{c2} and then H_p in magnitude, we obtain a chain of transitions AFS($\pi\pi$) \rightarrow AFN \rightarrow FN, as was described above. The switching off of external fields again returns the system into the initial state AFS($\pi\pi$). Such a S/FM/S/FM superlattice already has the maximum number of logically different states, i.e., four (AFS, FS, FN, and AFN).

Thus, FM/S superlattices can serve as the component base for the development of microelectronic devices of a fundamentally new type, which combines advantages of the superconducting and magnetic channels of recording infor-

mation in a *single* sample. We emphasize that these channels can be *separately* controlled by an external field. Note that the π -phase magnetism manifests itself most vividly in a quite narrow interval of the theory parameters. In particular, it is extremely sensitive to the parameters $2I\tau_f$ and n_{sf} . For example, at $2I\tau_f \gg 0.1$ and n_{sf} of the order of unity or smaller, the difference $|t(\text{AFS}) - t(\text{FS})|$ becomes less than 0.02, i.e., the π -magnetic and 0-magnetic states of the FM/S superlattice become virtually indistinguishable.

We established above that at large thicknesses of S layers, when $d_s > d_s^\pi$, the 00 and $\pi 0$ FS states are dominant. As is shown in Fig. 9, the behavior of $T_c(d_f)$ in the simplest 1D version of the theory admits a wide spectrum of nonmonotonic dependences, from a single spike (Fig. 9a) to periodically reentrant superconductivity (Fig. 9d). However, in contrast to the FM/S junctions (see Fig. 3), these dependences arise as a result of competition between the 00 and $\pi 0$ states. The mechanism of the nonmonotonic behavior of T_c depending on d_f is related to oscillations of the flux of Cooper pairs at S/FM interfaces owing to the pinning of antinodes or nodes of the pair amplitude in the centers of the FM interlayers (see analogous discussion in Section 3.2).

In comparison with the above-considered case where $d_s < d_s^\pi$, note that the appearance, along with the 1D states, of 3D LOFF states at $d_s > d_s^\pi$ dramatically changes the $T_c(d_f)$ phase diagram of FM/S superlattices (Fig. 10). Here, thin dashed and dotted lines show the 00-phase and $\pi 0$ -phase 1D solutions that were considered above (see Fig. 9). The thick solid lines show the results of the optimization of the $T_c(d_f)$ dependence, which are due to a complex competition of 1D and 3D solutions for both 00- and $\pi 0$ -phase LOFF states.

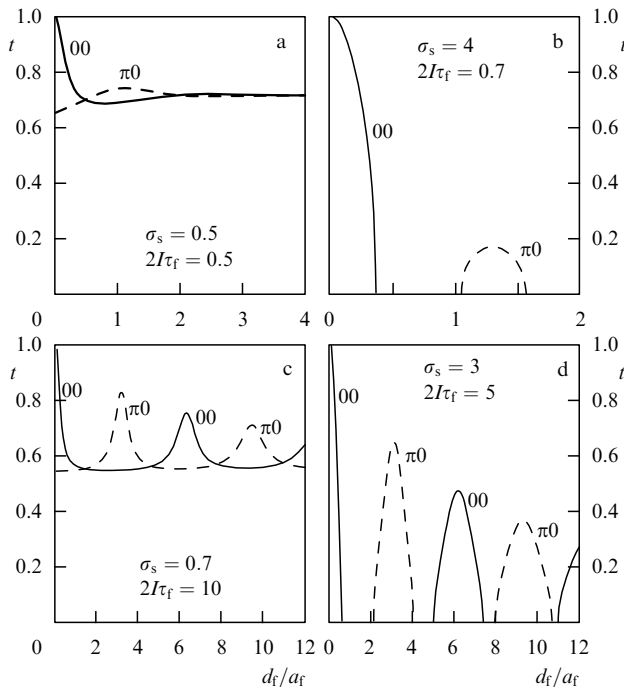


Figure 9. Reduced transition temperature $t = T_c/T_{cs}$ for FM/S superlattices as a function of the reduced thickness of the FM layer d_f/a_f in terms of the 1D theory ($q_f = 0$). Here, $l_s = 0.25\xi_{s0}$, $d_s = 1.25\xi_{s0}$ (except for Fig. 9b) and $n_{sf} = N_s v_s / N_f v_f = 1$; the values of the parameters σ_s and $2I\tau_f$ are given in the figures (a)–(d) taken from Refs [65, 66]: (a) passage onto a plateau through a minimum; (b) reentrant superconductivity ($d_s = \xi_{s0}$); (c) oscillations; and (d) periodically reentrant superconductivity.

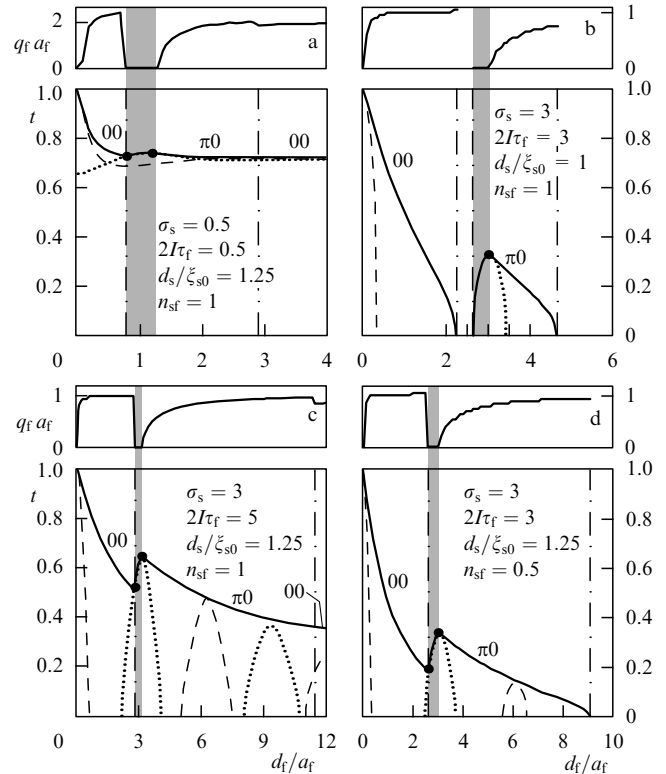


Figure 10. Phase diagrams of the FM/S superlattices at $l_s/\xi_{s0} = 0.25$ for various values of the parameters of the 3D theory. The main designations are the same as in Fig. 5. Thin dashed lines correspond to pure 1D 00-phase solutions; dotted lines correspond to $\pi 0$ -phase solutions. The regions of existence of optimized 00-phase and $\pi 0$ -phase states are separated by vertical dash-dot lines.

As follows from Fig. 10c, at certain values of the parameters of the superlattice, the behavior of the $T_c(d_f)$ function indeed reveals a single spike of the critical temperature caused by the 3D(00)–1D($\pi 0$)–3D($\pi 0$) cascade of transitions. At lower values of σ_s and $2I\tau_f$, the amplitude of the spike strongly decreases, and the $T_c(d_f)$ dependence after a monotonic fall-off directly passes onto a plateau (Fig. 10a). In addition, we also predict some new variants of the nonmonotonic behavior of $T_c(d_f)$ that are characteristic of only superlattices, such as the reentrant superconductivity in the form of an isolated 1D–3D($\pi 0$) peak (Fig. 10b) and the oscillatory approaching of T_c to zero as a result of 3D(00)–1D($\pi 0$)–3D($\pi 0$) transitions (Fig. 10d). The points of the phase transitions at which the period of the 2D modulation of the pair amplitude along FM/S boundaries tends to infinity ($q_f = 0$) correspond to Lifshitz triple points. Thus, even the seemingly simple (as in Fig. 10a) behavior of $T_c(d_f)$ observed in many experiments can lead to nontrivial physics of FM/S systems, consisting in a combined (BCS + LOFF) character of superconductivity and competition of 1D and 3D LOFF states in FM layers.

The one-dimensional LOFF states with vividly pronounced oscillations of $T_c(d_f)$ shown in Fig. 10c by thin dashed lines could be realized in pure form, e.g., in FM/S structures in which the FM layers are quasi-one-dimensional ferromagnets with conducting threads oriented perpendicular to the interface. Another possibility for the realization of only 1D LOFF states is provided by the replacement of FM layers by quasi-one-dimensional ferromagnetic bridges (whiskers). In these cases, the appearance of 3D states with spatial

changes in the pair amplitude along FM/S boundaries can be neglected.

It is important to note that both for bilayers and superlattices, the appearance of new 3D LOFF states along with 1D states prevents the premature vanishing of T_c with increasing d_f and increases the area of the superconducting regions in the phase diagrams in Figs 5 and 10. Moreover, it is the competition between the 1D and 3D states, leading to the multicritical behavior of the phase diagrams, that is responsible for the nonmonotonic behavior of $T_c(d_f)$ at some thicknesses of F layers and for the absence of oscillations at greater d_f .

3.5 Three-layer FM/S/FM system

We specially consider this particular case in view of the prospects for practical applications of the principle of modification of the superconducting state in such a trilayer depending on the mutual orientation of the magnetizations in ferromagnetic layers.

To find the critical temperature in a FM/S/FM trilayer, we can use Eqns (3.17) and (3.19), and we should replace the quantity d_s by $d_s/2$ in Eqn (3.18): in a two-layer FM/S system, the S layer is coupled with only one FM layer, whereas in a FM/S/FM system it is coupled with two layers.

Note that Figs 7 and 8a are also suitable for analyzing $T_c(d_s)$ and $T_c(d_f)$ phase diagrams of three-layer FM/S/FM structures in which the π -phase superconductivity is impossible in principle. To make this, it is sufficient to remove the curves $C(\pi/2)$ and $D(\pi)$ from these figures and replace d_f by $2d_f$. In particular, Fig. 8b with the reentrant superconductivity represents the $T_c(d_f)$ phase diagram for FM/S/FM trilayers.

It follows from Fig. 8b that with our choice of the parameters of the theory, it is possible to organize controlling the superconductivity of the FM/S/FM trilayers and superlattices with the help of a weak external magnetic field. However, as we saw above, the FM/S superlattices offer a significantly greater number of logically different variants for recording information as compared to the FM/S/FM trilayers.

Thus, the FM/S/FM trilayers that were earlier discussed in Refs [90, 91] represent a particular case of the above-described theory of superlattices. Moreover, it was assumed in the cited works that the AFS state has a greater T_c than the FS state at any thickness d_s of the S layer, although the estimates of the $T_c(d_s)$ were only performed in the Cooper limit ($d_s \ll \xi_s$). We showed above that the AFS state is dominating only while d_s is smaller than a certain threshold value d_s^π (see Fig. 7). In the opposite case, the FS state has a higher critical temperature. Recall that, in our case, $d_s \geq d_s^c \approx 0.4\xi_{s0} > \xi_s \approx 0.3\xi_{s0}$

Nevertheless, for the first time the idea of the development of similar switches of *current* with two possible states was suggested just for FM/S/FM trilayers by Buzdin, Vedyayev, and Ryzhanova [90] and Tagirov [91]. In these papers, the direction of the magnetization in one of the FM layers was fixed due to the magnetic coupling with one more external F layer, i.e., in fact a four-layer system F/FM/S/FM was suggested. A weak external magnetic field $H_{\text{coer}} < H < H_p$ transformed the system from the AFS into the FN state.

To close the consideration of switches of superconducting current, note some earlier works devoted to similar devices with a single channel of recording based on the transition from the superconducting into the normal state. In Ref. [92],

an experimental model of a device based on an FM/I/S system was suggested, in which the superconductivity was suppressed due to magnetic fringe fields arising because of the special geometry of the switch. A three-layer F'/F''/S device in which a weak magnetic field changed the direction of the magnetization in a sufficiently thin internal F'' layer, was theoretically investigated in Ref. [93]. Upon the change in the mutual ordering of the magnetizations M' and M'' from the antiparallel to the parallel arrangement, the device passed from the S into the N state.

So far, we have investigated F/S multilayers with particular phase relationships between two neighboring F layers $\chi = 0, \pi$ [see relations (3.28) and (3.30)]. In Ref. [94], the authors investigated the interaction between superconducting and magnetic OPs for the case where the angle χ between the magnetizations of two neighboring F layers was arbitrary. For the FM/S/FM system in the case of a dirty superconductor, the Usadel equations were solved using simplified boundary conditions corresponding to a high transparency of the boundaries. When the ratio of the conductivities of the metals in the normal state $\bar{\sigma}_{s,f}$ is small ($\gamma = \bar{\sigma}_f/\bar{\sigma}_s \ll 1$), the boundary-value problem leads to the following equation for T_c :

$$\ln \frac{T_c}{T_{cs}} = \Psi\left(\frac{1}{2}\right) - \text{Re} \Psi\left[\frac{1}{2} + \frac{d^*}{d_s} \frac{T_{cs}}{T_c} \left(1 + i \cos \frac{\chi}{2}\right)\right], \quad (3.33)$$

where d^* is a characteristic length written as

$$d^* = \frac{\gamma D_s}{4\pi T_{cs}} \sqrt{\frac{I}{D_f}}.$$

In the particular cases of $\chi = 0$ (parallel orientation of magnetizations) and $\chi = \pi$ (antiparallel orientation), we have from Eqn (3.33) the previously obtained result [90]: T_c is higher for the antiferromagnetic orientation. A numerical solution to Eqn (3.33) shows that at intermediate χ the critical temperature gradually passes from one limit to another, so that $T_c(0) < T_c(\chi) < T_c(\pi)$. Another result following from Eqn (3.33) is the determination of the critical thickness d_s^c at which the superconductivity disappears ($T_c = 0$):

$$\frac{d_s^c}{d^*} = \exp\left[-\Psi\left(\frac{1}{2}\right) + \text{Re} \ln\left(1 + i \cos \frac{\chi}{2}\right)\right]. \quad (3.34)$$

According to this formula, d_s^c gradually decreases as the angle increases, i.e., at the antiferromagnetic orientation the superconductivity is more stable with respect to the pair-breaking effect due to the proximity of the FM layer.

In another case, where $\gamma = 1$, superconductivity is retained only at small thicknesses d_f . Investigation [94] shows that, in this case as well, the antiferromagnetic orientation is energetically more favorable.

The same conclusion follows from the consideration of other systems, e.g., FM/S superlattices with atomic layers [94]. As an example of such a system, the layered superconducting ruthenate $\text{RuSr}_2\text{GdCu}_2\text{O}_8$ can be taken, in which the magnetic phase transition occurs at $T_m \approx 130\text{--}140$ K, and the superconducting transition, at $T_c \approx 30\text{--}40$ K. We can assume that in such compounds the CuO layers are responsible for superconductivity, while in the Gd layers a ferromagnetic ordering occurs in such a manner that the magnetizations of neighboring layers are antiparallel. Thus, this ruthenate could be considered as an example of an atomic

superlattice with a π -phase superconductivity and π -phase magnetism (see, e.g., Ref. [95] and references therein). However, recent neutron diffraction investigations [12] showed that the antiferromagnetic ordering in this compound occurs in all three directions. It is possible that the atomic FM/S superlattice is also realized in other ruthenates with a greater number of ruthenium layers.

3.6 Further development of the theory

So far, when studying the problem of the interaction of the superconducting state with the type of magnetic ordering between ferromagnetic layers, we ignored the exchange coupling between the surface atoms of the FM layers through the conduction electrons of the S layer. To the full extent, this problem will be considered in Section 5, in connection with the study of FI/S structures consisting of layers of a ferromagnetic insulator and a superconductor. In that section, we will consider in detail the problem of indirect interaction of localized spins through the conduction electrons in the superconductor on the basis of fundamental investigations [78, 80, 87].

Returning to the problem of magnetic ordering in FM/S structures, we note that the mechanism of the establishment of any magnetic order here is of purely correlation character. The type of magnetic order is determined by the minimization of the free energy of the entire FM/S structure. Thus, for a FM/S/FM trilayer, as we saw, the antiferromagnetic orientation of the magnetizations of neighboring FM layers proves to be energetically more favorable than the ferromagnetic orientation. Such an approach should be supplemented by the introduction of the indirect interaction of FM layers through the conduction electrons of the S layer.

For an FM/N/FM system consisting of two ferromagnetic layers separated by a normal metal, the indirect FM–FM interaction has the character of a modified RKKY interaction [96]. For FM/S/FM system, an investigation was performed for the zero temperature using numerical methods [97]. Recently [98], the problem was considered for finite temperatures analytically, using the method of functional integration, with the following assumptions: (1) the indirect interaction between FM layers exists when the superconductor that separates them is in the normal state; (2) superconductivity is not suppressed because of the proximity effects involving ferromagnetic layers; and (3) the boundary of the FM/S junction is smooth. The second condition requires that the ferromagnetic layer be a weak ferromagnet. For the model in which

$$T_m \gg T_c, \quad J_{sd} \langle S^z \rangle \ll 2\pi T_c, \quad d_f \gg d_s, \quad p_F d_s \gg 1, \quad (3.35)$$

where p_F is the Fermi momentum for the S metal, the following asymptotic for the indirect interaction between FM layers was obtained:

$$H_{\text{eff}} \sim J_{sd}^2 N(0) \frac{\cos 2p_F d_s}{(2p_F d_s)^2} \begin{cases} \exp\left(-\frac{d_s}{\xi_s}\right), & T \rightarrow 0, \\ \exp\left(-\frac{d_s}{\lambda_T}\right), & T \sim T_c. \end{cases} \quad (3.36)$$

Thus, the magnitude H_{eff} is controlled by the coherence length ξ_s at low temperatures and by the thermal length

$\lambda_T = v_s/\pi T_c$ in the vicinity of T_c (including the region of $T > T_c$). The oscillations of the effective interaction have a period of π/p_F , as for the RKKY interaction, but they fall off with distance by the law $\sim (p_F d_s)^{-2}$ rather than $\sim (p_F d_s)^{-3}$, as is the case for the indirect interaction between localized moments. It is important that near T_c no drastic changes in H_{eff} occurs, and formula (3.36) at $T \approx T_c$ agrees with the calculations [96] for the FM/N/FM system. Such oscillations in the FM/N/FM system have already been observed experimentally [99]. For the experimental observation of oscillations in the FM/S/FM systems, structures consisting of high-temperature superconductors and magnets with colossal magnetoresistance were suggested [98].

When studying the interaction of magnetic and superconducting states in FM/S systems, we assumed that the state of an isolated FM layer is ferromagnetic. At the same time, it was shown yet in earlier investigations [2] that the minimum of energy of the system in a uniform superconductor is associated with a cryptoferromagnetic (CF) phase with a spatial modulation of the magnetic moment. The loss in the exchange energy (in the case of the positive sign of the exchange integral) is compensated by the formation of the superconducting state in such a way that, at least under the condition that the period of the CF structure is much smaller than the size of Cooper pairs ($Q_0^{-1} \ll \xi_s$), the CFS phase proves to be stable, and the paramagnetic effect is weakened because of the averaging of spin polarization over distances of the order of the coherence length ξ_s .

In a nonuniform superconductor (FM/S junction), the cryptoferromagnetic state in the FM layer also proves to be stable. Recently, a detailed investigation of the possibility of the existence of such a state in the FM/S junction was performed under the conditions corresponding to the experiment, namely, for the case where the following inequalities are satisfied:

$$l_s \ll \xi_s, \quad d_f \ll a_f, \quad I\tau_f \gtrsim 1 \quad (3.37)$$

which means that there is a dirty superconductor and a thin sufficiently pure ferromagnetic layer. The last condition in Eqn (3.37) implies that we cannot use the Usadel equations for the FM layer, as for the S layer, but should write the Eilenberger equations [71].

The corresponding boundary-value problem with the Usadel equations for the superconductor and the Eilenberger equations for the ferromagnet was solved in Ref. [100], where the free energy of such a junction was calculated as a function of the modulation wave vector q . On the assumption that q is small, an expansion of the energy in powers of q was obtained. The zero coefficient at q^2 (and the positive sign of the coefficient at q^4) determines the boundary between the CF and F phases. An analysis shows that the appearance of the CF phase is favored by the small magnitude of the exchange integral J and the small thickness of the FM layer (at a sufficiently large exchange field I). Naturally, cryptoferromagnetism should arise not only in the junction but also in the lattice, including the π -phase magnetic ordering. This phenomenon will be studied in detail in Section 5, in which we will consider layered systems consisting of insulating magnetic and superconducting layers on the basis of the works performed by one of us [78, 79].

We now turn our attention to works [101, 102], in which some features in the density of states in a ferromagnetic metal being in contact with a superconductor have been studied.

The Usadel function for the FM layer is an oscillating and damped function of the distance from the FM/S interface:

$$F_f(z, \omega) = \frac{\Delta}{\sqrt{\Delta^2 + \omega^2}} \exp k_\omega z \quad (z < 0), \quad (3.38)$$

where

$$k_\omega = \sqrt{\frac{2(\omega + iI)}{D}}, \quad \text{Re } k_\omega > 0.$$

Since the normal Green's function G_f and the anomalous function F_f for the Usadel equations are linked by the known relation $G_f^2 + F_f \tilde{F}_f = 1$, we can easily obtain the expression for the density of states in the F layer [101]

$$\begin{aligned} N_\uparrow(z, \omega) &= N_f \text{Re } G_f(\omega) \\ &= N_f \text{Re} \sqrt{1 - \frac{\Delta^2}{\Delta^2 - \omega^2} \exp \left[2z(1+i) \sqrt{\frac{I+\omega}{D}} \right]}. \end{aligned} \quad (3.39)$$

The density of states $N_\downarrow(z, \omega)$ of electrons with the opposite spin is obtained from Eqn (3.29) by the substitution $I \rightarrow -I$. The expression $N_f(z, \omega) = N_\uparrow + N_\downarrow$ determines the local density of states in the ferromagnetic metal.

It is seen from Eqn (3.39) that $N_f(z, \omega)$ strongly changes on moving away from the F/S boundary within several units of coherence length $\xi_f \sim \sqrt{D/2I}$; the character of this dependence is determined by the magnitude of the frequency ω . At a fixed distance z , $N_f(z, \omega)$ nonmonotonically depends on energy; namely, a sharp peak appears at energies $E_f \pm I$. This peak remains quite marked at distances $|z| \gg \xi_f$. Thus, at the above energies the proximity effect becomes long-range.

In Ref. [102], Koshina and Krivoruchko solved a kind of the inverse problem of the effect of a ferromagnetic layer on the density of single-particle states of a superconducting metal. The density of states $N_s(\omega)$ proved to be spin-polarized, as is the case in the ferromagnetic metal. This is due to the proximity effect on the ferromagnet side. Usually, $N_s(\omega)$ has an ordinary BCS singularity at $\omega = \pm \Delta_0(T)$, but the height of the corresponding peaks decreases with increasing I . In addition, there is another singularity, which is due to the presence of a true gap $\Delta_s(T)$ in the system.

4. FM/S systems: a review of experimental data, a comparison of theory and experiment

4.1 A brief review of experiments

The experimental study of the proximity effect in artificially produced systems consisting of layers of ferromagnetic and superconducting metals stems to the pioneering work of Hauser, Theuerer, and Werthamer [30]. To prepare two-layer FM/Pb sandwiches, they used the method of rf sputtering (rfS). Beginning from the 1980s, numerous new works began appearing [31–60].

Figure 2 schematically displays the multilayer structures that have been studied in experiments. The description of the experimental procedure of preparation of multilayer FM/S systems can be found both in the cited works and in the excellent review by Jin and Ketterson [29]. To prepare FM interlayers, Fe, Co, Gd, and Ni were used, i.e., metals whose Curie temperatures T_m are much greater than the

superconducting transition temperatures of the metals Nb, Pb, and V used for the preparation of S layers.

The main results of experiments on the investigation of multilayer FM/S systems are given in Table 1. Table 2 lists analogous results for the cases where one of the metals was replaced by an alloy and where concentration dependences were mainly studied.

Among all possible experimental parameters and dependences (Tables 1 and 2), the dependence of the critical temperature of the multilayer FM/S system on the thickness d_f of the FM layer and on the thickness d_s of the S layer appears to be of most interest. Experiments show a sufficiently large variety of $T_c(d_f)$ dependences at a fixed d_s , including quite unexpected (at first glance) nonmonotonic dependences and the phenomenon of reentrant superconductivity. Figure 11 shows the main types of experimental dependences of the critical temperature T_c on the thickness of the FM layer. Several experimental dependences of the critical temperature are reproduced in Figs 12–14. The $T_c(d_s)$ dependence, on the contrary, has a completely expected character: it monotonically falls off with decreasing d_s (Figs 12c and 14b).

The various aspects of the dependences of the critical temperature on the layer thicknesses will be discussed in more detail in the next sections; here, we only consider some other

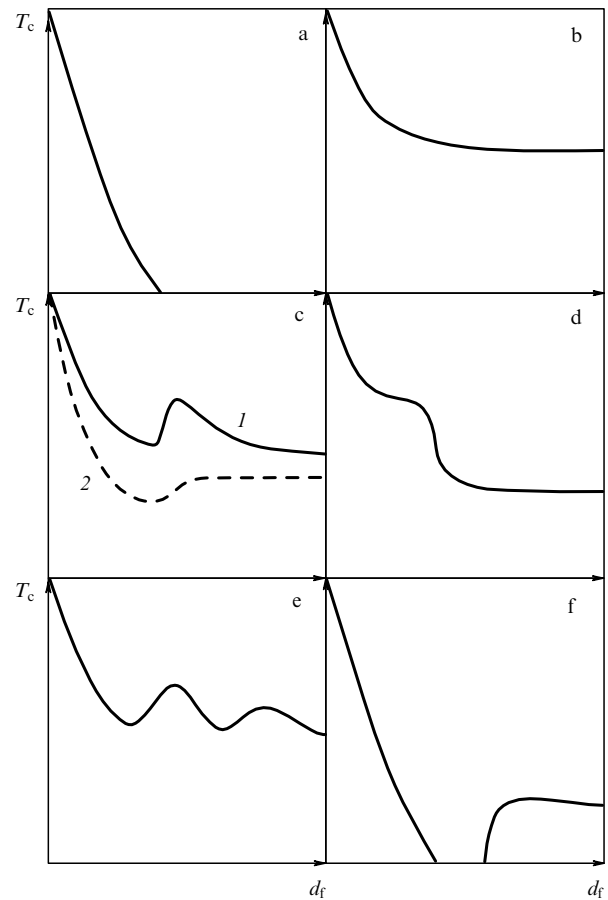


Figure 11. Types of dependences of the critical temperature T_c on the thickness of the FM layer d_f observed in experiments on multilayer FM/S systems (schematic): (a) rapid fall-off to zero; (b) rapid initial fall-off with subsequent monotonic passage onto a plateau; (c) passage onto a plateau via a local minimum (two variants); (d) monotonic decrease with a sharp drop; (e) oscillations (two or more local minima); and (f) reentrant superconductivity.

Table 1. Summary table of experimental results on the FM/S structures.

| <i>n</i> -System (S/FM) | References | $d_s, \text{\AA}$ | $d_f, \text{\AA}$ | Method | $T_c(d_f)$ | $T_c(d_s)$ | M | T_{cs}, K | $\xi_{90}, \text{\AA}$ | $\xi_s, \text{\AA}$ | $I_s, \text{\AA}$ | T_c, K | $d_f^m, \text{\AA}$ | H_{c2} | $d_g^c, \text{\AA}$ | |
|-----------------------------------|------------|-------------------|-------------------|--------|------------|------------|----------|--------------------|------------------------|---------------------|----------------------|-----------------|---------------------|----------|---------------------|---------|
| 2- Nb/Fe | [50] | 260–615 | 0–25 | MBE | d | | + | 8.5 | 400 | 270–330 | 250–375 | | 5 | | | |
| 2- Nb/Fe | [50] | 260 | 7–23 | MBE | d | | + | 8.5 | 400 | 270–330 | 250–375 | | 5 | | | |
| 2- Nb/Fe | [52] | 220–250 | 4–26 | MBE | d | | $M(d_f)$ | | | 180 | 250 | | | | | |
| 3- Fe/Nb/Fe | [42] | 350, 400, 450 | 0–30 | rFS | ? | | + | 7 | | | | | 7 | | | |
| 3- Fe/Nb/Fe | [42] | 200, 400 | 1.5–300 | rFS | b | | + | 7 | | | | | | + | | |
| 3- Fe/Nb/Fe | [45] | 300–800 | 0–30 | rFS | + | + | $M(d_f)$ | 7 | | | | | 7 | + | | |
| 3- Fe/Nb/Fe | [45] | 400 | 0–30 | rFS | c | | | | | | 60–68(1S), 87(F/S/F) | 29 | | | | |
| 3- Fe/Nb/Fe | [45] | 450 | 0–12 | rFS | b | | | | | | | | | | | |
| 3- Fe/Nb/Fe | [45] | 300–800 | 7, 16 | rFS | | | | | | | | | | | | ~ 305 |
| 3- Fe/Nb/Fe | [57] | 200 | 3–40 | eBE | b | | + | | | | | | 4 | + | | |
| <i>n</i> - Nb/Fe | [34] | 0–50 | 0–50 | | | | $M(d_s)$ | | | | | | 3.5 | | | |
| <i>n</i> - Nb/Fe | [35] | | | | | | + | | | | | | | | | |
| <i>n</i> - Nb/Fe | [38] | | | | b | | | | | 80? | | | | | | |
| <i>n</i> - Nb/Fe | [49] | 400 | 2–34 | MBE | d(b) | | + | | | | | | 16 | + | | |
| <i>n</i> - Nb/Fe | [49] | 250–670 | 25 | MBE | | + | + | 9.15 | | 82 | | | | | | ~ 315 |
| <i>n</i> - Nb/Fe _{1-x} N | [46] | 0–200 | 11–28 | | | + | $M(d_s)$ | 17 | | 50 | | | | + | | ~ 100 |
| 3- Co/Nb/Co | [58] | 560–1500 | 20 | dcMS | | | | 9.2 | 500 | | | | | | | |
| 3- Nb/Co/Nb | [58] | 560–1500 | 10, 25, 40 | dcMS | | | + | 9.2 | 500 | | | | 4 | + | | |
| <i>n</i> - Nb/Co | [43] | 200, 400 | 1.5–300 | rFS | b | | $M(d_f)$ | 8.5 | | | | | | + | | |
| <i>n</i> - Nb/Co | [53] | 400 | 2–100 | rFS | e | | $M(d_f)$ | | | | | | 7 | | | |
| <i>n</i> - Nb/Co | [59] | 500 | 18–42 | MBE | e | | | 9.52 | | | | | | + | | |
| 2- Nb/Gd | [37] | 168 | 4–40 | eBE | d | | | | 420 | | | > 1.5 | 12–15 | | | |
| 3- Nb/Gd/Nb | [37] | 188–350 | 34 | eBE | | + | | 8.57 | 420 | 78–90 | | > 1.5 | | + | | ~ 165 |
| 3- Nb/Gd/Nb | [37] | 191 | 4–40 | eBE | b | | | 8.57 | 420 | 78–79.5 | | > 1.5 | 12–15 | | | |
| 3- Nb/Gd/Nb | [37] | 154–180 | 4–40 | eBE | d | | | | 420 | | | > 1.5 | 12–15 | | | |
| 3- Nb/Gd/Nb | [41, 48] | 250 | 0–50 | dcMS | c | | | | | | | | | + | | |
| <i>n</i> - Nb/Gd | [37] | 360, 500, 700 | 34 | eBE | | + | | 8.57 | 420 | 80–108 | | > 1.5 | | + | | ~ 330 |
| <i>n</i> - Nb/Gd | [40, 48] | 81–600–(5000) | 5–55 | dcMS | c | | + | 8.8 | 407 | | | > 0.05 | > 12 | | | 200–350 |
| | | 500 | | | | | | | | 115–130 | 110–141 | | | | | |
| | | 600 | | | | | | | | 145 | | | | | | |

Table 1 (continued).

| n -System (S/FM) | References | $d_s, \text{\AA}$ | $d_f, \text{\AA}$ | Method | $T_c(d_f)$ | $T_c(d_s)$ | M | T_{es}, K | $\xi_{s0}, \text{\AA}$ | $\xi_s, \text{\AA}$ | $l_s, \text{\AA}$ | T_c, K | $d_f^m, \text{\AA}$ | H_{c2} | $d_s^c, \text{\AA}$ | |
|--------------------|------------|-------------------|-------------------|--------|------------|------------|----------|---------------------------|------------------------|---------------------|-------------------|-----------------|---------------------|----------|---------------------|------------|
| n -Nb/Ni | [47] | 0–234 | 18.7 | dcMS | + | + | $M(d_s)$ | 9.2(6.3?) | | 80 | | | | | | ~ 100 |
| n -Nb/Ni | [47] | 87 | 0–19.2 | dcMS | d(b) | | $M(d_f)$ | | | 80 | | | 14 | | | |
| 2-Pb/Fe | [30] | 275–1200 | 1000 | dcMS | | + | | 7.2 | | | | > 1 | | | | ~ 300 |
| 2-Pb/Fe | [56] | 375–1500 | 30 | rFS | | + | + | | | | | | 8 | + | | ~ 350 |
| 3-Fe/Pb/Fe | [56] | 730, 620 | 0–52 | rFS | c | | + | 7.1 | 830 | 170 | 230 | | | + | | |
| 3-Fe/Pb/Fe | [56] | 740–3000 | 30 | rFS | | + | + | | | | | | | + | | ~ 700 |
| 3-Fe/Pb/Fe | [51] | 620 | 4–30 | rFS | a | | + | | 830 | 200 | 200 | | | | | |
| n -Pb/Fe | [33] | | | | | | | | | | | | | | | |
| 2-Pb/Gd | [30] | 220–1200 | 80 | rFS | | + | | 7.2 | | | | > 1 | | | | ~ 250 |
| 2-Pb/Ni | [30] | 350–1200 | 50 | rFS | | + | | 7.2 | | | | > 1 | | | | ~ 350 |
| 3-V/Pb/V | [60] | 335 | 0–35 | | f | | | 5.3 | 435 | 130 | | > 0.5 | | | | |
| n -V/Fe | [31] | (84–400) ap | (0–30) ap | MBE | b(c) | + | | | 440 | | | > 1.9 | | + | | |
| n -V/Fe | [31] | (297–400) ap | (0–30) ap | MBE | c | + | | | 440 | | | > 1.9 | | + | | |
| n -V/Fe | [31] | 102 ap | (0–30) ap | MBE | a | + | | | 440 | | | > 1.9 | | + | | |
| n -V/Fe | [36] | 100–1000 | 6–60 | dcMS | a | + | | 5.1 | | 88.5 | | > 1.4 | 2 | + | | ~ 280 |
| n -V/Fe | [36] | 400 | 6–60 | MBE | a | + | | 5.1 | | 88.5 | | > 1.4 | 2 | | | |
| n -V/Fe | [39] | 100–1000 | 5–60 | dcMS | | | | | | 88.5 | | > 1.4 | 1 | | | 280 |
| n -V/Fe | [44] | 250–1500 | 0–30 | dcMS | c | + | + | 5.1 | | 88 | | > 1.5 | 1 | | | 280 |
| n -V/Co | [39] | 100–1000 | 10–50 | dcMS | | + | + | 5.11 | | 78 | | > 1.4 | 4 | + | | 230 |
| n -V/Co | [43] | 220, 400 | 1.5–300 | rFS | b | | | 4.2 | | | | | | + | | |
| n -V/Co | [53] | 400 | 2–100 | rFS | e | | | | | | | | 7 | + | | |
| n -V/Ni | [32] | 306, 518 | 7–25 | dcMS | | | | 5.4 | | 400 | | | | + | | |
| n -V/Ni | [39] | 100–1000 | 10–50 | dcMS | | + | + | 5.11 | | 70–77 | | > 1.4 | 8 | + | | 190 |

Here, '2-' denotes a bilayer; '3-' denotes a trilayer; 'n-', a superlattice; ap, atomic planes; cBE, electron-beam evaporation; rFS, rf sputtering; dcMS, dc magnetron sputtering. Letters a–f in the column $T_c(d_f)$ correspond to Fig. 11; the sign '+' shows that the measurements were performed in that work; M , magnetization; T_c , temperature range in which the measurements were carried out; d_f^m , critical thickness of the FM layer (at $d_f < d_f^m$, the FM layer is not ferromagnetic); H_{c2} , upper critical field; d_s^c , critical thickness of the S layer (at $d_s < d_s^c$, the sample exhibits no superconductivity).

Table 2. Experimental results on the FM/S structures with alloys (T_m is the Curie temperature; μ_f is the average atomic magnetic moment; for the other designations, see Table 1).

| n - System (S/FM) | References | x | $d_s, \text{Å}$ | $d_f, \text{Å}$ | Method | $T_c(d_f)$ | $T_c(d_s)$ | M | T_{cs}, K | $\xi_s, \text{Å}$ | T_c, K | $d_f^m, \text{Å}$ | H_{c2} | $d_s^c, \text{Å}$ | $T_m(d_f), \text{K}$ | $\mu_f(d_f), \mu_B$ | |
|-------------------------------|--|-------|-----------------|-----------------|--------|------------|------------|-----|--------------------|-------------------|-----------------|-------------------|----------|-------------------|----------------------|---|---|
| n - V/Fe $_x$ V $_{1-x}$ | [39, 44] [44] [44] [39, 44] [39, 44] [44] | 1 | 100–1500 | 0–60 | dcMS | c | + | + | 5.1 | 88 | > 1.4 | 1 | | 280 | | 2 | |
| | | 0.88 | 250–1500 | 0–30 | dcMS | a | + | + | 5.1 | | | > 1.5 | 3 | | 320 | | 1.74 |
| | | 0.77 | 250–1500 | 0–30 | dcMS | b | + | + | 5.1 | | | > 1.5 | 2 | | 350 | | 1.57 |
| | | 0.53 | 100–1500 | 0–30 | dcMS | b | + | + | 5.1 | | | > 1.4 | 2 | + | 340 | | 1 |
| | | 0.38 | 100–1500 | 0–60 | dcMS | b | + | + | 5.1 | | | > 1.4 | 3 | + | 300 | | 0.39 |
| | | 0.34 | 250–1500 | 0–30 | dcMS | b | + | + | 5.1 | | | > 1.5 | 4 | | 280 | | 0.25 |
| | | 0.65 | 400 | 2–100 | rfS | a | | | | 9.4 | 46 | | 7 | | | | |
| n - Nb $_x$ Ti $_{1-x}$ /Co | [53] [53] | 0.28 | 400 | 2–100 | rfS | a | | | 10.2 | 32 | | 7 | | | | | |
| | | 1 | 200 | 3–40 | eBE | b | | | + | 9–9.2 | | 4 | + | | | | |
| 3- Nb/Fe $_x$ Pb $_{1-x}$ /Nb | [57] | 0.4 | 200 | 3–50 | eBE | b | | + | | | | | + | | | | |
| | | 0.2 | 200 | 3–80 | eBE | c | | + | | | | | + | | | 70 (9 Å) 175 (12 Å) > 300 (17 Å) 440 (∞) | 0.13 (9 Å) 0.1 (12 Å) 0.96 (17 Å) 0.91 (∞) |
| | | 0.13 | 200 | 3–80 | eBE | c | | + | | | | | | + | | 150 (15 Å) 320 (∞) | 0.2 (9 Å) 0.66 (∞) |
| | | 0.05 | 200 | 3–60 | eBE | b | | + | | | | | | + | | 60 (18 Å) 162 (∞) | 0.17 (9 Å) 0.3 (∞) |
| | | 0.01 | 200 | 3–60 | eBE | b | | + | | | | | | + | | < T_c | |
| 2- Pb/Fe $_x$ Mo $_{1-x}$ | [30] | 0.0 | 200 | 3–80 | eBE | b | | + | | | | | + | | < T_c | | |
| | | 0.01 | 100–1200 | 300 | rfS | | + | | | 7.2 | | | | | 50–200 | | |
| 2- Pb/Gd $_x$ Pb $_{1-x}$ | [30] | 0.029 | 0–1000 | 5200 | rfS | | + | | 7.2 | | | | | No | | | |

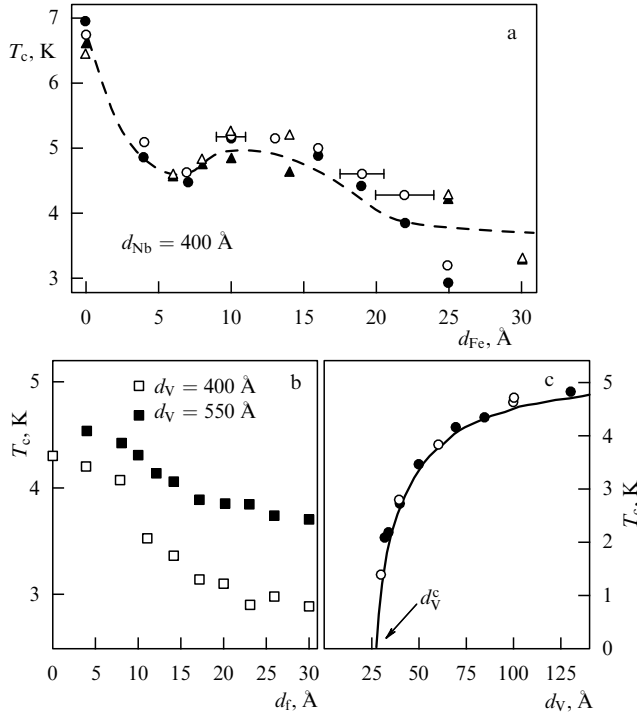


Figure 12. Experimental dependences of the critical temperature T_c on the thickness of the FM layer (d_f) and S layer (d_s). The various symbols correspond to different samples and measurement techniques. (a) Non-monotonic $T_c(d_f)$ dependence for the three-layer Fe/Nb/Fe system [42]; the dashed line was drawn by the authors of Ref. [42] as a guide for the eye. (b), (c) Two dependences for the Fe/V_{0.34}Fe_{0.66} superlattice [44]: (b) passage onto a plateau in the $T_c(d_f)$ dependence; (c) typical $T_c(d_s)$ dependence (solid line corresponds to a fit [44] based on the theory of Ref. [61, 62]).

parameters of the FM/S systems, both those listed in Tables 1 and 2 and omitted from them.

Because of the effect of various technological, metallurgical, and chemical factors that act upon the preparation of FM/S systems, the multilayer systems, even when having the same constituents can strongly differ in their properties. Following the review [29], we enumerate some of them:

- mutual diffusion and noticeable solubility, resulting in the appearance of an intermediate layer between the S and F metals and a deterioration of the boundary quality. In this sense, better properties are characteristic of the FM/S multilayers based on Nb and rare-earth F metals. The latter virtually do not mix with Nb; therefore, very pure Nb/FM junctions with a sharp boundary can be grown on their basis [40]. The same may be said of the boundary between Pb and Fe [30, 51, 56], in contrast to, e.g., systems based on Nb and Fe, which are well soluble in one another. The quality of the transition layer in such multilayer systems depends on the method of preparation [51];

- the appearance of an oxide interlayer and the problem of the irreversibility (dependence of the critical temperature T_c on the order in which the layers are sputtered);

- the possibility of an electrochemical reaction between the constituents of layered structures and the effects of annealing;

- the dependence of the critical temperature on the substrate material; the following materials were used: glass [30]; sapphire [30–32, 37, 46, 47]; silicon [39–41, 44, 48, 54, 55, 58, 59]; Al₂O₃ [42, 45, 50–52, 56, 57]; MgO [49]; quartz glass [30, 43].

In addition to the superconducting properties of the FM/S systems [i.e., the critical temperature T_c and parallel ($H_{c2\parallel}$) and perpendicular ($H_{c2\perp}$) upper critical fields], magnetic properties of the FM layers (such as the magnetization M and the Curie temperature T_m) were studied in much detail. To this end, magneto-optical Kerr effect (MOKE), ferromagnetic resonance (FMR), and SQUID magnetometry were employed. For example, it was found in Ref. [52] that the effective magnetization in the Fe layer decreases upon the transition of the Nb layer into the superconducting state (see also Ref. [100]). In Ref. [37], it was shown using the magneto-optical Kerr effect that in Nb/Gd/Nb trilayers the Curie temperature of the FM interlayer decreased on decreasing its thickness: it was 255 K at $d_f = 34 \text{ Å}$, 220 K at $d_f = 25 \text{ Å}$, 140 K at $d_f = 20 \text{ Å}$, and no ferromagnetic ordering was observed at $d_f \lesssim 15 \text{ Å}$. The existence of a critical thickness d_f^m of the FM layer was also observed in other FM/S systems (see Tables 1 and 2). In particular, it was shown in Ref. [36] for the V/FM systems that the magnetization M of FM layers decreases linearly with decreasing thickness d_f and vanishes at d_f^m .

Naturally, the above theory (Section 3) is applicable only to multilayer systems with $d_f > d_f^m$. Therefore, e.g., no sharp drop of the $T_c(d_f)$ curve of the type shown in Fig. 11d can be obtained in terms of this theory, since it is most frequently associated just with the transition of the FM layer to the ferromagnetic state at $d_f \approx d_f^m$ (see, e.g., the paper devoted to the Nb/Fe superlattice [49] and the corresponding drop at $d_{Fe}^m \approx 16 \text{ Å}$).

A contribution to the formation of the transition layer at the S/FM boundary also comes from the mismatch of the lattice parameters of the contacting metals (from 2 to 18%), depending on the mutual orientation of their crystallographic axes. As is shown by crystallographic investigations, this effect manifests itself over a distance of about 1–3 atomic planes (ap) on each side of the interface [36, 37, 47, 57]. In Ref. [44], the choice of the system Fe/V_{1-x}Fe_x is caused not only by the fact that it is convenient to trace the change in the magnitude of the effective magnetic moment per Fe atom depending on x (see Table 2), but also by the fact that these metals yield minimum disordering at the boundary, completely vanishing within two atomic planes on each side of the boundary, since the difference in the lattice parameters for these pure metals does not exceed 5%.

Measurements of the perpendicular and parallel critical magnetic fields give additional information on the coherence length in the system. Sufficiently thick FM interlayers cannot ensure coherent coupling of S layers (see discussion of Fig. 4). Over the entire temperature range, such FM/S samples behave as two-dimensional superconducting slabs with a well-known 2D temperature dependence of $H_{c2\parallel}$:

$$H_{c2\parallel}(T) = H_{c2\parallel}(0) \sqrt{1 - \frac{T}{T_c}}. \quad (4.1)$$

In this case, they say of a decoupled character of superconductivity. In systems with thinner FM layers, the superconductivity at $T \lesssim T_c$ has a coupled character: the S layers are coupled with one another, and the superlattice behaves as a massive superconductor, which is described by the 3D dependence of $H_{c2\parallel}$

$$H_{c2\parallel}(T) = H_{c2\parallel}(0) \left(1 - \frac{T}{T_c}\right). \quad (4.2)$$

It was in just this case that a 3D–2D crossover with respect to $H_{c2\parallel}(T)$ was observed with decreasing T/T_c in many works [31, 35, 39, 41, 42, 48, 57]. Note that the temperature dependence of $H_{c2\perp}$ mainly obeys the ‘three-dimensional’ relationship

$$H_{c2\perp}(T) = H_{c2\perp}(0) \left(1 - \frac{T}{T_c}\right). \quad (4.3)$$

The value of $H_{c2\perp}(0)$ found in experiments permits one to estimate the Ginzburg–Landau (GL) coherence length ξ_{GL} in terms of the Ginzburg–Landau theory:

$$\xi_{GL}(0) = \sqrt{\frac{\phi_0}{2\pi H_{c2\perp}(0)}} \quad (4.4)$$

(where ϕ_0 is the quantum of the magnetic flux) and find the important parameter of the proximity-effect theory, i.e., the coherence length ξ_s ,

$$\xi_s = \frac{2\xi_{GL}(0)}{\pi}. \quad (4.5)$$

On the other hand, ξ_s can be estimated from l_s found from the resistance of the S layers in the normal phase. In the dirty limit, this relation looks as follows:

$$\xi_s = \left(\frac{\hbar D_s}{2\pi k_B T_{cs}}\right)^{1/2} = \left(\frac{l_s \xi_{s0}}{3.4}\right)^{1/2}. \quad (4.6)$$

Note that an additional complexity in the interpretation of experimental results comes from the dependence of the parameters of even isolated film on its thickness. For example, it was shown in Ref. [58] that, as the thickness of Nb films changes from 560 to 1500 Å, the critical temperature T_{cs} changes from 5.8 to 8.5 K, remaining smaller than the critical temperature of the massive sample $T_c^{\text{bulk}} = 9.2$ K. Experiments on measurements of the resistance in such a system [57] show that as d_s changes from 100 to 460 Å, the coherence length ξ_s changes from 50 to 80 Å; close estimates follow from measurements of the critical field $H_{c2\parallel}$: $\xi_s = 57.7\text{--}66$ Å. At the same time, measurements of $H_{c2\perp}$ at $d_s = 400\text{--}460$ Å gave $\xi_s = 116\text{--}133$ Å. These data once more emphasize the degree of anisotropy of the system studied.

To conclude this section, we note works [54, 55] whose results have not been included in the tables. In these works, the role of a ferromagnet in the Nb/F superlattice was played by spin glass $\text{Cu}_{1-x}\text{Mn}_x$ (at $x = 0.7\text{--}4.5\%$ and 7.5%). In Ref. [55], $T_c(d_f)$ dependences of the type shown in Fig. 11a and curve 2 in Fig. 11c were observed.

4.2 Dependence of the critical temperature on the thickness of FM and S layers and other parameters of the theory

For the interpretation of experimental data on the $T_c(d_f)$ and $T_c(d_s)$ dependences, the Buzdin–Radović theory [61, 62] was mainly used (see, e.g., Refs [36, 37, 39, 40, 46, 48, 49, 51, 55–57]). Recall that the nonmonotonicity of $T_c(d_f)$ in this theory arises as a consequence of the competition between the superconductivities of 0 and π types, which takes place in superlattices. However, the nonmonotonicity was also observed experimentally in FM/S/FM trilayers, for which the π -phase superconductivity is impossible in principle. In addition, the values of the adjustable parameters often do not

agree with the known characteristics of the metals studied (see, e.g., Ref. [56]); therefore, below, we will use the more general formulas given in Section 3 for the description of experiments.

According to the theory developed in Section 3, the following parameters of the system should be specified: l_s/ξ_{s0} , the reduced mean free path in a dirty superconductor [or ξ_s/ξ_{s0} ; for the relation between them, see Eqn (4.6)]; σ_s , the transparency of the S/FM boundary [see also (3.9) and (3.14)]; the parameter $2I\tau_f (= l_f/a_f)$, which simultaneously takes into account the magnitude of the exchange splitting and the degree of contamination of the FM layer; the parameter $n_{sf} = v_s N_s/v_f N_f$ [see (3.14)]; and the characteristic spin-stiffness length a_f (see its definition in Section 2.3).

The investigation of changes in the behavior of the $t(d_f/a_f)$ curve under the effect of a change in only one parameter of the theory with other parameters being fixed was performed for the 1D theory of the proximity effect in Refs [64–67] and for the 3D version of the theory in Ref. [68]. Here, note only that the general rise in the $t(d_f/a_f)$ curve can be due to an *increase* in one of the following parameters: n_{sf} , d_s , or $2I\tau_f$ (the latter, in the case of $2I\tau_f > 1$). A similar effect is observed upon a *decrease* in one of the following parameters: σ_s , l_s (or ξ_s), or $2I\tau_f$ (the latter, if $2I\tau_f < 1$). A successive changeover of virtually all types of the $t(d_f/a_f)$ dependences can be observed, i.e., from that shown in Fig. 11a to that given in Fig. 11f. Recall that the existence of an additional degree of freedom in the 3D version of the theory ($q_f \neq 0$) also leads to a general rise in the curve and to smoothing of the oscillations (only the first local maximum is retained).

The various $t(d_f)$ dependences at reasonable values of the parameters of the theory are given in Figs 3, 5, and 7–10. The corresponding $q_f(d_f)$ curves for the 3D version of the theory are given in Figs 5 and 10. As was noted in Section 3, the shape of the curves is very sensitive to the magnitudes of the parameters of the theory and the relationships between them. Note that the regions of existence of reentrant superconductivity predicted for the 1D case [64–66] are restricted in the 3D theory to a very narrow range of parameters. Thus, virtually all the various types of experimental dependences are qualitatively reproduced by the theory suggested.

When comparing theoretical and experimental $T_c(d_{f(s)})$ dependences, many parameters are, as a rule, either given (d_s or d_f , ξ_{s0} , T_{cs}) or can be found from independent measurements (ξ_s , l_s , n_{sf} , $2I\tau_f$), or, finally, can be determined using a fitting procedure. The parameter n_{sf} is determined by the band structure of the contacting metals and cannot take on arbitrary values; however, estimates of it lead to a sufficiently wide scatter in values. On the one hand, we can roughly estimate this parameter within the simple model of nearly free electrons [89]; according to this model, $n_{sf} \approx v_s^2/v_f^2$, and this ratio can be calculated for S/FM pairs used in known experiments. Then, in this simple model, the value of n_{sf} lies between 0.73 (Nb/Co) and 1.36 (V/Gd); therefore, we used the value $n_{sf} \sim 1$ when constructing phase diagrams in Section 3. On the other hand [30, 89], when estimating the ratio of the density of states at the Fermi surface N_s/N_f , we can use the ratio γ_s/γ_f of the (known from experiment) coefficients of electron heat capacities in the normal phase. The ratio of the Fermi velocities v_s/v_f for real metals can be obtained from experiments or (and) from band structure calculations (see, e.g., Refs [105–108]). In this model, the value of n_{sf} lies between 0.18 (Pb/Fe) to 10.4 (Nb/Gd). Such a wide scatter in values tells us that this parameter can be used

as an adjustable one. The boundary transparency σ_s and the parameter $2l\tau_f$, which can vary between very wide limits, also should be used as adjustable parameters. As we saw above, the quality of the S/FM boundary and the presence of the transition layer depend not only on the nature of the contacting metals but also on the technique of the preparation of multilayers.

If we say of the $t(d_s)$ dependence, we should note the importance of the critical value of the S-layer thickness d_s^c . At given d_f and $d_s < d_s^c$, no superconductivity arises in the FM/S system. The critical thickness d_f^c of the FM layer can be determined as a thickness at which the superconductivity is destroyed at a given d_s . Our analysis shows that the $d_s^c(d_f)$ dependence may be strongly nonmonotonic, representing a nearly mirror reflection of the $t(d_f)$ dependence: the minimum in t corresponds to the maximum of d_s^c and *vice versa*. This is sufficiently evident: at a fixed d_f , the FM/S system with thicker S layers has a greater reduced temperature t .

At finite d_s and d_f , the critical thicknesses d_s^c and d_f^c of a two-layer FM/S contact at $2l\tau_f < 1$ are linked by a transcendental equation such as Eqn (3.18) [or (3.26)]:

$$D_s k_s^c \tan k_s^c d_s^c = \sigma_s v_s \left[4 - \frac{\sigma_s v_f n_{sf} \cot k_f d_f^c}{D_f(I) k_f} \right]^{-1}. \quad (4.7)$$

Here, the complex wave vector k_s^c can be found from Eqn (3.17) [or (3.25)] under the condition that $t \rightarrow 0$, which yields the expression

$$|k_s^c|^2 = \frac{1}{2\gamma \xi_s^2}, \quad (4.8)$$

where k_f is specified by the known equation (3.19), and $\gamma = 1.781$ is the Euler constant.

Note that for finite d_f , we cannot use the estimates of the parameters σ_s and n_{sf} that follows from expression (4.7) as $d_f \rightarrow \infty$ (see discussion of Fig. 14).

4.3 Comparison of the theory and experiment

As was noted in Section 3.4, to analyze the behavior of the $T_c(d_f)$ function in the region of S-layer thicknesses $d_s > d_s^\pi$, where the FM/S superlattice is magnetically quasi-two-dimensional, it is sufficient to use simpler 00 and $\pi 0$ solutions of the 3D proximity-effect theory [68, 69] that does not take into account π magnetic states (0π and $\pi\pi$ AFS states). The thing is that the overwhelming majority of available experiments on FM/S multilayers were performed at thicknesses $d_s \gg d_s^\pi$, in which case the AFS states have a slightly smaller critical temperature than the FS states have. Of special interest, from the viewpoint of the comparison of the theory with experiment, are the nonmonotonic $T_c(d_f)$ dependences that permit us to obtain the maximum information on the FM/S structures under study.

Gd/Nb superlattice. In Figure 13, the theoretical results obtained in preceding sections are compared with the experimental behavior of $T_c(d_f)$ for the Gd/Nb superlattice [40]. It is seen in the figure that the dependence shown corresponds to curve 1 in Fig. 11c, i.e., to the 3D theory with $2l\tau_f > 1$.

In Figure 13a, the $T_c(d_f)$ dependence [109] was fitted for samples with thicker Nb layers ($d_{Nb} = 600 \text{ \AA}$) and only two parameters were varied, namely, $2l\tau_f$ and σ_s . The spin-stiffness length a_f was determined from the position of the

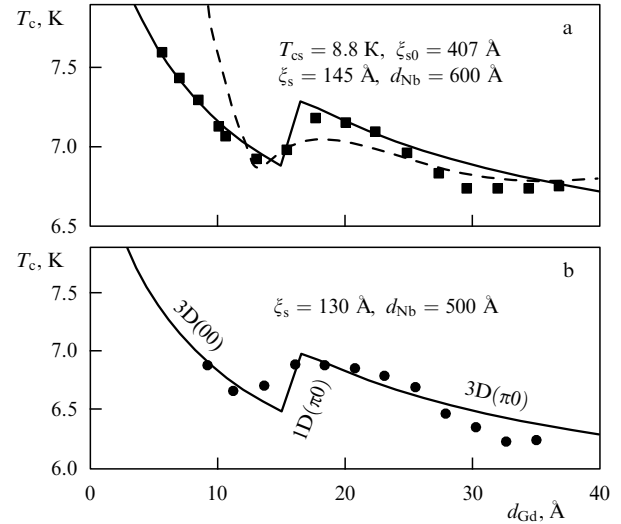


Figure 13. Fitting of the 3D theory of the proximity effect [68, 69] to experimental data on the Gd/Nb superlattice [40]. The known experimental values are given above the curves. The dashed line in Fig. 13a represents the best result of fitting using the theory of Refs [61, 62]. The parameters of the theoretical curve (solid line) are as follows: $2l\tau_f = 5.60$, $\sigma_s = 0.527$, $n_{sf} = 1.15$, $a_f = 5.34 \text{ \AA}$.

maximum ($a_f \approx d_f^{\max}/\pi$ for $2l\tau_f > 1$), and the parameter n_{sf} was estimated within the model of free electrons. The parameters of the curve are given in the figure.

The theoretical curve in Fig. 13b for the superlattice with thinner Nb layers was obtained by simply substituting these parameters and experimental values $d_{Nb} = 500 \text{ \AA}$ and $\xi_s = 130 \text{ \AA}$ into the formulas (3.23)–(3.25) with allowance for the π -phase superconducting states that can arise in the superlattice (see Section 3.4). In this case, the asymptotic theoretical value corresponding to the passage of $T_c(d_f \rightarrow \infty)$ onto a plateau coincided with the value of the critical temperature known from experiment, i.e., $T_c = 6.1 \text{ K}$.

We emphasize that, using the Buzdin–Radović theory [61, 62], Jiang et al. [40] obtained only a partial qualitative agreement with experimental data (see the dashed line in Fig. 13a), and for samples with $d_{Nb} = 500 \text{ \AA}$, in which the position of the local minimum of T_c proved to be higher than the asymptotic value (Fig. 13b), the Buzdin–Radović theory [61, 62] cannot give even a qualitatively satisfactory description.

It is seen from Fig. 13 that the description of the nonmonotonic $T_c(d_f)$ dependence in the Gd/Nb superlattice in terms of the 3D(00)–1D($\pi 0$)–3D($\pi 0$) cascade of phase transitions through Lifshitz triple points (in which the 2D momentum of pairs $q_f \rightarrow 0$) yields quite satisfactory agreement with experiments [40]. In addition, in contrast to the Buzdin–Radović theory [61, 62], our approach makes it possible to obtain realistic data on the transparency coefficient σ_s of the S/FM interface and the parameter $2l\tau_f = l_f/a_f$ that is responsible for the relationship between the diffusion and wave modes of motion of quasi-particles in the strong exchange field of ferromagnetic layers.

Fe/Pb/Fe trilayers. Experimental $T_c(d_f)$ and $T_c(d_s)$ dependences for the Fe/Pb/Fe trilayer were obtained in Ref. [56]. Here, we give the results of fitting our 1D and 3D theories of the proximity effect to these data.

Figure 14a presents the $T_c(d_f)$ dependences. Two theoretical curves are reproduced according to Ref. [56]. These are

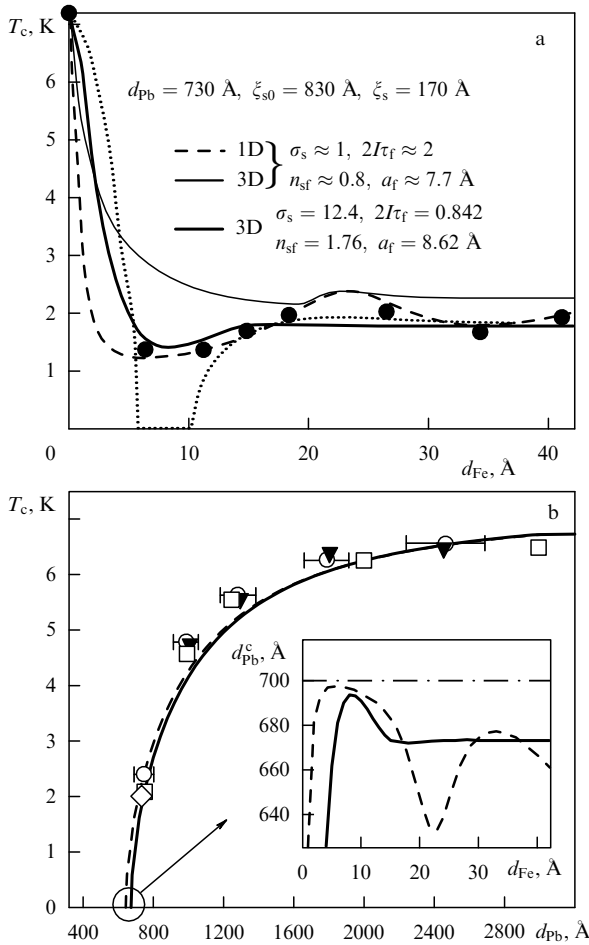


Figure 14. Fitting of the theory to experimental data for the three-layered Fe/Pb/Fe system [56] (different symbols correspond to different samples and measurement methods). The two fits are taken from Ref. [56]: the dashed line, the theory of Refs [61, 62]; and the dotted line, the 1D theory. The curve calculated using the 3D theory (at the values of the parameters used for the latter fit) is shown by the thin solid line. Fitting using the 3D theory [68, 69] is given by the thick solid line. The fitting parameters and the known experimental values are given in Fig. 14a. (a) $T_c(d_f)$ dependence; (b) $T_c(d_s)$. In the inset, the critical thickness of the S layer d_s^c is given as a function of the thickness d_f of the FM layer (see discussion in the main text).

the results of fitting using the Buzdin – Radović theory [61, 62] (thin dotted line) and the 1D theory (dashed line). The parameters of the latter are given in the figure.

The thin solid line lying above the experimental points represents the result of the solution to the equations of the 3D theory for the same parameters that were found in Ref. [56] for the 1D case. This means that the parameters found as a result of fitting of the 1D theory [56] are not suitable when 3D LOFF states are realized in this system.

In our opinion, the experimental points in this figure fall onto a dependence of the ‘passage onto a plateau through a minimum’ type (curve 2 in Fig. 11c) rather than onto an oscillatory dependence. As we saw when analyzing the types of the $T_c(d_f)$ dependences, this corresponds to the 3D theory of the proximity effect with $2I\tau_f < 1$. The thick solid line in Fig. 14a just represents the result of fitting of the 3D theory with corresponding parameters. It is seen from the comparison of the parameters of fitting for the 1D and 3D versions of the theory that the greatest differences are observed for the

values of the transparency σ_s , which questions the conclusion of the authors of Ref. [56] on the low transparency of the Fe/Pb boundary.

Figure 14b shows the dependences of the critical temperature of the trilayer on the thickness of the Pb interlayer at $d_{Fe} = 30$ Å. The dependences were calculated for the same values of the parameters that are shown in Fig. 14a. It is seen from the figure that both the 1D and 3D theories satisfactorily agree with the experimental points.

The inset in Fig. 14b depicts the dependence of the critical thickness of the Pb layer d_s^c on the thickness of the Fe layer d_{Fe} calculated by the general formulas (4.7) and (4.8). The horizontal dash-dot line in the inset corresponds to the approximation $d_f \rightarrow \infty$ used in Ref. [56] to obtain the relationship between σ_s and n_{sf} [in contrast to (4.8), the wave vector k_s^c was assumed to be purely real]. It is seen from Fig. 14a and the inset in Fig. 14b that the obtained nonmonotonicity of $d_s^c(d_f)$ is an almost mirror reflection of the nonmonotonicity of $T_c(d_f)$.

General conclusions. It is seen from the above tables that a large number of FM/S systems with various combinations of FM and S metals, which formed various n -layered structures, have been investigated experimentally. In the majority of works, the dependences of the critical temperature on the thickness of FM and S interlayers were studied. The type of the $T_c(d_f)$ dependence is determined not only by the nature of the contacting metals but also, to a significant extent, by the technique of fabrication of FM/S structures. This indicates the extreme importance of taking into account, in the theory developed, the finite transparency of the S/FM boundary (parameter σ_s), along with parameter $2I\tau_f$, for the description of various forms of the $T_c(d_f)$ dependence in layered FM/S systems.

The 3D theory of the proximity effect yields virtually all types of $T_c(d_f)$ behavior observed experimentally. Above, we compared the theory with experiment for Gd/Nb and Fe/Pb/Fe structures. Analogous agreement of the results of fitting in the 3D theory was also obtained for other sets of experimental data: for the dependences with a monotonic passage onto a plateau (see the curve given in Fig. 11b) for the V/Fe_{0.66}V_{0.34} superlattices [44]; for the dependences with a monotonic decrease to zero (Fig. 11a); for the dependence with a single local maximum (curve 1 in Fig. 11c) for Fe/Nb/Fe trilayers; for the dependence with a single falloff of the curve (Fig. 11d) but only for the ferromagnetic region of thicknesses $d_{Fe} > d_f^m$ for Fe/Nb superlattices [49] (these figures are not given here).

At present, the oscillatory dependences with two minima (such as the curve in Fig. 11e), obtained for the V/Co [53] and Nb/Co [53, 59] superlattices, cannot be explained by the competition between 3D and 1D states. The presence of such dependences characteristic of the 1D version of the theory (Fig. 9c) for the S/Co superlattices indicates that a one-dimensional LOFF lattice with $q_f = 0$ is realized in Co layers (see Section 3.3), apparently because of the anisotropy of these layers.

All the results of this paper were obtained on the assumption of a sharp (on the atomic level) FM/S boundary, with a ferromagnetic ordering even in very thin F layers. It is obvious that in realistic FM/S systems used in experiments the situation is much more complicated. Sometimes, because of the mutual solubility of the FM and S metals, but sometimes for purely technological reasons, the FM/S boundary turns out to be diffuse; therefore, the thin

layers of ferromagnet can become paramagnetic or even nonmagnetic. In principle, the FM/S model investigated can easily be extended for a case including a thin nonmagnetic interlayer between the FM and S layers or a case where a paramagnet–ferromagnet transition occurs after the FM-layer thickness reaches a certain critical value. Physically, it is, however, clear that if the penetration depth is substantially greater than the typical thickness of nonferromagnetic interlayers $d_1^m \approx 5-12 \text{ \AA}$, then the oscillations of the flux of Cooper pairs through such a diffuse S/FM boundary will be retained. The effect of buffer interlayers at sufficiently large thicknesses of FM layers can roughly be taken into account using the simple renormalization of the exchange field I or the constant of electron-electron interaction λ_s .

In Refs [103, 104], when considering the boundary-value problem for an FM/S contact, the authors took into account the spin–orbit coupling (see also Ref. [66]). This coupling leads to the appearance in the Usadel equation for a ferromagnetic metal of an additional term $\sim (1/\tau_{so})F_T(z, \omega)$, where τ_{so} is the electron relaxation time due to the spin–orbit coupling. Numerical analysis shows that all features in the critical temperature T_c of the junction become smooth as $1/\tau_{so}$ grows. This fact should be taken into account when interpreting experimental results.

In many experimental works, various dependences of H_{c2} were investigated. Of special interest is the 2D–3D crossover observed in the temperature dependence of $H_{c2\parallel}$. The dependence of the crossover occurrence on the thickness of the FM layer was investigated in Ref. [110] based on another variant of the proximity-effect theory developed in Ref. [111]. As was shown in Ref. [112], this approach is equivalent to the Buzdin–Radović theory [61, 62]. The theory that was suggested in this paper in Section 3 can also be extended to the case of the presence of an external magnetic field.

5. Theory of FI/S systems consisting of layers of a ferromagnetic insulator and a superconductor

5.1 Indirect exchange of localized spins in a dirty superconductor

In contrast to the above-considered FM/S systems, the superconducting layers in FI/S systems do not interact with one another, if the separating layers of the ferromagnetic insulator are sufficiently thick to neglect electron tunneling through them. At the same time, the localized spins of surface atomic layers of the ferromagnet interact with one another via the conduction electrons of the superconducting metal. This indirect interaction of the RKKY type provides coupling between various ferromagnetic layers. Since this long-range interaction has an antiferromagnetic character, the ferromagnetic orientation of the magnetic moments of one FI layer can be distorted by the RKKY interaction, which finally can result in a cryptoferrimagnetic state at a sufficiently strong indirect interaction as compared to the direct exchange interaction in FI layers.

At the same time, there is an inverse influence of the magnetic order on superconductivity due to the pair-breaking paramagnetic effect in the subsurface layer. Since electrons do not penetrate deep into the FI layer, only the monoatomic surface layer of the ferromagnet is involved and the related effect should not depend on the thickness of the FI layer, in contrast to the FM/S systems. Below, we will study the

mutual influence of ferromagnetism and superconductivity in FI/S junctions and FI/S superlattices, but first we will discuss the problem of RKKY interaction in superconductors [80, 78, 87].

The dependence of the RKKY exchange integral on the distance between the localized spins \mathbf{S}_i and \mathbf{S}_j is determined by the spatial dispersion of the spin susceptibility of conduction electrons $\chi(\mathbf{r}, \mathbf{r}')$. The Hamiltonian of indirect exchange has the form

$$H_{\text{ex}} = -\frac{1}{8} J_{\text{sd}}^2 \sum_{ij} \chi(\mathbf{r}_i, \mathbf{r}_j) \mathbf{S}_i \cdot \mathbf{S}_j, \quad (5.1)$$

where J_{sd} is the sd exchange integral. In the normal phase, the spatial dependence of the susceptibility $\chi_n(\mathbf{r}, \mathbf{r}')$ has the form of Friedel oscillations, and the integral over the entire space from this susceptibility yields the uniform Pauli susceptibility.

It was shown in Ref. [80] that in a dirty superconductor the spin polarization $\chi_n(\mathbf{r}, \mathbf{r}')$ corresponding to the normal phase is compensated by a long-range additional term of antiferromagnetic sign. This additional contribution to the RKKY exchange arises as a consequence of exclusion of the contribution of paired electrons from the uniform spin polarization. A superconducting contribution to the susceptibility, $\delta\chi_s(\mathbf{r}, \mathbf{r}')$, can be written as

$$\delta\chi_s(\mathbf{r}, \mathbf{r}') = \chi(\mathbf{r}, \mathbf{r}') - \chi_n(\mathbf{r}, \mathbf{r}') = -2T \sum_{\omega} A_s(\mathbf{r}, \mathbf{r}', \omega). \quad (5.2)$$

For an infinite dirty superconductor, the two-particle correlator in the hydrodynamic limit, i.e., at distances $R = |\mathbf{r} - \mathbf{r}'|$ exceeding the mean free path l , is described by the expression [78, 80, 87]

$$A_s(\mathbf{r}, \mathbf{r}', \omega) = \frac{N(0)A^2}{2D_s R(\omega^2 + A^2)} \exp\left(-\frac{R}{\xi_{\omega}}\right), \quad (5.3)$$

$$\xi_{\omega} = \sqrt{\frac{D_s}{2(\omega^2 + A^2)^{1/2}}},$$

where ξ_{ω} is the range of the correlator $A_s(\mathbf{r}, \mathbf{r}', \omega)$, which depends on the frequency ω . Since the uniform spin polarization in the superconductor should vanish at $T = 0$, the sum rule for $A_s(\mathbf{r}, \mathbf{r}', \omega)$ should be satisfied. In the case of a uniform superconductor with a coordinate-independent OP A and density of states $N(0)$, this sum rule has the form

$$\int d\mathbf{r}' A_s(\mathbf{r}, \mathbf{r}', \omega) = \pi N(0) \frac{A^2}{(\omega^2 + A^2)^{3/2}}. \quad (5.4)$$

Note that Eqn (5.4) is a fundamental relation and can be derived in a general way, e.g., by analogy with the derivation of the sum rule for the kernel of the Gor'kov equation suggested by de Gennes [26].

To find the long-range part of the RKKY exchange in the case of superconductors restricted in space by the surface σ , it is convenient to represent $A_s(\mathbf{r}, \mathbf{r}', \omega)$ as a solution to the boundary-value problem. Using Fourier analysis, it can easily be shown that expression (5.3) is the solution to the differential equation of diffusion type

$$\begin{aligned} & \left(2\sqrt{\omega^2 + A^2} - D_s \nabla_{\mathbf{r}}^2\right) A_s(\mathbf{r}, \mathbf{r}', \omega) \\ & = 2\pi N(0) \frac{A^2}{\omega^2 + A^2} \delta(\mathbf{r} - \mathbf{r}'). \end{aligned} \quad (5.5)$$

The boundary conditions for this equation can be found by integrating (5.5) with respect to $d\mathbf{r}$ using the sum rule (5.4) and can be written in the form

$$D_s \mathbf{n} \nabla_{\mathbf{r}} A_s(\mathbf{r}, \mathbf{r}', \omega) \Big|_{\sigma} = 0, \quad (5.6)$$

where \mathbf{n} is the normal to the superconductor–vacuum (insulator) interface. Physically, Eqn (5.6) corresponds to the absence of a flux of Cooper pairs through the superconductor surface.

Solving Eqn (5.5) simultaneously with (5.6) on the assumption that the density of states $N(0)$ and the parameter Δ are constant and vanish jumpwise only at the surface of the superconductor σ , we can obtain the coordinate dependence of the correlator $A_s(\mathbf{r}, \mathbf{r}', \omega)$ for all practically interesting geometries. Here, we consider a superconducting half-space and a superconducting slab.

In the case of the superconducting half-space $z, z' \geq 0$, we have [78, 87]

$$A_s(\mathbf{r}, \mathbf{r}', \omega) = \frac{\pi N(0) \Delta^2}{\omega^2 + \Delta^2} \int \frac{d\mathbf{q}_{\perp}}{(2\pi)^2} \frac{\exp[i\mathbf{q}_{\perp}(\boldsymbol{\rho} - \boldsymbol{\rho}')] }{D_s k} \times \{ \exp[-k|z - z'|] + \exp[-k(z + z')] \}, \quad (5.7)$$

where $k^2 = \mathbf{q}_{\perp}^2 + \xi_{\omega}^{-2}$, and $\mathbf{q}_{\perp} = q_x \mathbf{i} + q_y \mathbf{j}$; $\boldsymbol{\rho} = x \mathbf{i} + y \mathbf{j}$. Note that a pair of spins on the surface of the superconductor ($z = z' = 0$) interacts twice as strongly as in the bulk at $z = z' > \xi$, where formula (5.3) is valid for $A_s(\mathbf{r}, \mathbf{r}', \omega)$. Thus, the elastic reflection of Cooper pairs from the surface of the superconductor leads to a kind of constructive interference, which occurs because of the increase in the effective time of pair correlations near the boundary.

For a superconducting slab of thickness d_s , i.e., when $0 \leq z, z' \leq d_s$ (with $d_s \gg l$), we obtain [78, 87]

$$A_s(\mathbf{r}, \mathbf{r}', \omega) = \frac{2\pi N(0) \Delta^2}{\omega^2 + \Delta^2} \int \frac{d\mathbf{q}_{\perp}}{(2\pi)^2} \frac{\exp[i\mathbf{q}_{\perp}(\boldsymbol{\rho} - \boldsymbol{\rho}')] }{D_s k \sinh kd_s} \times \cosh(kz) \cosh[k(z' - d_s)] \quad (5.8)$$

at $z < z'$. If, on the contrary, $z > z'$, the places of these variables in Eqn (5.8) should be reversed. It can easily be shown that in the case of a massive slab ($d_s > \xi$), the antiferromagnetic coupling between localized spins at either surface will be twice as strong as that in the bulk. As $d_s \rightarrow \infty$, we obtain expression (5.7) for the half-space from Eqn (5.8). However, result (5.8) is most vividly illustrated by a quasi-two-dimensional situation, when the film thickness d_s is much smaller than the coherence length ξ . In this case, the interaction between the localized spins is virtually independent of the variables z and z' and is determined only by the projection of the radius vector \mathbf{R} onto the plane $z = 0$, i.e., by the magnitude of $R_{\perp} = |\boldsymbol{\rho} - \boldsymbol{\rho}'|$:

$$A_s(\mathbf{r}, \mathbf{r}', \omega) = \frac{N(0) \Delta^2}{D_s d_s (\omega^2 + \Delta^2)} K_0 \left(\frac{R_{\perp}}{\xi_{\omega}} \right). \quad (5.9)$$

In this case, as follows from the MacDonald function asymptotes

$$K_0 \left(\frac{R_{\perp}}{\xi_{\omega}} \right) \sim \ln \frac{\xi_{\omega}}{R_{\perp}}, \quad R_{\perp} < \xi_{\omega},$$

$$K_0 \left(\frac{R_{\perp}}{\xi_{\omega}} \right) \sim \left(\frac{\xi_{\omega}}{R_{\perp}} \right)^{1/2} \exp \left(- \frac{R_{\perp}}{\xi_{\omega}} \right), \quad R_{\perp} > \xi_{\omega},$$

a power-type fall-off of the RKKY potential with increasing spacing between the localized spins becomes slow as compared to the three-dimensional case (5.3), and their antiferromagnetic correlations over distances $R_{\perp} \leq \xi$ become stronger.

Thus, the antiferromagnetic correlations between localized spins, induced by the transition of the metal to the superconducting state, become stronger on approaching the surface of the massive dirty superconductor or with decreasing the dimensionality of the sample. It can be shown by direct integration that all the results obtained satisfy the sum rule (5.4), which ensures the vanishing of the uniform spin susceptibility $\chi_s(0)$ of the superconductor at $T = 0$. Further, we investigate the interaction of the magnetic and superconducting states in FI/S junctions and FI/S superlattices.

5.2 FI/S multilayers at zero temperature.

Ground states

FI/S junctions. We first consider a planar junction consisting of a thin ferromagnetic film occupying the region $-d_f < z < 0$ with a superconducting slab occupying the region $0 < z < d_s$. The subsystems of localized spins of the FI film and conduction electrons of the S layer, which are coupled with one another via the FI/S boundary can be described by the Hamiltonian

$$H = H_F + H_S + H_{FS}, \quad (5.10)$$

consisting of the Hamiltonians of the ferromagnet H_F , superconductor H_S , and interaction H_{FS} . Here,

$$H_F = -J \sum_{i,j} \mathbf{S}_i \mathbf{S}_j + K \sum_j (S_j^z)^2 \quad (5.11)$$

describes the direct exchange of neighboring spins of the FI layer with allowance for the in-basal-plane anisotropy ($K > 0$), H_S is the superconductor Hamiltonian of the BCS model, and H_{FS} is the Hamiltonian of the sd exchange interaction of localized spins with conduction electrons of the superconductor,

$$H_{FS} = \frac{J_{sd}}{2} \sum'_{j,\alpha,\beta} \psi_{\alpha}^{+}(j) (\mathbf{S}_j \cdot \boldsymbol{\sigma}_{\alpha\beta}) \psi_{\beta}(j), \quad (5.12)$$

where the prime at the sum over j means that summing is performed only over localized spins located directly at the boundary. The interaction H_{FS} leads, on the one hand, to splitting of the states of conduction electrons in the S layer by the exchange field of the localized spins of the FI/S boundary and, on the other hand, to the indirect exchange of the same localized spins via electrons of the superconducting layer.

For certainty, we assume that the Curie temperature T_m is above T_c and that at $T_c < T < T_m$ the ferromagnetism of the surface of the FI film is not disturbed by oscillations of the normal part of the RKKY interaction. The latter assumption means that the direct exchange at distances of about nearest-neighbor spacings is stronger than the indirect exchange, i.e., $J > N(0) J_{sd}^2$. In fact, this implies that we can neglect the contribution of the oscillating part, retaining only the short-range ferromagnetic and long-range antiferromagnetic parts of the exchange interaction, which are most important in the problem under consideration. We assume that the FI layers are so thin that the surface distortions of magnetic order due to the proximity of the S layers will be transferred over the entire thickness of the FI layer via the strong direct exchange.

Averaging Hamiltonian (5.10) over electron and spin variables in the spirit of Ref. [7] and specifying the magnetic order in the FI film in the form

$$\langle S_j^\pm \rangle = \langle S_j^x \pm iS_j^y \rangle = S \exp(\pm i\mathbf{q}_\perp \cdot \boldsymbol{\rho}), \quad \langle S_j^z \rangle = 0, \quad (5.13)$$

where $\mathbf{q}_\perp = q_x \mathbf{i} + q_y \mathbf{j}$, we obtain the following functional for the surface density of free energy of the FI/S junction at $T = 0$ [78]:

$$f = f_F^0 + f_N^0 + JS^2 q_\perp^2 \frac{d_f}{a} - I(\mathbf{q}_\perp, 0, 0) \frac{S^2}{a^2} - \frac{d_s N(0)}{2a^3} \Delta^2 \ln \frac{e\Delta_0^2}{\Delta^2}, \quad (5.14)$$

where f_F^0 and f_N^0 are the free energies per unit junction area for the FI film and S layer in the normal phase, respectively. The third term describes the loss in the energy of the direct exchange because of the long-wavelength ($q_\perp a \ll 1$) modulation of the ferromagnetic order. The fourth term is the two-dimensional Fourier transform of the superconducting contribution $\delta\chi_s(\boldsymbol{\rho} - \boldsymbol{\rho}', z, z')$ to the RKKY potential, which is found by the substitution of Eqn (5.8) into Eqn (5.2), i.e.,

$$I(\mathbf{q}_\perp, z, z') = -\frac{a}{2} N(0) J_{sd}^2 \pi T \times \sum_{\omega} \frac{\Delta^2}{\omega^2 + \Delta^2} \frac{\cosh(kz) \cosh[k(z' - d_s)]}{D_s k \sinh kd_s}. \quad (5.15)$$

The term that is proportional to $I(\mathbf{q}_\perp, 0, 0)$ in Eqn (5.14) plays a double role. On the one hand, it describes long-range magnetic correlations of the near-boundary ($z = z' = 0$) localized spins via Cooper pairs of the superconductor; on the other hand, it takes into account the suppression of the order parameter Δ due to the paramagnetic effect. Finally, the last term in Eqn (5.14) describes the gain in the energy of condensation (see Ref. [23]) related to the transition of the S layer to the superconducting state. Here, $\Delta_0 = 1.76T_{cs}$, and we neglect the difference in the lattice parameters of the FI and S layers ($a_f = a_s = a$).

In terms of the model (5.14), we investigate the mutual accommodation of superconductivity and ferromagnetism in the FI/S junction at $T = 0$. To find the magnetic configuration corresponding to minimum free energy (5.14), we should know the behavior of the quantity (5.15) as a function of q_\perp at $z = z' = 0$. After summing over the frequency ω , the low-temperature ($\pi T \ll \Delta$) asymptotics of $I(\mathbf{q}_\perp, 0, 0)$ for various ranges of q_\perp can be written in the form

$$\begin{cases} I(\mathbf{q}_\perp, 0, 0) = -\frac{a}{4d_s} N(0) J_{sd}^2 \times \left(1 + \frac{\pi d_s^2}{6\xi_s^2} - \frac{\pi}{4} q_\perp^2 \xi_s^2 + \frac{2}{3} q_\perp^4 \xi_s^4 + \dots \right), & q_\perp < \frac{1}{\xi_s}, \\ I(\mathbf{q}_\perp, 0, 0) = -\frac{\pi}{d_s} N(0) J_{sd}^2 (q_\perp^2 \xi_s)^{-2}, & \xi_s^{-1} < q_\perp < d_s^{-1}, \\ I(\mathbf{q}_\perp, 0, 0) = -\frac{\pi}{\xi_s} N(0) J_{sd}^2 (q_\perp^2 \xi_s)^{-1}, & d_s^{-1} < q_\perp < l_s^{-1}, \end{cases} \quad (5.16)$$

where $\xi_s = \sqrt{D_s/2\Delta}$ is the coherence length of the superconductor.

The minimization of functional (5.14) with respect to Δ and q_\perp using the first of the expressions (5.16) for $I(\mathbf{q}_\perp, 0, 0)$ at $q_\perp \xi < 1$ leads to the presence of three different ground states or phases of the FI/S contact, whose realization depends on

the magnitudes of the parameters A and h (see Ref. [78]):

$$A = \frac{N(0)h^2 \pi \xi_s^2 d_s}{JS^2 4a^2 d_f}, \quad h = \frac{SJ_{sd}}{2} \frac{a}{d_s}. \quad (5.17)$$

The parameter A has the sense of the ratio of the absolute values of the antiferromagnetic and ferromagnetic molecular fields (per each localized spin of the FI/S boundary) corresponding to the RKKY exchange via the superconducting electrons of the S layer and via the direct exchange in the FI layer, respectively. The quantity h is the average exchange field acting on the conduction electrons from the localized spins of the FI/S boundary.

If $A < 1$, the ferromagnetic ordering is stable with respect to the long-wavelength modulation (a tendency to such a modulation arises due to the RKKY exchange). If the exchange field h is not too large, the superconductivity in the S layer arises against the background of ferromagnetism in the FI film, and they coexist (FS phase). In the FS phase, the equilibrium values of the order parameter Δ and of the wave vector of the magnetic structure Q_\perp are determined by the expressions

$$\Delta^2 \ln \frac{\Delta_0}{\Delta} = \frac{\pi h^2}{12} \left(\frac{d_s}{\xi_s} \right)^2, \quad Q_\perp = 0. \quad (5.18)$$

The surface density of the free energy in this phase is equal to

$$f_{FS} = f_F^0 + f_N^0 - \frac{d_s N(0)}{2a^3} \left[\Delta^2 - 2h^2 \left(1 + \frac{\pi d_s^2}{12\xi_s^2} \right) \right]. \quad (5.19)$$

At $A > 1$, the ferromagnetic ordering is unstable with respect to the long-wavelength modulation, and the minimum of the free energy (5.14) is now associated with the cryptoferrimagnetic superconducting phase (CFS), whose parameters Δ and Q_\perp are determined from the self-consistent conditions of equilibrium:

$$\begin{aligned} \Delta^2 \ln \frac{\Delta_0}{\Delta} &= \frac{\pi h^2}{4} \left[\frac{d_s^2}{3\xi_s^2} + \frac{(Q_\perp \xi_s)^2}{2A} \right], \\ Q_\perp &= \left[\frac{3\pi}{16} \left(1 - \frac{1}{A} \right) \right]^{1/2} \xi_s^{-1}. \end{aligned} \quad (5.20)$$

The density of the free energy in the CFS phase is determined as follows:

$$f_{CFS} = f_F^0 + f_N^0 - \frac{d_s N(0)}{2a^3} \left[\Delta^2 - 2h^2 \left(1 + \frac{\pi d_s^2}{12\xi_s^2} - \frac{\pi}{8} Q_\perp^2 \xi_s^2 \right) \right]. \quad (5.21)$$

It follows from a comparison of the free energies (5.19) and (5.21) that the transition from one ground state, FS, into another ground state, CFS, occurs at $A = 1$ and is accompanied by a mutual adjustment of the superconducting and magnetic order parameters. In this case, the vicinity $A - 1 \ll A$ of the transition point corresponds to a large-scale sinusoidal modulation of the magnetic order of localized spins in the FI film. This modulation leads, on the one hand, to a partial compensation of the paramagnetic effect and, on the other hand, to a minimum loss in the energy of the direct exchange, since $Q_\perp^{-1} \gg \xi_s \gg a$.

On increasing the exchange field h , when the energy gain connected with the energy of condensation is compensated by the paramagnetic effect and by the loss in the energy of direct exchange, the FI/S junction passes into a ferromagnetic

normal state FN with $\Delta = 0$, $Q_{\perp} = 0$, and free energy $f_{\text{FN}} = f_{\text{F}}^0 + f_{\text{N}}^0$, and this transition can occur both from the CFS and FS phase.

It follows from the above low-temperature analysis that with an increase in the exchange field h and the corresponding increase in the balance of the molecular fields A , the FI/S junctions may behave in various ways. Two possible variants of the dependence of the superconducting order parameter Δ and the wave vector Q_{\perp} of the magnetic-structure modulation on h are shown schematically in Fig. 15.

In the case of the FI/S contacts of the first type (Fig. 15a), the magnitude of A remains less than unity up to a certain critical value of the exchange field h_c . The critical parameters of the point (h_c, Δ_c) of the first-order phase transition from the FS to FN state are found from the equality of the free energies of these phases and are given as follows:

$$h_c \approx \frac{\Delta_0}{\sqrt{2}} \left(1 - \frac{\pi d_s^2}{12 \xi_0^2} \right), \quad \Delta_c \approx \Delta_0 \left(1 - \frac{\pi d_s^2}{24 \xi_0^2} \right), \quad (5.22)$$

where $\xi_0 = (D_s/2\Delta_0)^{1/2}$ is the coherence length at $T = 0$ and $h = 0$. The small corrections [of the order of $(d_s/\xi_0)^2$] to the result known for the uniform ferromagnet superconductor [19, 20] $h_c = \Delta_0/\sqrt{2}$ and $\Delta_c = \Delta_0$ are due to the fact that the exchange field that breaks Cooper pairs is generated by localized spins that are located at the surface rather than in the bulk of the sample.

For the FI/S junctions of the second type (Fig. 15b), the ratio of the molecular fields A is less than unity only up to a certain lower critical value of the exchange field, h_{c1} . At $h = h_{c1} (< h_c)$, a second-order phase transition occurs, which is accompanied by a steeper (as compared to the FS phase) decrease in the superconducting OP Δ in the S layer (a kind of kink) and by the appearance of a nonzero wave vector Q_{\perp} of the modulation of the ferromagnetic ordering in the film. The parameters of the transition point (h_{c1}, Δ_{c1}) as determined from the equality of the free energies of these phases are as follows:

$$h_{c1} \approx \frac{h_c}{\sqrt{A_c}} \left[1 + \frac{\pi d_s^2}{48 \xi_s^2} \left(1 - \frac{1}{A_c} \right) \right], \quad (5.23)$$

$$\Delta_{c1} \approx \Delta_c \left[1 + \frac{\pi d_s^2}{24 \xi_s^2} \left(1 - \frac{1}{A_c} \right) \right].$$

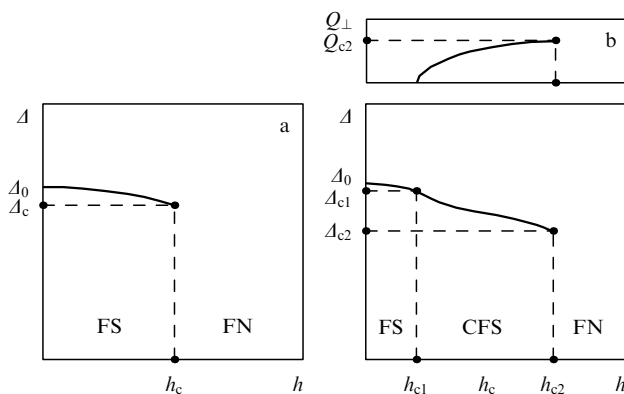


Figure 15. The superconducting order parameter Δ and wave vector Q_{\perp} of the magnetic structure as a function of the exchange field h for FI/S contacts: (a) contacts of the first type [with $A_c < 1$ ($Q_{\perp} = 0$)] and (b) of the second type (with $A_c > 1$) [78].

Here, A_c is the value of the parameter A at $h = h_c$ and $\Delta = \Delta_c$ ($A_c > 1$). As the exchange field increases further, a first-order phase transition CFS \rightarrow FN occurs at the point $h = h_{c2}$. The upper critical field h_{c2} and the corresponding values of OP Δ_{c2} and modulation wave vector Q_{c2} in the case where $A_c - 1 \ll A_c$ are determined as follows:

$$h_{c2} \approx h_c \left[1 + \frac{\pi^2}{256} \left(1 - \frac{1}{A_c} \right)^2 \right],$$

$$\Delta_{c2} \approx \Delta_c \left[1 - \frac{3\pi^2}{256} \left(1 - \frac{1}{A_c} \right) \right], \quad (5.24)$$

$$Q_{c2} \approx \left[\frac{3\pi}{16} \left(1 - \frac{1}{A_c} \right) \right]^{1/2} \xi_s^{-1}.$$

It can be shown that in the case of FI/S junctions the quantity A_c plays a role analogous to the role the Ginzburg–Landau parameter κ plays in distinguishing type I and type II superconductors. Indeed, the balance of the molecular fields, which plays the key role in determining whether the junctions are of type I or type II, may be expressed through A_c as

$$A = A_c \left(\frac{h}{h_c} \right)^2 \frac{\Delta_c}{\Delta}, \quad A_c = \frac{N(0)h_c^2 \pi \xi_s^2 d_s}{JS^2 4a^2 d_f}. \quad (5.25)$$

It follows from these expressions that the FI/S junctions with $A_c < 1$ refer to the first type and the junctions with $A_c > 1$ refer to the second type. In addition, the FI/S contacts with $A_c - 1 \ll A_c$ are characterized by a wide range of coexistence of ferromagnetism and superconductivity and a narrow range of existence of the cryptoferromagnetic superconducting phase, since the critical values h_{c1} and h_{c2} are close to h_c in this case. At $A_c \gg 1$, the region occupied by the CFS phase becomes substantially wider and the region corresponding to the FS phase, on the contrary, substantially narrows, since in this case $h_{c1} \ll h_c \ll h_{c2}$ (see Ref. [78]).

FI/S superlattices. Now, we consider a superlattice obtained by the alternation of layers of a ferromagnetic insulator of thickness d_f and a superconductor of thickness d_s (as before, $d_s \ll \xi_s$). To study the mutual accommodation of the superconducting and magnetic order parameters in such a system, it is sufficient to investigate the density of the free energy f^* of a unit cell consisting of two magnetic FI half-layers, $-d_f/2 < z < 0$ and $d_s < z < d_s + d_f/2$, separated by a superconducting interlayer S. The functional f^* in this case differs from Eqn (5.14) in that, apart from the term $I(q_{\perp}, 0, 0)$, it should include an analogous surface RKKY exchange $I(q_{\perp}, d_s, d_s)$ of localized spins of the neighboring ferromagnetic layer ($z = z' = d_s$) between themselves, as well as the RKKY exchange $I(q_{\perp}, 0, d_s)$ between the localized spins that refer to the magnetic surfaces $z = 0$ and $z' = d_s$ separated by a superconducting interlayer.

We will seek magnetic order in the superlattice in the form

$$\langle S_j^{\pm} \rangle = S \exp[\pm i(\mathbf{q}_{\perp} \mathbf{p} + q_{\parallel} z)], \quad \langle S_j^z \rangle = 0, \quad (5.26)$$

where q_{\parallel} is the component of the wave vector parallel to the superlattice axis. The translational invariance of the superlattice will result only in the multiplication by a constant phase factor upon the transition from a given FI layer to a neighboring layer, i.e.,

$$\langle S^{\pm}(\mathbf{p}, z + d_s + d_f) \rangle = \langle S^{\pm}(\mathbf{p}, z) \rangle \exp[\pm i q_{\parallel} (d_s + d_f)]. \quad (5.27)$$

At the same time, we neglect the effects of electron tunneling from one S layer into another through the magnetic FI interlayer. Therefore, the phases of the superconducting OPs Δ in neighboring S layers are not coupled and the π -phase (in the sense of superconductivity) variant of the mutual accommodation will not be considered here. Taking into account that $I(q_{\perp}, d_s, d_s) = I(q_{\perp}, 0, 0)$ and $I(q_{\perp}, d_s, 0) = I(q_{\perp}, 0, d_s)$, we obtain for the density of the free energy f^* per unit cell of the superlattice [78]

$$f^* = f_F^0 + f_N^0 + JS^2 q_{\perp}^2 \frac{d}{a} - 2I(q_{\perp}, 0, 0) - 2I(q_{\perp}, 0, d_s) \cos(q_{\parallel} d_s) - \frac{d_s N(0)}{2a^3} \Delta^2 \ln \frac{eA_0^2}{\Delta^2}, \quad (5.28)$$

where $I(q_{\perp}, 0, d_s)$ is determined from Eqn (5.8) and has asymptotes similar to Eqn (5.16) for $I(q_{\perp}, 0, 0)$. A difference between them arises only for wave vectors q_{\perp} comparable with d_s^{-1} . Indeed, at $q_{\perp} d_s \ll 1$, we obtain

$$I(q_{\perp}, 0, d_s) = I(q_{\perp}, 0, 0) + \frac{\pi d_s}{2\xi_s^3} N(0) \left(1 - \frac{q_{\perp}^2 d_s^2}{12} + \frac{q_{\perp}^4 d_s^4}{120} \right), \quad (5.29)$$

from which we see that the corrections to $I(q_{\perp}, 0, 0)$ are small because of (and to the extent) of smallness of the ratio d_s^2/ξ_s^2 . In this case, the RKKY exchange between localized spins belonging to different magnetic surfaces $z = 0$ and $z' = d_s$ has the same order of magnitude as the RKKY exchange between localized spins at each of these surfaces $z = z' = 0$ or $z = z' = d_s$. In the opposite limit, when $q_{\perp} d_s \gg 1$, we have

$$I(q_{\perp}, 0, d_s) \approx 2I(q_{\perp}, 0, 0) \exp(-q_{\perp} d_s), \quad (5.30)$$

i.e., the exchange coupling between magnetic surfaces through a superconducting interlayer is exponentially small as compared to the exchange between localized spins at each of these surfaces (although, as before, $d_s \ll \xi_s$). This is due to a significant averaging of the spin polarization of electrons in the superconductor upon the strong modulation of the ferromagnetic ordering in FI layers, for which reason the RKKY exchange in this case is of purely surface nature.

The minimization of free energy (5.28) with respect to the parameters Δ , q_{\perp} , and q_{\parallel} using expression (5.29) for $I(q_{\perp}, 0, d_s)$ leads to two possible variants of the ground state of the superlattice combining magnetic and superconducting types of long-range order. The result turns out to depend on the magnitude of A_c^* representing the ratio of antiferromagnetic to ferromagnetic exchange. In superlattices for which $A_c^* < 1$, at $h < h_c^*$ superconductivity coexists with the antiferromagnetic arrangement of the spontaneous moments of neighboring layers (AFS phase). At $h = h_c^*$, a phase transition occurs to the FN phase, in which all metallic layers are in the normal state and the coherent coupling between FI layers is broken. Thus, the FN phase in magnetic aspect behaves as a 2D ferromagnet.

In a superlattice for which $A_c^* > 1$, the AFS phase exists up to fields $h < h_{c1}^*$. In fields $h_{c1}^* < h < h_{c2}^*$, a CFS phase arises, in which cryptoferromagnetism coexists with superconductivity and in which a coherent π coupling exists between the spins of neighboring FI layers. At the point $h = h_{c2}^*$, the system passes, via a first-order phase transition, to the FN state, in which 2D ferromagnetism takes place. The phase diagrams for FI/S superlattices topologically coincide

with those for FI/S junctions. They can be represented by Fig. 15, where FS should be replaced by AFS and all critical fields and parameters should be labeled by asterisks.

The critical points in the phase diagram of the FI/S superlattice can be expressed through the parameters of the system. Thus, we have

$$h_c^* = A_0 \frac{\xi_0}{d_s} \sqrt{\frac{2}{\pi\sqrt{e}}}, \quad A_c^* = \frac{A_0}{\sqrt{e}}.$$

The values of h_{c1}^* and h_{c2}^* for the case $A_c^* - 1 \ll A_c^*$ are

$$h_{c1}^* \approx h_c^* \left(1 - \frac{1}{2} \sqrt{1 - \frac{1}{A_c^*}} \right),$$

$$h_{c2}^* \approx h_c^* \left[1 + \frac{5}{28} \left(1 - \frac{1}{A_c^*} \right)^2 \right],$$

and the modulation wave vector in the CFS phase is

$$Q_{c2}^* \approx \frac{1}{d_s} \sqrt{\frac{60}{7} \left(1 - \frac{1}{A_c^*} \right)}.$$

As $A_c^* \rightarrow 1$, the cryptoferromagnetism region contracts to point.

The very quantity A_c^* under these conditions is defined as

$$A_c^* = \frac{2}{3\pi e} \left(\frac{d_s}{\xi_0} \right)^2 A_c,$$

where A_c is the critical balance of molecular fields corresponding to the junction [second formula in (5.25)].

The differences in the character of the mutual accommodation of superconductivity and magnetism in FI/S junctions and FI/S superlattices are mainly due to the presence in the last case (apart from the RKKY exchange between spins along FI/S boundaries) of an antiferromagnetic exchange between localized spins of neighboring FI layers via the S interlayers. The very idea of the antiferromagnetic coupling of two ferromagnetic insulators through a superconductor was first discussed by de Gennes [113].

5.3 FI/S multilayers at finite temperatures.

Multicritical points in phase diagrams

An elementary qualitative analysis of the possible variants of coexistence and mutual accommodation of superconductivity and ferromagnetism in FI/S junctions at finite temperatures can be made on the basis of the Landau theory of phase transitions. Within the framework of the self-consistent field approximation, we define the magnetic order in the FI film in the form (5.13), where $\langle S \rangle$ denotes the thermodynamic average of the localized spin in a site with \mathbf{p} . Then, for the free energy per unit area of the junction near the critical temperature we obtain the following functional [79]:

$$f = f_F^0 + f_N^0 + J \langle S \rangle^2 q_{\perp}^2 \frac{df}{a} - I(q_{\perp}, 0, 0) \frac{\langle S \rangle^2}{a^2} + \frac{d_s}{a^3} \left(\alpha_0 \frac{A^2}{2} + \beta_0 \frac{A^4}{4} + \gamma_0 \frac{A^6}{6} \right), \quad (5.31)$$

which formally differs from Eqn (5.14) at $T = 0$ in only the replacement of the term responsible for the energy gain due to the superconducting transition of the S layer by the Landau

expansion in powers of Δ . The coefficients α_0 , β_0 , and γ_0 of this expansion are known from the microscopic theory of superconductivity [114]:

$$\alpha_0 = -2N(0) \left(1 - \frac{T}{T_{cs}}\right), \quad \beta_0 = \frac{7\zeta(3)N(0)}{(2\pi T_{cs})^2}, \quad (5.32)$$

$$\gamma_0 = \frac{93\zeta(5)N(0)}{2(2\pi T_{cs})^4}.$$

For further analysis, it is convenient, using the high-temperature expansion of the RKKY potential (5.15) in powers of Δ and q_\perp (at $\Delta \ll 2\pi T_{cs}$, $q_\perp \xi_s \ll 1$), to rewrite functional (5.31) in the form

$$f = f_F^0 + f_N^0 + J(S)^2 q_\perp^2 \frac{df}{a} + \frac{d_s}{a^3} \left(\alpha \frac{\Delta^2}{2} + \beta \frac{\Delta^4}{4} + \gamma \frac{\Delta^6}{6} \right). \quad (5.33)$$

Here, the renormalized coefficients α , β , and γ are given by the expressions

$$\alpha = \alpha_0 + 2N(0)\eta \left(\frac{h}{h_t}\right)^2 [1 - b(q_\perp \xi_s)^2 + g(q_\perp \xi_s)^4],$$

$$\beta = \beta_0 \left[1 - \left(\frac{h}{h_t}\right)^2\right], \quad \gamma = \gamma_0 \left[1 + p \left(\frac{h}{h_t}\right)^2\right],$$

$$h = \frac{I(S)a}{2d_s}, \quad h_t = \sqrt{\frac{7\zeta(3)}{186\zeta(5)}} 2\pi T_{cs} \simeq 1.312 T_{cs},$$

where ξ_s is the coherence length at $T = T_{cs}$, and the numerical values of the coefficients are as follows:

$$\eta \simeq 0.367, \quad b \simeq 0.963, \quad g \simeq 0.955, \quad p \simeq 1.303.$$

The summands that are proportional to the product of h^2 and Δ^2 in the last term in Eqn (5.33) are responsible for the coupling between the magnetic and superconducting OPs.

The minimization of functional (5.33) with respect to Δ and q_\perp results in three different states (see Ref. [79]):

- (1) a ferromagnetic normal phase (FN) with $\Delta = q_\perp = 0$;
- (2) a ferromagnetic superconducting phase (FS) with $\Delta = \Delta_1$, $q_\perp = 0$, and $A < 1$ with

$$\Delta_1^2 = \frac{-\beta + \sqrt{\beta^2 - 4\gamma\alpha_1}}{2\gamma}, \quad \alpha_1 = \alpha_0 + 2N(0)\eta \left(\frac{h}{h_t}\right)^2;$$

- (3) a cryptoferromagnetic superconducting phase (CFS) with $\Delta = \Delta_2$, $q_\perp = q_0$, and $A > 1$ with

$$\Delta_2^2 = \frac{-\beta + \sqrt{\beta^2 - 4\gamma\alpha}}{2\gamma}, \quad q_0^2 = \left(1 - \frac{1}{A}\right) \frac{b}{2g\xi_s^2}.$$

The realization of each of these phases depends on the magnitudes of three parameters: temperature T ; exchange field h produced by localized spins of the FI/S boundary and acting on the conduction electrons of the superconductor; and the ratio

$$A = \frac{\pi^2 N(0) h^2 \xi_s^2 d_s}{12 J(S)^2 a^2 d_f} \left(\frac{\Delta}{2T_{cs}}\right)^2 \quad (5.34)$$

of the antiferromagnetic and ferromagnetic molecular fields. Note that the smallness of the ratio of the amplitudes of the

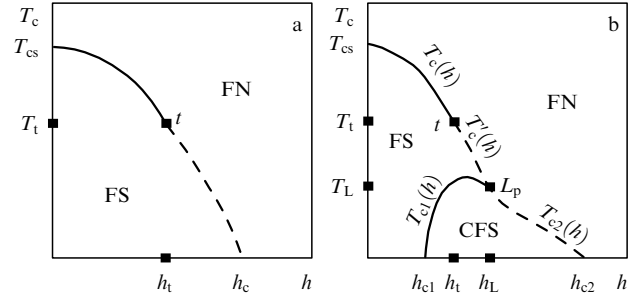


Figure 16. (T_c, h) phase diagrams for the FI/S contacts of (a) the first type and (b) second type. Solid lines show curves of second-order phase transitions; the dashed lines correspond to first-order phase transitions [79].

antiferromagnetic and ferromagnetic polarizations in Eqn (5.34) is compensated by the extremely large ratio of their domains of existence $\xi_s^2 d_s / a^2 d_f$. Therefore, the parameter A can be varied within wide limits. At $A > 1$, the ferromagnetic state is unstable, and the long-wavelength modulation arising at the FI/S boundary will be transferred via the strong interatomic exchange J over the entire thickness of the FI film. The loss in the energy of direct exchange in this case proves to be smaller than the energy gain due to the transition of the S layer to the superconducting state and a decrease in the paramagnetic effect. The phase diagrams for the two types of FI/S junctions are shown schematically in Fig. 16.

The contacts of the first type (Fig. 16a) with $A_c < 1$, where $A_c = A(h = h_c, T = 0)$, and h_c is the critical exchange field, admit the superconductivity coexistence with only a uniform ferromagnetic ordering. The critical temperature $T_c(h)$ at the $T_{cs} - T_t$ line of second-order phase transitions is specified by the equation $\alpha_1 = 0$. At the $h_t - h_c$ line of first-order phase transitions ($\beta < 0$), the function $T_c'(h)$ is determined from the equation $\alpha_1 = 3\beta^2/16\gamma$. When the exchange field h reaches its critical value $h_c \simeq 1.74h_t$, the temperature T_c' tends to zero. The magnitude of Δ_1 corresponding to h_c is $\Delta_c \simeq 1.11h_t$. It can be seen that the balance of molecular fields A , which can be conveniently represented in the form

$$A = A_c \left(\frac{h}{h_t}\right)^2 \left(\frac{\Delta}{\Delta_c}\right)^2, \quad A_c = \frac{\pi^2 N(0) h_c^2 \xi_s^2 d_s}{12 J(S)^2 a^2 d_f} \left(\frac{\Delta_c}{2T_{cs}}\right)^2, \quad (5.35)$$

remains less than unity when moving along the $T_{cs} - t - h_c$ line of FS–FN phase transitions, since $A_c < 1$. The coordinates of the tricritical point t ($h = h_t, T = T_t$) at which a changeover of the phase-transition order occurs, are determined from the simultaneous fulfillment of the conditions $\beta = 0$ and $\alpha_1 = 0$. It is the existence of a tricritical point t that dictates the necessity of retaining terms up to Δ^6 in the expansion (5.33). Note, however, that the phase diagrams and the magnitudes of critical parameters obtained here and below in terms of the Landau theory have only a qualitative nature because of the neglect of the realistic temperature dependences of the coefficients α , β , and γ in the expansion (5.33).

A distinctive feature of the FI/S junctions of the second type (Fig. 16b) with $A_c > 1$ is the existence of a Lifshitz point L_p [81] in the line of first-order phase transitions. At this point, three possible phases meet: FN, FS, and CFS. The coordinates of the Lifshitz point (T_L, h_L) are determined from the simultaneous fulfillment of the conditions $\alpha_1 = 3\beta^2/16\gamma$

and $A = 1$. The latter condition ($A = 1$) corresponds to the period of modulation q_0^{-1} of the magnetic order in the FI layer tending to infinity; this condition, along with the expression for Δ_1 , determines the line of second-order phase transitions $T_{c1}(h)$, which separates the commensurate (FS) and incommensurate (CFS) superconducting magnetic phases. Note that the $T_{c1}(h)$ curve passes through a maximum, thus ensuring the reentrant (FS–CFS–FS) behavior of the system in a certain range of exchange fields between h_{c1} and h_L at a fixed temperature. Near the Lifshitz point, the $T_{c2}(h)$ curve of the first-order phase transitions separating the ferromagnetic normal phase (FN) from the superconducting phase (CFS) with a sinusoidally modulated magnetic order is determined from the equality of the free energies of these phases.

In the case of the FI/S superlattice, the analysis of the corresponding free energy f^* is performed as in the case of the FI/S junctions, and the phase diagram (T, h) is topologically equivalent to that for the FI/S junction. Between these diagrams, the same connection exists as was the case for $T = 0$, namely, FS in Fig. 16 should be replaced by AFS. As in the case of $T = 0$, the AFS and CFS states are three-dimensional, and the FS states are two-dimensional, i.e., in these states the coherence in the orientation of magnetic moments of the FI layers is lost. A detailed discussion of the multicritical points t and L_p in these diagrams is given in Ref. [79].

Thus, the ratio of the antiferromagnetic and ferromagnetic molecular fields A_c or A_c^* permits classification of the FI/S systems into two types, similar to the Ginzburg–Landau parameter κ serving to distinguish type I and type II superconductors. The FI/S systems of the first type with A_c and $A_c^* < 1$ admit the coexistence of the superconductivity in S layers with only a uniform ferromagnetic ordering in FI layers (Figs 15a, 16a). It follows from the phase diagrams of the FI/S systems of the second type ($A_c, A_c^* > 1$, Figs 15b and 16b) that under certain conditions changes in the temperature T or in the exchange field h can result in the appearance of a cascade of alternating magnetic and superconducting transitions, e.g., CFS \rightarrow FS \rightarrow FN for junctions and CFS(2D–3D) \rightarrow FS(3D) \rightarrow FN(2D) for superlattices. A similar chain of transitions arising under the effect of an external magnetic field parallel to the plane of the FI/S interface can explain the increase and subsequent saturation of the exchange splitting of the BCS peak in the density of states for quasi-particles of aluminum in EuO/Al junction [73] and EuS/Al [74] junction. A further growth of magnetic field results in a *first-order* phase transition to the normal state, as was observed in these experiments.

Note also that the relatively weak suppression of superconductivity in the EuO/V superlattice [77] can be explained by the strong compensation of the exchange field in the vanadium interlayers due to the π -phase matching of the magnetic structures of localized spins of neighboring FI layers in the AFS or CFS states. The existence of an incommensurate magnetically ordered superconducting phase of CFS type in the EuO/Al and EuS/Al contacts and the possible existence of such a phase in the EuO/V superlattices suggests the probable existence of a Lifshitz point in them and, therefore, makes these systems attractive candidates for further experimental investigation. A direct observation of changes in the spin ordering in FI layers due to the competition between superconductivity and ferromagnetism can be performed, e.g., by the method of

magnetic neutron scattering. To experimentally study phase diagrams, we may use the circumstance that the vicinities of multicritical points can be passed through by varying the temperature T , as well as by changing the magnitude of the exchange field $h = I\langle S \rangle a/2d_s$ at the expense of variation of the S-layer thicknesses d_s or fabrication of the wedge-shaped S layers.

6. FI/S systems with pure superconductors

6.1 Boundary conditions for a ferromagnetic insulator/pure superconductor junction

In the preceding section, FI/S junctions and superlattices were studied in the limiting case of dirty superconductors. Here, we consider another limit — the case of a pure superconductor. The most important element of the theory is the derivation of boundary conditions at the FI/S junction. This problem was solved in Refs [115, 116] in 1988. The authors simulated the boundary as a high-energy barrier for electrons in the superconducting metal. Many properties of the sought boundary conditions proved to be determined by the symmetry of the system. For a smooth, ideally reflecting interface, the relationship between the incident and reflected electron waves is given by the scattering matrix S that relates the two-component spinors of a quasi-particle, representing the incident ψ_{in} and scattered ψ_{out} waves with quasi-momenta \mathbf{p}_{in} and \mathbf{p}_{out} : $\psi_{out} = S\psi_{in}$. Since we assume the reflection to be ideal, the matrix should be unitary, i.e., $SS^+ = S^+S = 1$. For a magnetically active surface possessing a spontaneous moment that is characterized by a unit vector $\boldsymbol{\mu}$, S is a matrix of dimension 2×2 of the form $S = s + \mathbf{m} \cdot \boldsymbol{\sigma}$, where $\mathbf{m} \sim \boldsymbol{\mu}$.

The general form of the S matrix that agrees with the conditions of unitarity is

$$S = \exp\left(-\frac{i\theta\boldsymbol{\mu}\boldsymbol{\sigma}}{2}\right), \quad (6.1)$$

where θ is the angle of mixing of spin states in the reflected wave. Indeed, let the spontaneous moment be directed along the y axis and let the incident wave has spin directed along the z axis (perpendicular to the interface) with a projection $\sigma_z = 1$ (state $\psi_{in} = |\uparrow\rangle$). Then, the reflected wave will represent a superposition of spin states with both projections of spin:

$$\psi_{out} = \cos\left(\frac{\theta}{2}\right)|\uparrow\rangle + \sin\left(\frac{\theta}{2}\right)|\downarrow\rangle. \quad (6.2)$$

Thus, the spin of a quasi-particle upon reflection from a magnetized interface is rotated by an angle $\theta/2$. This rotation is a consequence of the tunnel penetration of a quasi-particle into the ferromagnetic region, which is forbidden for it in the classical model, and therefore represents a quantum effect.

The mixing angle θ depends on the quasi-momentum \mathbf{p}_{\parallel} , which is conserved along the interface. If the Fermi surface is considered to be spherical, then $\mathbf{p}_{\parallel} = \mathbf{p} - (\mathbf{p} \cdot \mathbf{z})\mathbf{z}$. The matrix S does not take into account the dynamic reorientation of the spin of the quasi-particle upon its tunneling into the ferromagnetic region, but only allows for the interaction of the spin with the mean field acting on the quasi-particle in the ferromagnet.

A model for the potential barrier at the FI/S boundary was suggested in Ref. [116]. It is assumed that the ferromagnet is a semiconductor with a bandgap E_g and that it is this gap

that controls the height of the barrier. The solution to the Schrödinger equation for an electron with such a potential barrier permits one to calculate the scattering matrix S . It proves to be dependent on two dimensionless parameters:

$$r = \left(\frac{2mE_g}{p_F} \right)^{1/2}, \quad \lambda = \frac{h}{E_g},$$

where m and p_F are the mass and the Fermi momentum of an electron in the metal, and h is the exchange field in the ferromagnet that acts on its spin; it is also assumed that $\lambda < 1$. The matrix S also depends on the angle ϑ between the reflected electron and the z axis. The mixing angle is expressed through the eigenvalues of the matrices S_+ and S_- as follows:

$$\tan \frac{\theta}{2} = - \frac{2 \operatorname{Im} S_+ S_-^*}{|S_+ + S_-|^2}.$$

Hence, for $r \gg 1$, we have $\theta \approx (2\lambda/r) \cos \vartheta$. Thus, under these conditions, the angle θ is small and proportional to the exchange field h . Naturally, the mixing angle θ should depend in a complex manner on the angle ϑ , which is determined by the shape of the Fermi surface and orientation of the crystal axes of the superconductor with respect to the interface of the junction. In the available theoretical investigations [115–117], it is assumed for simplicity that the Fermi surface is spherical and the mixing angle θ is independent of the angle ϑ and is a certain parameter that characterizes the interface.

The boundary conditions at the FI/S interface can be formulated in terms of the matrix Green's function $\hat{g}(\mathbf{p}, \mathbf{R}, \omega_n)$ of the superconductor. Since the single-particle Green's function is constructed of two eigenvectors of the single-particle state, it is obvious that at the interface a relation between its values for the quasi-momenta \mathbf{p}_{in} and \mathbf{p}_{out} should exist. This relation has the following form [116]:

$$\hat{g}(\mathbf{p}_{\text{out}}, \mathbf{R}_0, \omega_n) = \hat{S} \hat{g}(\mathbf{p}_{\text{in}}, \mathbf{R}_0, \omega_n) \hat{S}^+, \quad (6.3)$$

where \mathbf{R}_0 are the coordinates of the surface points and \hat{S} is a matrix of dimension 4×4 composed of the spin matrix S :

$$\begin{aligned} \hat{S} &= \begin{pmatrix} S(\mathbf{p}, \boldsymbol{\mu}) & 0 \\ 0 & S^+(-\mathbf{p}, -\boldsymbol{\mu}) \end{pmatrix} \\ &= \begin{pmatrix} \exp \left[-i \frac{\theta}{2} (\boldsymbol{\mu} \boldsymbol{\sigma}) \right] & 0 \\ 0 & \exp \left[-i \frac{\theta}{2} (\boldsymbol{\mu} \boldsymbol{\sigma})^{\text{tr}} \right] \end{pmatrix}. \end{aligned} \quad (6.4)$$

The lower element of the matrix \hat{S} corresponds to holes reflected from the boundary, and the upper element is associated with electrons that constitute a quasi-particle in the superconductor.

The authors of Ref. [116] solved the problem of a system consisting of a ferromagnetic insulator and superconductor occupying a half-space. The use of boundary conditions in the form (6.3) with Green's functions in the quasi-classical approximation led to the following main results: the superconducting gap of the FI/S system decreases on approaching the interface as soon as z is of the order of several coherence lengths ξ_0 . On the other hand, the exchange field induced in the superconductor rapidly falls off at the same distances, which is a sufficiently obvious result.

The critical temperature T_c for a superconducting layer of a finite thickness $d_s \ll \xi_0$ decreases with increasing parameter

$$\rho = \frac{\xi_0}{2d_s} \tan \frac{\theta}{2}, \quad (6.5)$$

vanishing at $\rho = \rho_c \simeq 0.38$. At small $\rho \ll 1$, we have

$$\frac{T_c}{T_{cs}} = 1 - \frac{7\zeta(3)}{3} \rho^2 + \dots \quad (6.6)$$

Thus, the presence of a boundary with a ferromagnetic insulator leads to pair breaking in the superconductor because of the appearance of mixing of spin states in reflected waves. Of most interest is a system in which there are ferromagnetic layers of an arbitrary thickness on both sides of the superconducting film. This situation was studied in [117] for superconductors of singlet and triplet types.

6.2 FI/S/FI system with singlet superconductivity

Studying superconducting states in such a trilayer depending on the mutual orientation of the magnetization vectors of FI layers is of special interest in view of possible engineering applications. In this section, we follow Ref. [117].

An inhomogeneous system consisting of two ferromagnetic layers with a thin film of a superconducting metal between them (Fig. 17) is described by a Green's function $\hat{g}(\mathbf{p}, \mathbf{R}, \omega_n)$ depending on the momentum \mathbf{p} and coordinate \mathbf{R} of the quasi-particle. The matrix structure of this Green's function is as follows:

$$\hat{g}(\mathbf{p}, \mathbf{R}, \omega_n) = \begin{pmatrix} g(\mathbf{p}, \mathbf{R}, \omega_n) & f(\mathbf{p}, \mathbf{R}, \omega_n) \\ f^*(-\mathbf{p}, \mathbf{R}, \omega_n) & g^{\text{tr}}(-\mathbf{p}, \mathbf{R}, -\omega_n) \end{pmatrix}, \quad (6.7)$$

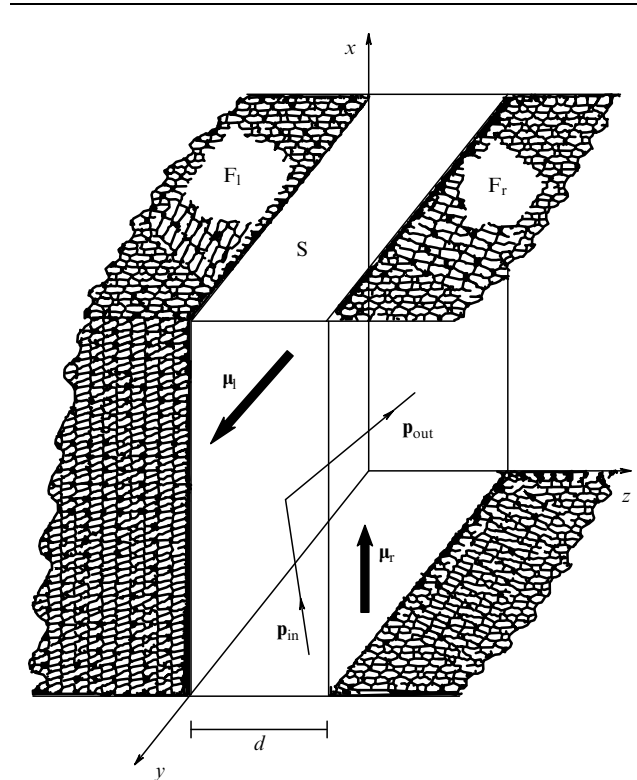


Figure 17. FI/S/FI contact with a different orientation of the spontaneous moments $\boldsymbol{\mu}_l$ and $\boldsymbol{\mu}_r$ for the left-hand and right-hand F layers [117].

where the normal Green's function g is diagonal in spin and the anomalous f (for singlet state) function has the form

$$f = f_s i \sigma_2. \quad (6.8)$$

For a pure superconductor in the quasi-classical approximation, \hat{g} obeys the Eilenberger equation [71]

$$[i\omega_n \tau_3 - \hat{\Delta}(\mathbf{p}, \mathbf{R}, \omega_n), \hat{g}(\mathbf{p}, \mathbf{R}, \omega_n)] + i v_F \mathbf{V}_R g(\mathbf{p}, \mathbf{R}, \omega_n) = 0 \quad (6.9)$$

with the following normalization:

$$\hat{g}^2(\mathbf{p}, \mathbf{R}, \omega_n) = -1. \quad (6.10)$$

On the other hand, the OP $\hat{\Delta}$ is a solution to the self-consistent equation

$$\hat{\Delta}(\mathbf{p}, \mathbf{R}) = N(0) T \sum_n \int \frac{d\Omega'}{4\pi} V(\mathbf{p}, \mathbf{p}') \hat{f}(\mathbf{p}', \mathbf{R}, \omega_n), \quad (6.11)$$

where $V(\mathbf{p}, \mathbf{p}')$ is the pairing potential, and the angle Ω specifies integration over the Fermi surface.

To calculate the Green's function of the entire system, we should solve the set of equations (6.9), (6.10) with boundary conditions (6.3) for the left-hand and right-hand boundaries. The momenta entering into the boundary conditions are linked by the relation

$$\mathbf{p}_{\text{out}} = \mathbf{p}_{\text{in}} - 2\mathbf{z}(\mathbf{p}_{\text{in}} \cdot \mathbf{z}). \quad (6.12)$$

The mixing angle θ that parametrizes the S matrix will further be considered as a phenomenological parameter independent of the momenta \mathbf{p}_{in} and \mathbf{p}_{out} .

Under conditions where $d_s \ll \xi_0$, the solution to equation (6.9) can be found using the substitution

$$\hat{g}(\mathbf{p}, \mathbf{R}, \omega_n) = \hat{g}_0(\mathbf{p}, \omega_n) + \left(z - \frac{d_s}{2}\right) \hat{g}_1(\mathbf{p}, \omega_n),$$

where $|\mathbf{g}_0| \gg |d_s \mathbf{g}_1|$. Using boundary conditions (6.3) for the left-hand and right-hand boundaries of the double junction, we can eliminate \hat{g}_1 and obtain the equation for \hat{g}_0 :

$$\left\{ [i\omega_n \tau_3 - \hat{\Delta}, \hat{g}_0], \hat{S}_l \hat{S}_r \right\} + 2i \frac{v_F |p_z|}{d_s} [\hat{g}_0, \hat{S}_l \hat{S}_r] + \hat{S}_l [i\omega_n \tau_3 - \hat{\Delta}, \hat{S}_l^+ \hat{g}_0 \hat{S}_l + \hat{S}_r^+ g_0 \hat{S}_r] \hat{S}_r = 0. \quad (6.13)$$

Here, the brackets $[\dots]$ and braces $\{\dots\}$ denote the commutator and anticommutator, respectively.

In the case of a singlet superconductor, the 4×4 matrix $\hat{\Delta}$ should have the form

$$\hat{\Delta} = i \Delta_s \sigma_2 \tau_1. \quad (6.14)$$

Near T_c , the solution for \hat{g}_0 in Eqn (6.13) is sought in the form $\hat{g}_0 = \hat{g}_0^{(0)} + \hat{f}_0^{(1)}$, where $g_0^{(0)}$ is independent of Δ , and $\hat{f}_0^{(1)}$ is linear in Δ . The condition of renormalization (6.10) is then resolved into two equations:

$$[\hat{g}_0^{(0)}]^2 = -1, \quad \{\hat{g}_0^{(0)}, \hat{f}_0^{(1)}\} = 0.$$

For a singlet superconductor, the orientation of the magnetization in the junction is insignificant, and T_c depends

only on the mutual orientation of the vectors $\boldsymbol{\mu}_l$ and $\boldsymbol{\mu}_r$. At the parallel magnetization, the scattering matrices S_l and S_r on the left-hand and right-hand junctions are equal, and Eqn (6.13) then reduces to the equation

$$[i\omega_n \tau_3 - \hat{\Delta} - \alpha \sigma_2 \tau_3, \hat{g}_0] = 0, \quad \text{where } \alpha = \frac{v_F |p_z|}{2d_s} \tan \theta.$$

Then, from the linearized equation (6.11) we obtain the equation in $t_c = T_{c\perp}/T_{cs}$:

$$\ln t_c = - \sum_{n=0}^{\infty} \frac{1}{n+1/2} \left[1 - \left(n + \frac{1}{2}\right) \frac{t_c}{\rho} \arctan \frac{\rho}{T_c(n+1/2)} \right], \quad (6.15)$$

where

$$\rho = \rho_0 \frac{\tan \theta}{\tan(\theta/2)}, \quad \rho_0 = \frac{\xi_0}{2d_s} \tan \frac{\theta}{2}. \quad (6.16)$$

Here, as usual, T_{cs} is the critical temperature for a bulk superconductor and ρ_0 is the parameter that describes the breaking of Cooper pairs at one of the FI/S boundaries. In this case, T_c at $\rho_0 \ll 1$ is determined by relationship (6.6).

If $\rho \ll 1$ in Eqn (6.15), we obtain the following conditions for suppression of T_c in the presence of a trilayer FI/S/FI and a bilayer FI/S:

$$\frac{\delta T_{c2}}{T_{cs}} = 4 \frac{\delta T_{c1}}{T_{cs}}, \quad (6.17)$$

where $\delta T_{c2} = T_{c2} - T_{cs}$ and $\delta T_{c1} = T_{c1} - T_{c0}$. The results of numerical solutions for T_c in these cases are shown in Fig. 18. We see that the interaction with FI/S boundaries leads to a pair-breaking effect. Another mechanism arises in the case of an antiparallel orientation of the vectors $\boldsymbol{\mu}_l$ and $\boldsymbol{\mu}_r$. In this case, the matrices of scattering from junctions are linked by relationship $S_l S_r = 1$. As a result, Eqn (6.13) reduces to the following equation:

$$[i\omega_n \tau_3 - a \hat{\Delta} - b \sigma_2 \hat{\Delta}, \hat{g}_0] = 0, \quad (6.18)$$

where $a = \cos^2(\theta/2)$ and $b = i \sin(\theta/2)$. Linearized equation (6.11) yields

$$T_{c,\text{anti}} = T_{cs} \exp\left(-\frac{1}{\lambda} \tan^2 \frac{\theta}{2}\right). \quad (6.19)$$

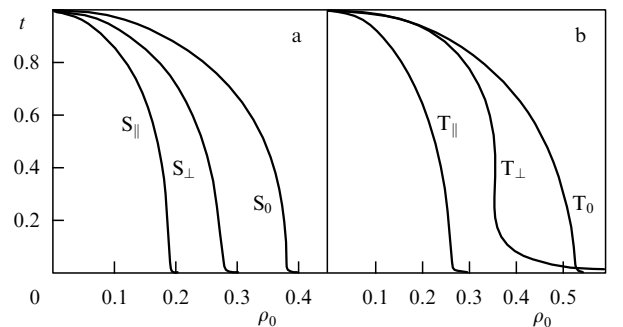


Figure 18. Temperature of the superconducting transition as a function of the pair-breaking parameter for (a) singlet and (b) triplet superconductors in the FI/S/FI system [117].

Thus, in this case, we simply have a weakening of pairing. Finally, in the case of a perpendicular orientation of the μ_1 and μ_r vectors, the dependence on the pair-breaking parameter is shown in Fig. 18a. At small ρ , we have

$$\delta T_{c\perp} = 2\delta T_{c1} = \frac{1}{2} \delta T_{c2}. \quad (6.20)$$

In the case of a superconductor with triplet pairs, the situation becomes more complex. The matrix $\hat{\Delta}$ contains a vector order parameter Δ_t ,

$$\hat{\Delta} = \begin{pmatrix} 0 & (\Delta_t \sigma) i\sigma_2 \\ i\sigma_2 (\Delta_t^* \sigma) & 0 \end{pmatrix}, \quad (6.21)$$

and to find it, we should solve the self-consistent equation (6.11). The results of calculations of T_c at various orientations of the vectors μ_1 and μ_r are given in Fig. 18b.

In both cases, the superconductivity of the FI/S/FI system strongly depends on the mutual orientation of the vectors μ_1 and μ_r . At the parallel orientation, T_c decreases with increasing pair-breaking parameter ρ_0 more rapidly than at the perpendicular (or antiparallel) orientation of the vectors μ_1 and μ_r . This means that if at a fixed ρ_0 the temperature T satisfies the condition $T_{c2} < T < T_{c\perp}$ and the three-layer junction is in the superconducting state at the perpendicular (antiparallel) orientation of μ_1 and μ_r , then if the orientation of the magnetic field in one of the FI layers changes in such a way that μ_1 and μ_r become parallel, the system passes into the normal state. Thus, in this situation, a sharp change in the conductivity will occur with changing orientation of the magnetic field at the second contact. This phenomenon can be employed for producing superconducting spin switches of current.

7. Transport properties of S/F systems

7.1 Josephson effect in S/F/S structures

Up to this point, we have mainly considered the thermodynamics of F/S systems, in particular, the phase diagrams of F/S junctions and F/S superlattices. However, there exist a number of remarkable phenomena related to the passage of electric current through double junctions. Among these, the Josephson effect in three-layer S/F/S structures should be noted, which permits one to directly study the π -phase superconductivity. Another example is a three-layer F/S/F junction, in which the transport properties of spin-polarized electrons and the Andreev reflection are used. At present, numerous theoretical investigations devoted to these problems are available, which could already constitute a subject of a separate review. Here, we restrict ourselves to a brief report of the main results obtained to date.

For the first time, the idea of using current oscillations in the S/F/S junction for the investigation of π -phase superconductivity was suggested by Buzdin et al. [118], who considered the junction in the pure limit. Later, the realistic case corresponding to the dirty limit was considered by Buzdin and Kupriyanov [119] and then in more detail by Buzdin et al. in Ref. [62]. Given the Usadel function $F(z, \omega)$ in each layer of an S/F/S junction, we can calculate the current through the junction depending on the phase difference in the superconducting order parameter at the first and second S layers. As in the case of an ordinary Josephson junction,

the current is $j(\varphi) = J_c \sin \varphi$. Calculations show that the critical current j_c through the S/F/S contact is determined by the formula [119]

$$j_c \sim F\left(\frac{\Delta}{T}\right) y \exp(-y) \sin\left(y + \frac{\pi}{4}\right), \quad (7.1)$$

where

$$y = \frac{d_f}{\xi_f} \left(\frac{2I}{\pi T_{cs}}\right)^{1/2}. \quad (7.2)$$

Thus, the current amplitude decreases with increasing parameter y and vanishes at $y = n\pi - \pi/4$ ($n = 0, 1, 2, \dots$). Formula (7.1) is valid at $y \gg 1$; however, it can be shown that $j_c(y)$ has a maximum value at $y = 0$. The quantity $F(\Delta/T)$ is a decreasing function of temperature and vanishes at $T = T_{cs}$.

We see that j_c oscillates with increasing thickness of the F layer or (at fixed d_f) with increasing temperature, since $I \sim \langle S^z \rangle$ falls off on approaching the Curie point T_m . The temperature oscillations can occur when T_m and T_c are close to one another in order of magnitude. Note that with the boundary conditions used in Ref. [119], the results obtained are valid only in the limit of a high transparency of the barrier.

Similar (in physical meaning) results were recently obtained in Ref. [120], where the authors used the microscopic model of a layered metal in which atomic planes with ferromagnetic and superconducting order parameters alternate [121]. In this ‘atomic’ limit of an S/F superlattice, they obtained the condition for the appearance of π -phase superconductivity and calculated the critical current that passed perpendicular to the layers. It turned out that j_c as a function of the parameter I/T_c has a maximum at $I = 0$ and falls off to zero at the critical point I_c corresponding to the appearance of π -phase superconductivity. In contrast to Eqn (7.1), which is valid for an S/F/S junction, in the case of an atomic F/S superlattice there is only one zero of the critical current.

The experimental observation of such a nonmonotonic behavior of the critical current with decreasing temperature was made on a S/F/S trilayer in which Nb was taken as the superconducting layer and a $\text{Cu}_x\text{Ni}_{1-x}$ alloy with x close to 0.5 was taken as the ferromagnetic layer [122]. Figure 19 displays the variation of the critical current measured on two such junctions (curves *A* and *B*) with a ferromagnetic layer thickness $d_f = 22$ nm. The curve *A* shows that j_c increases with decreasing temperature, passes through a maximum, vanishes, and again increases. This corresponds to the supposition that π -phase superconductivity is realized in the S/F/S system. The point where the critical current becomes zero corresponds to the transition from the 0-phase to the π -phase superconductivity. Thus, the measurements performed in Ref. [122] appear to be the first evidence that confirms the existence of π -phase superconductivity.

Another observation of π -phase superconductivity was made on F/S junctions by the same authors [123]. They studied the temperature and field dependences of the critical current in a circuit composed of three F/S junctions in a triangular geometry. At a temperature $T_{cr} = 2.2$ K, a crossover from the 0-phase superconductivity (at $T > T_{cr}$) to the π -phase superconductivity (at $T < T_{cr}$) was observed. The occurrence of a crossover can be judged from the shift of the periodic $j_c(H)$ dependence. In the case of the standard 0-phase superconductivity, peaks are observed in $j_c(H)$ which correspond to integer quanta of the flux Φ_0 passing through

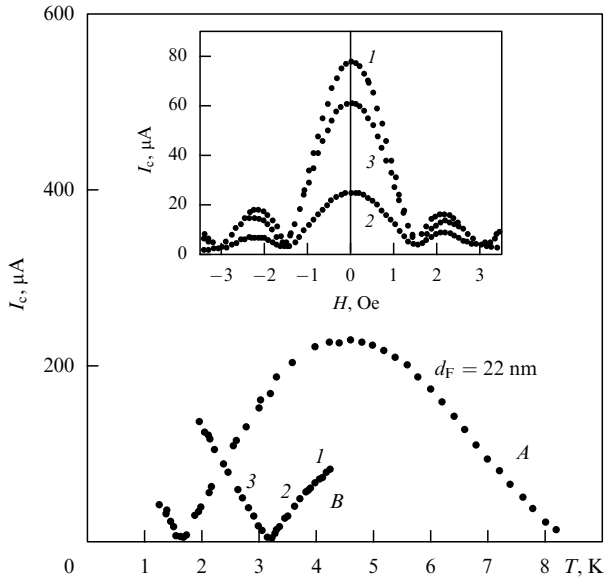


Figure 19. Temperature dependence of the critical current in a Nb/Cu_{0.48}Ni_{0.52}/Nb trilayer. The inset shows the dependence of I_c on the external magnetic field at various temperatures: (1) $T = 4.19$, (2) 3.45 , and (3) 2.61 K [122].

the Josephson junctions. In the case of the π -phase superconductivity, the $j_c(H)$ curve should be shifted by a half-period, which was observed in reality. With decreasing temperature the critical current j_c vanishes at the point T_{cr} and then again increases already in the π -phase.

The shift of the $j_c(H)$ curve by a half-period is due to the appearance of a spontaneous current (corresponding to a half-quantum of the flux) in the triangular circuit consisting of π -contacts. In this case, the ground state degenerates because of the possibility of two directions of this current. Since such an object has a double-degenerate ground state, it can be used as a quantum bit of information (qubit). Earlier, analogous suggestions were made in Refs [124, 125].

The authors of Ref. [126] considered a Josephson S/I/S junction formed by two magnetic superconductors in which superconductivity coexisted with a spiral magnetic order. Such a coexistence phase in a uniform metal was earlier investigated in Refs [4, 127]. The spiral phase arises in a ferromagnetic superconducting metal as a result of the adjustment of the superconducting and magnetic order parameters under the conditions where $Q_0^{-1} \ll \xi_0$, when the paramagnetic effect in the system is weakened. If the phases of the magnetic OP θ_1 and θ_2 at the surface of the insulating layer are fixed, the calculation shows that the Josephson tunneling current is determined by the formula [126]

$$J(\varphi, \theta) = (J_c - J'_c \cos \theta) \sin \varphi,$$

where $\varphi = \varphi_1 - \varphi_2$ and $\theta = \theta_1 - \theta_2$. The additional current J'_c , which is determined by the phase difference θ , also depends on the chirality (i.e., on whether the spiral is left-hand or right-hand) of the first and second superconductors. The strength of the current depends on the magnitudes of the parameters Δ/h and Qv_F/h . In such a junction, π -phase superconductivity can be realized if the phase difference θ can be changed with the help of an external magnetic field applied to one of the superconductors.

In another work [128], a complex Josephson junction S/F/I/F/S was considered, which consisted of two S/F bilayers separated by an insulating layer. In such a heterosystem, one can study the critical current depending on the mutual orientation of magnetic moments in the ferromagnetic layers. Calculations show that at low temperatures ($T \ll \Delta$), the critical current J_c increases with increasing exchange field h at the antiferromagnetic orientation of the F layers. In the case of the parallel orientation, J_c is suppressed. In principle, such an effect can be used for controlling current with the use of an external magnetic field.

7.2 Transport of spin-polarized electrons in F/S/F structures

In recent years, great attention has been paid to transport properties in F/S structures connected into an electric circuit, which are due to the passage of spin-polarized electrons from the ferromagnetic layer into the superconductor [72, 129–135]. Depending on the applied potential difference, new physical phenomena arise, which are promising for engineering applications [129, 130]. The most interesting phenomena were found in F/S/F structures, in which the current was studied as a function of the applied potential V in two different configurations: when the mutual orientation of spontaneous moments in F layers was ferromagnetic or antiferromagnetic.

The phenomena that occur in the F/S/F junction upon the application of a potential difference to it consist in the following. Because of the magnetic biasing of conduction electrons in the F layer, they pass into the S layer with the preferred orientation of their spins directed upward (\uparrow , in the direction of the spontaneous moment). It is assumed that the time of spin relaxation τ_s in the S layer is greater than all other characteristic times; therefore, an electron with spin up (\uparrow) that passed from the left-hand F layer (Fig. 20) rapidly relaxes to the Fermi distribution of quasi-particles in the superconductor but retains its spin up to the passage into the right-hand F layer. If the junction has an antiferromagnetic configuration, a nonequilibrium spin polarization is accumulated in the S layer; for the ferromagnetic orientation, no such polarization occurs. Owing to the spin polarization, the chemical potential of quasi-particles in the superconductor is shifted by $\delta\mu$ for quasi-particles with spin up (\uparrow) and by $-\delta\mu$ for quasi-particles with spin down (\downarrow). Thus, there arises a paramagnetic effect, which results in a decrease in the magnitude of the superconducting gap Δ ; at a certain $\delta\mu$ (i.e., at a certain potential V), this gap can vanish. The $\Delta(\delta\mu)$ dependence is determined by the same equation as in the case of the paramagnetic effect in a superconductor [133, 134], namely,

$$\ln \frac{\Delta_0}{\Delta} = \int_0^{\hbar\omega_D} \frac{d\varepsilon}{E(\varepsilon)} \left\{ \frac{1}{\exp[(E(\varepsilon) + \delta\mu)/T] + 1} + \frac{1}{\exp[(E(\varepsilon) - \delta\mu)/T] + 1} \right\}. \quad (7.3)$$

Here, $E(\varepsilon) = \sqrt{\varepsilon^2 + \Delta^2}$, and Δ_0 is the magnitude of the gap at $T = 0$ in the absence of spin density ($\delta\mu = 0$).

For the normal state in the antiferromagnetic configuration, we have $\delta\mu = PeV/2$, where P is the spin polarization; for the superconducting state, $\delta\mu$ can be calculated as a function of T and V [133, 134].

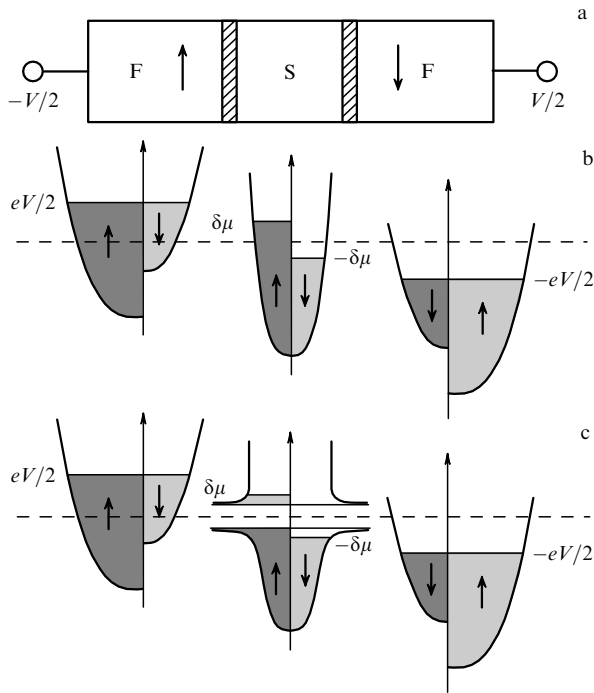


Figure 20. (a) Double tunnel F/S/F junction under an applied potential V for the antiferromagnetic configuration. (b), (c) Density of states of quasiparticles with spins up (\uparrow) and down (\downarrow) in (b) the normal and (c) superconducting states [133].

The authors of Ref. [133] calculated, in terms of a phenomenological model, the width of the gap Δ and the spin density (normalized to the density of states in the normal phase in the S layer) as a function of the applied potential V . The results of calculations at a fixed spin polarization of the ferromagnetic layer $P = 0.4$ and various temperatures are given in Fig. 21. We see that for each temperature $T < T_c$ there is a critical value $V = V_c$ at which the gap vanishes. The suppression of superconductivity is due to the accumulation of spin polarization in the S layer to a certain critical value corresponding to breaking of Cooper pairs because of the paramagnetic effect. The critical value V_c turns out to be inversely proportional to the spin polarization of the F layer ($V_c \sim 1/P$), which seems to be quite reasonable, since the greater P , the greater the spin polarization in the S layer (and, consequently, the greater the pair-breaking factor), and the smaller the magnitude of the gap Δ . The authors of Ref. [134] calculated the conductance of the junction as a function of the applied potential for the antiferromagnetic and ferromagnetic configurations, as well as the tunneling magnetoresistance. Both quantities are quite specific functions of V in the range $|eV| < 2\Delta_0$.

Experimental investigations of spin-polarized transport in F/S structures were carried out in Refs [72, 136–138]. In Ref. [139], along with experimental data for an Fe/Nb/Fe trilayer, the dependence of the depairing critical current J_{c0} on the thickness of the superconducting layer d_s was calculated theoretically based on the boundary-value problem for the Usadel function with boundary conditions for the case of high transparency of the barrier. From a comparison of the experimental data with calculations of $T_c(d_s)$ in the Fe/Nb/Fe system, the microscopic parameters of the junction were determined, which were then used to calculate $J_{c0}(d_s)$. The results obtained agree well with the direct

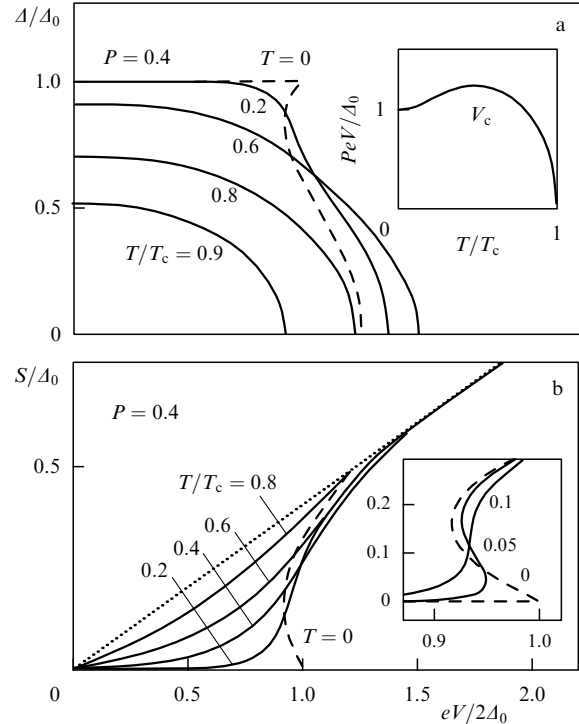


Figure 21. Theoretical calculation of the F/S/F contact with the antiferromagnetic configuration for (a) the gap and (b) spin density depending on the applied potential difference. The dashed line in Fig. 21b shows the value of polarization $S_A = PeV/2$ in the normal state of the junction [133].

measurements of the pair-breaking current in this junction. Both the $J_{c0}(d_s)$ and $T_c(d_s)$ curves begin from a critical value $d_{Nb} = 35$ nm and saturate at $d_{Nb} = 150$ nm.

7.3 Role of the Andreev reflection

The phenomenological theory developed in Ref. [133] ignored the Andreev reflection at the boundaries of the normal ferromagnetic and superconducting metals in the double F/S/F junction. As is shown in Ref. [134], this reflection can play an important role if the height of the corresponding barrier is small. The Andreev reflection is known [140, 141] to arise upon the passage of an electron from the normal into superconducting metal. The chemical potentials of both metals are equal; therefore, if the energy ω of the electron incident onto the boundary (measured from the chemical potential) is smaller than the superconducting gap ($\omega < \Delta$), the electron should be reflected. Its energy and quasi-momentum in this case are conserved but the velocity changes (becomes opposite). This means that the reflected electron should be considered as a hole (upon ordinary reflection, only the normal component of the velocity usually changes to the opposite). Another aspect of this extraordinary reflection is that the electron current passing through the normal and superconducting metals transforms at the boundary into a current of Cooper pairs, but in the normal metal it is accompanied by a current of holes produced at the boundary.

If the normal metal is in the ferromagnetic state, we should take into account magnetic biasing of electrons and a shift of the Fermi surface for the electrons with spins up and down. Consider an electron with spin up and energy ω moving along the normal to the junction surface. The wave

function for the left-hand layer can be written in the form

$$\begin{aligned} \psi_f(z) = & \exp(ik_{e\uparrow}z) \begin{pmatrix} 1 \\ 0 \end{pmatrix} + a_{\uparrow} \exp(ik_{h\uparrow}z) \begin{pmatrix} 0 \\ 1 \end{pmatrix} \\ & + b_{\uparrow} \exp(-ik_{e\uparrow}z) \begin{pmatrix} 1 \\ 0 \end{pmatrix}, \end{aligned} \quad (7.4)$$

where $k_{e\uparrow} = \sqrt{2m(E_F + \omega)}$, $k_{h\uparrow} = \sqrt{2m(E_F - \omega - 2I)}$ are the quasi-momenta of the electron and ‘reflected hole’. The third term in Eqn (7.4) takes into account the usual reflection of electrons.

In the S layer, the wave function includes the electron-like and hole-like parts:

$$\psi_s(z) = c_{\uparrow} \exp(ik_{e\uparrow}^s z) \begin{pmatrix} u_k \\ v_k \end{pmatrix} + d_{\uparrow} \exp(-ik_{h\uparrow}^s z) \begin{pmatrix} v_k \\ u_k \end{pmatrix}, \quad (7.5)$$

where

$$\begin{aligned} k_{e\uparrow}^s &= \sqrt{2m \left[E_F + \sqrt{(\omega - \delta\mu)^2 - \Delta^2} \right]}, \\ k_{h\uparrow}^s &= \sqrt{2m \left[E_F - \sqrt{(\omega + \delta\mu)^2 - \Delta^2} \right]}. \end{aligned}$$

In view of the smallness of ω , $\delta\mu$, and Δ in comparison with E_F , we may approximately assume $k_{e\uparrow}^s \simeq k_{h\uparrow}^s = \sqrt{2mE_F} = p_F$. In expression (7.5), u_k and v_k are the coefficients of the $u-v$ transformation for the quasi-particles of the superconductor.

The use of the conditions of joining solutions (7.4) and (7.5) at the boundaries of the FM/S junction permits one to calculate the amplitudes a_{\uparrow} , b_{\uparrow} , c_{\uparrow} , and d_{\uparrow} and the current passing through the F/S/F junction. Note that in Ref. [134] the authors also (phenomenologically) included the potential barrier for electrons at the F/S boundaries of the junction:

$$U_0 \left[\delta \left(z - \frac{d_s}{2} \right) + \delta \left(z + \frac{d_s}{2} \right) \right], \quad (7.6)$$

so that the complete solution of the problem depends on the dimensionless parameter $Z = U_0/\hbar v_F$. Numerical calculations show the significant influence of Z on the behavior of the tunneling magnetoresistance of the F/S/F junction, which is determined as the ratio $(j_F - j_A)/j_A$ of the difference of currents passing through the junction upon the ferromagnetic and antiferromagnetic configurations to the current corresponding to the antiferromagnetic configuration. For low height of the barrier ($Z \rightarrow 0$), the magnetoresistance effect as a function of the applied potential is positive (the resistance of the junction in the ferromagnetic configuration is less than that in the antiferromagnetic configuration) and only weakly depends on Z up to $eV \approx 0.75(2\Delta)$. With increasing V , the effect begins decreasing more rapidly, the greater Z , and finally becomes negative. Since the Andreev reflection is especially efficient at low barriers, it follows from the calculated data obtained that taking this effect into account is of great importance when considering the problem of magnetoresistance of the F/S/F junctions.

Note also the importance of Andreev reflection in considering Josephson currents in S/F/S junctions [120]. This problem has been considered in numerous papers [142–157], and the list of papers is continually growing. Andreev [147] showed that in a thin layer of a normal metal sandwiched between two superconductors, bound localized states arise with energies lying inside the superconducting gap (Andreev states). The structure of these states and their density were later investigated in many works (see, e.g.,

Ref. [146] and references therein). It was clearly shown in Ref. [146] that the Josephson current in an S/N/S junction was transferred through Andreev states. It also turned out that the structure of the localized states (or the local density of states in the spectrum of quasi-particles) in the normal part of the junction strongly depends on the macroscopic phase difference ϕ of the wave function in the left-hand and right-hand superconductors [146]. Another remarkable property related to Andreev reflection is the appearance of states with zero energy in junctions formed by superconductors with a d symmetry of the OP [143].

These properties of the S/N/S contacts are superimposed by special properties of the S/F/S contacts containing a ferromagnetic (metallic or insulating) layer. The exchange field I leads to a spin splitting of the localized Andreev levels. This splitting is described by the equation that determines the energies ω_+ and ω_- of the localized states inside the S/F/S junction [150]:

$$\tan \left[\frac{\omega_{\pm}}{v_0 |\cos \theta|} + \text{sgn}(\cos \theta) \frac{\phi}{2} \pm \frac{Id_f}{v_0 |\cos \theta|} \right] = \sqrt{\frac{\Delta^2 - \omega_{\pm}^2}{\omega_{\pm}}}. \quad (7.7)$$

Here, θ is the angle between the momentum of an electron incident from the superconducting layer onto the interface and the normal to this interface, and Δ is the magnitude of the gap in the superconducting layer. At $I = 0$, Eqn (7.7) defines the spectrum of the Andreev quasi-particle in the S/N/S junction, with the condition $\phi \neq 0$ corresponding to the current state. In the special case of a narrow barrier ($d_f \ll \xi_s$) and an excitation propagating along the normal to the boundary ($\cos \theta = 1$) under the conditions $\phi = 0$ and $I = 0$, there is a single (degenerate in spin) level $\omega_0 = \Delta(1 - d_f^2/2\xi_s^2)$. The introduction of a weak exchange field splits this level:

$$\omega_{\pm} = \omega_0 \mp I \frac{d_f^2}{2\xi_s^2}.$$

With increasing I , the level ω_- increases whereas the level ω_+ decreases. Under certain conditions, the upper level is expelled into the region of continuum ($\omega_- = \Delta$), so that the remaining level belongs to a spin-polarized state.

In later works [144, 145, 151–156], the results obtained in [150] were generalized in various directions. The most comprehensive investigation of Josephson S/F/S junctions can be found in Ref. [151]. We borrow from it, for example, the equation that determines the spectrum of a quasi-particle in the case of a superconductor of s type

$$\cos \left(\frac{\phi}{2} - \bar{d} \frac{\omega - I}{\Delta \cos \theta} \right) = \pm \frac{\omega}{\Delta}, \quad (7.8)$$

and d type

$$\cos \left(\frac{\phi}{2} - \bar{d} \frac{\omega - I}{\Delta \cos \theta} \right) = \pm \frac{\omega}{\cos 2\theta \Delta}, \quad (7.9)$$

where $\bar{d} = d_f/\xi_s$ is the reduced thickness of the F layer. Equation (7.8) is equivalent to Eqn (7.7), and Eqn (7.9) describes a situation in which a superconducting OP has a $d_{x^2-y^2}$ symmetry, and the crystal axes a of both superconductors are perpendicular to the interface. With allowance for the main factors that characterize the S/F/S junction, i.e., the phase difference ϕ , exchange field I , and symmetry of the OP, the physics of Andreev states and Josephson currents passing through the junction becomes

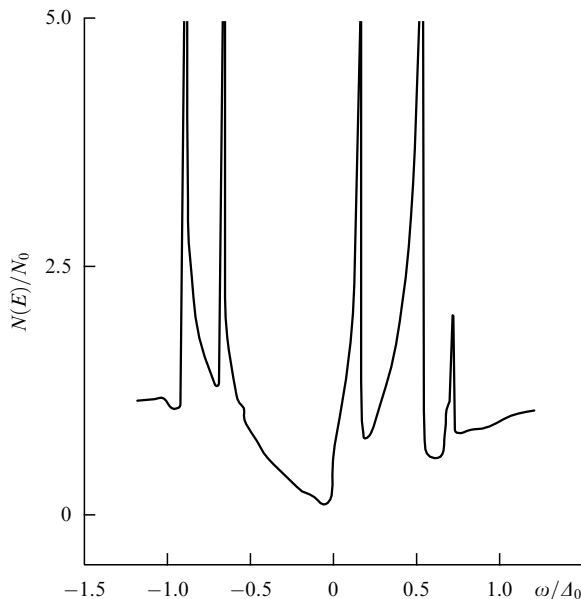


Figure 22. Density of states inside the ferromagnetic layer of the S/F/S junction with superconductors of d type [151]. The calculation was performed for the parameter values $I = 0,5\Delta$ and $\bar{d} = 1$, at which the ground state of the junction corresponds to $\phi = 0$.

very rich. We also give, for example, Fig. 22 from Ref. [151], which illustrates the complex structure of Andreev states in the S/F/S junction.

Experimental investigations of S/F/S junctions that require extremely thin ferromagnetic layers ($d_f \lesssim 1$ nm) are in the incipient stage (see Refs [122, 157]). The theoretical investigations of this problem, on the contrary, have been in progress quite long and quite intensively. We also mention Refs [104, 158–161] devoted to separate theoretical problems related to transport properties of multilayer F/S structures.

8. Conclusions

The aim of this review was to discuss the mutual accommodation of the superconducting and magnetic states in F/S systems where the superconducting and ferromagnetic regions are spatially separated but coupled with one another through the interfaces between the layers. To summarize the investigations of this problem, we may say the following.

In the decade passed since the publication of the pioneering works [61, 62], in which the fundamentals of the theory of FM/S junctions were developed, numerous theoretical and experimental investigations of heterogeneous systems consisting of layers of a ferromagnetic metal and a superconductor have been carried out. For conditions corresponding to experiments (dirty superconductor), it was shown that such systems are described by a boundary-value problem for a pair amplitude (Usadel function). Superconductivity in such a heterogeneous system proves to be a superposition of the superconductivities of the Bardeen–Cooper–Schrieffer (BCS) type in S layers and of the Larkin–Ovchinnikov–Fulde–Ferrel (LOFF) type in FM layers. The most important success of the theory is the explanation of the nonmonotonic dependence of the critical temperature T_c on the thickness of the ferromagnetic layer d_f . Oscillations of T_c are caused by conditions at the boundary: the flux of Cooper pairs is proportional to the jump in the pair amplitude at the ferromagnet–superconductor interface. The

solution of the boundary-value problem makes it possible to calculate T_c as a function of d_f . Depending on the microscopic parameters that characterize the S layer, the FM layer, and the boundary, varied behavior of the FM/S junctions and superlattices can be expected and is observed in numerous experiments.

Another problem concerning the behavior of FM/S systems (of superlattices, in particular) is the problem of the mutual orientations of the magnetizations of FM layers as an effect of the inverse influence of superconductivity on magnetism. Analysis of the boundary-value problem makes it possible to find conditions under which a ferromagnetic or antiferromagnetic arrangement of the magnetizations of FM layers is realized (the antiferromagnetic orientation proves to be more favorable). Thus, the theory of FM/S junctions and superlattices based on the boundary-value problem for the Usadel function is capable of explaining the experimentally observed behavior of these systems.

As to the FI/S systems consisting of layers of a ferromagnetic insulator and a superconductor, their theoretical description is performed on the basis of minimization of the Ginzburg–Landau functional for two interacting order parameters (OPs). Based on this approach, phase diagrams on the (T, h) plane were obtained, where h is the exchange field acting from the near-surface atomic layer of the ferromagnet on the electron spins in the superconductor. The possible phases in such a system are determined by the competition between the direct ferromagnetic exchange interaction in the FI layer and indirect antiferromagnetic interaction via the conduction electrons of the S layer. This proves that, depending on the relationship between these exchange energies, two types of behavior of FI/S systems can exist. In one case, two phases compete on the (T, h) plane: an antiferromagnetic superconducting (AFS) and a ferromagnetic normal (FN) phase, whereas in the second case, three phases can exist: AFS, FN, and cryptoferrimagnetic superconducting (CFS) phases. Thus, the mutual adjustment of the superconducting and magnetic OPs in the FI/S systems manifests itself in the appearance of either AFS or CFS phases. Experimental investigations of FI/S systems are much more scarce than for the corresponding FM/S systems. In order to test the theory, it was expedient to primarily determine phase diagrams for these systems on the (T, h) plane.

So far, we have spoken of the thermodynamic properties of F/S systems. Now, we summarize the investigations of the main features of their transport properties. They manifest themselves most vividly in three-layer junctions. Thus, an S/F/S junction can most conveniently be used to study π -phase superconductivity by the observation of oscillations of the Josephson current across the junction. Vanishing of the critical current at a certain thickness of the ferromagnetic layer (or at a certain temperature if d_f is fixed) with its subsequent increase is persuasive evidence of the existence of π -phase superconductivity in such systems.

Another class of phenomena arise in F/S/F junctions depending on the mutual orientations of magnetizations of the F layers. For the antiferromagnetic orientation, a nonequilibrium spin polarization due to the injection of magnetized electrons from the ferromagnetic layer is accumulated in the superconducting layer. As a result, the superconducting characteristics of the entire junction, e.g., the superconducting gap or the tunneling magnetoresistance, depend quite specifically on the applied voltage.

Thus, owing to intense theoretical and experimental investigations, a significant understanding of the effects of the mutual influence of superconductivity and magnetism in nonuniform F/S systems has been achieved. There are also numerous suggestions for engineering applications of some of the above considered phenomena in microelectronics, in particular, for the fabrication of electric current switches, in which the switching is effected using a weak magnetic field, or for the production of devices based on quantum bits of information. This stimulates the further study of layered F/S systems.

Along with the investigation of inhomogeneous F/S systems, interest in the problems of the coexistence of superconductivity and ferromagnetism in homogeneous systems has arisen again in recent years [162–164], especially after the discovery of such a coexistence in UGe_2 , which belongs to the class of heavy-fermion compounds [165]. Superconductivity is observed in this compound below 1 K in the ferromagnetic phase over a narrow range of pressures near the boundary of existence of the ferromagnetic state. Thus, the superconductivity in UGe_2 exists in the region of the ferromagnetic phase. The UGe_2 compound is an itinerant ferromagnet, and the same electrons form in it both the ferromagnetic and superconducting states, in contrast to other systems in which the coexistence of F and S order parameters was observed earlier [7].

In Ref. [164], a mean-field theory has been constructed for the one-fermion model of an itinerant magnet with singlet superconductivity, and in Ref. [162], a theory of an itinerant ferromagnet with a p symmetry of the superconducting OP has been developed. In such a superconductor, triplet Cooper pairs apparently should be formed. The theory suggested employs the Eliashberg equations for electrons interacting with one another via the fluctuations of the ferromagnetic OP, which lead, as is well known, to attraction in the triplet Cooper channel. Numerical solution of the Eliashberg equations shows that T_c increases as the system approaches the critical point where the ferromagnetic OP appears. We also give the latest references concerning the topic of the review [166–176].

There is no doubt that the problems of the coexistence of superconductivity and ferromagnetism will in the near future be at the peak of interest of theoreticians, experimentalists, and research engineers.

This work was supported in part by the Russian Foundation for Basic Research (Grants 01-02-17534, 01-02-17822, and 00-15-96544) and the Civilian Research and Development Foundation (Grant REC-007).

References

- Ginzburg V L *Zh. Eksp. Teor. Fiz.* **31** 202 (1956) [*Sov. Phys. JETP* **4** 153 (1957)]; Zharkov G F *Zh. Eksp. Teor. Fiz.* **34** 412 (1958) [*Sov. Phys. JETP* **7** 278 (1958)]; **37** 1784 (1959) [*Sov. Phys. JETP* **10** 1257 (1959)]
- Anderson P W, Suhl H *Phys. Rev.* **116** 898 (1959)
- White R M *Quantum Theory of Magnetism* (Berlin: Springer-Verlag, 1983) [Translated into Russian (Moscow: Mir, 1985)]
- Bulaevskii L N, Rusinov A I, Kulić M *Solid State Commun.* **30** 59 (1979); *J. Low Temp. Phys.* **39** 256 (1980)
- Bulaevskii L N et al. *Solid State Commun.* **44** 1247 (1982); *Phys. Rev. B* **28** 1370 (1983)
- Bulaevskii L N, Panjukov S V *J. Low Temp. Phys.* **52** 137 (1983)
- Buzdin A I et al. *Usp. Fiz. Nauk* **144** 597 (1984) [*Sov. Phys. Usp.* **27** 927 (1984)]
- Bernhard C et al. *Phys. Rev. B* **59** 14099 (1999)
- Pickett W E, Weht R, Shick A B *Phys. Rev. Lett.* **83** 3713 (1999)
- Shimahara H, Hata S *Phys. Rev. B* **62** 14541 (2000)
- Chmaissem O et al. *Phys. Rev. B* **61** 6401 (2000)
- Lynn J W et al. *Phys. Rev. B* **61** R14964 (2000)
- Eisaki H et al. *Phys. Rev. B* **50** 647 (1994)
- Huang Q et al. *Phys. Rev. B* **51** 3701 (1995)
- Cho B K et al. *Phys. Rev. B* **52** 3676 (1995)
- Abrikosov A A, Gor'kov L P *Zh. Eksp. Teor. Fiz.* **39** 1781 (1960) [*Sov. Phys. JETP* **12** 1243 (1961)]
- Baltensperger W *Physica* (Suppl.) **24S** 153 (1958)
- Sarma G J *Phys. Chem. Solids* **24** 1029 (1963)
- Chandrasekhar B S *Appl. Phys. Lett.* **1** 7 (1962)
- Clogston A M *Phys. Rev. Lett.* **9** 266 (1962)
- Larkin A I, Ovchinnikov Yu N *Zh. Eksp. Teor. Fiz.* **47** 1136 (1964) [*Sov. Phys. JETP* **20** 762 (1965)]
- Fulde P, Ferrell R A *Phys. Rev.* **135** A550 (1964)
- Saint-James D, Sarma G, Thomas E J *Type II Superconductivity* (Oxford: Pergamon Press, 1969) [Translated into Russian (Moscow: Mir, 1970)]
- Aslamazov L G *Zh. Eksp. Teor. Fiz.* **55** 1477 (1968) [*Sov. Phys. JETP* **28** 832 (1968)]
- Takada S *Prog. Theor. Phys.* **43** 27 (1970)
- de Gennes P G *Rev. Mod. Phys.* **36** 225 (1964)
- Khusainov M G *Pis'ma Zh. Eksp. Teor. Fiz.* **53** 554 (1991) [*JETP Lett.* **53** 579 (1991)]
- Khusainov M G *Sverkhprovodimost: Fiz., Khim., Tekh.* **5** 1789 (1992)
- Jin B Y, Ketterson J B *Adv. Phys.* **38** 189 (1989)
- Hauser J J, Theuerer H C, Werthamer N R *Phys. Rev.* **142** 118 (1966)
- Wong H K et al. *J. Low Temp. Phys.* **63** 307 (1986)
- Homma H et al. *Phys. Rev. B* **33** 3562 (1986)
- Moodera J S, Meservey R, Tedrow P M *J. Magn. Magn. Mater.* **54–57** 769 (1986)
- Mattson J E et al. *Phys. Rev. Lett.* **68** 3252 (1992)
- Kawaguchi K, Sohma M *Phys. Rev. B* **46** 14722 (1992)
- Koorevaar P et al. *Phys. Rev. B* **49** 441 (1994)
- Strunk C et al. *Phys. Rev. B* **49** 4053 (1994)
- Verbanck G et al. *Physica C* **235–240** 3295 (1994)
- Koorevaar P, Coehoorn R, Aarts J *Physica C* **248** 61 (1995)
- Jiang J S et al. *Phys. Rev. Lett.* **74** 314 (1995)
- Jiang J S et al. *Phys. Rev. B* **54** 6119 (1996)
- Mühge Th et al. *Phys. Rev. Lett.* **77** 1857 (1996)
- Obi Y et al. *Czech. J. Phys.* **46** 721 (1996)
- Aarts J et al. *Phys. Rev. B* **56** 2779 (1997)
- Mühge Th et al. *Phys. Rev. B* **55** 8945 (1997)
- Mattson J E et al. *Phys. Rev. B* **55** 70 (1997)
- Mattson J E et al. *J. Vac. Sci. Technol. A* **15** 1774 (1997)
- Chien C L et al. *J. Appl. Phys.* **81** 5358 (1997)
- Verbanck G et al. *Phys. Rev. B* **57** 6029 (1998)
- Mühge Th et al. *Physica C* **296** 325 (1998)
- Garif'yanov N N et al. *Eur. Phys. J. B* **1** 405 (1998)
- Mühge Th et al. *Phys. Rev. B* **57** 5071 (1998)
- Obi Y et al. *Physica C* **317–318** 149 (1999)
- Attanasio C et al. *Phys. Rev. B* **57** 6056 (1998)
- Attanasio C et al. *Phys. Rev. B* **57** 14411 (1998)
- Lazar L et al. *Phys. Rev. B* **61** 3711 (2000)
- Schöck M, Sürgers C, Löhneysen H V *Eur. Phys. J. B* **14** 1 (2000)
- Lee S F et al. *J. Magn. Magn. Mater.* **209** 231 (2000)
- Ogrin F Y et al. *Phys. Rev. B* **62** 6021 (2000)
- Tagirov L R et al. *J. Magn. Magn. Mater.* **240** 577 (2002)
- Radović Z et al. *Phys. Rev. B* **44** 759 (1991)
- Buzdin A I, Vučičich B, Kupriyanov M Yu *Zh. Eksp. Teor. Fiz.* **101** 231 (1992) [*Sov. Phys. JETP* **74** 124 (1992)]
- Bulaevskii L N, Kuzii V V, Sobyenin A A *Pis'ma Zh. Eksp. Teor. Fiz.* **25** 314 (1977) [*JETP Lett.* **25** 290 (1977)]
- Proshin Yu N, Khusainov M G *Pis'ma Zh. Eksp. Teor. Fiz.* **66** 527 (1997) [*JETP Lett.* **66** 562 (1997)]
- Khusainov M G, Proshin Yu N *Phys. Rev. B* **56** 14283 (1997); **62** 6832 (2000)
- Proshin Yu N, Khusainov M G *Zh. Eksp. Teor. Fiz.* **113** 1708 (1998); **116** 1882 (1999) [*JETP* **86** 930 (1998); **89** 1021 (1999)]
- Tagirov L R *Physica C* **307** 145 (1998)
- Izyumov Yu A, Proshin Yu N, Khusainov M G *Pis'ma Zh. Eksp. Teor. Fiz.* **71** 202 (2000) [*JETP Lett.* **71** 138 (2000)]

69. Khusainov M G, Izyumov Yu A, Proshin Yu N *Physica B* **284**–**288** 503 (2000)
70. Usadel K D *Phys. Rev. Lett.* **25** 507 (1970)
71. Eilenberger G Z *Phys.* **214** 195 (1968)
72. Tedrow P M, Meservey R *Phys. Rep.* **238** 173 (1994)
73. Tedrow P M, Tkaczyk J E, Kumar A *Phys. Rev. Lett.* **56** 1746 (1986)
74. Hao X, Moodera J S, Meservey R *Phys. Rev. Lett.* **67** 1342 (1991)
75. Moodera J S et al. *Phys. Rev. Lett.* **61** 637 (1988)
76. Tokuyasu T, Sauls J A, Rainer D *Phys. Rev. B* **38** 8823 (1988)
77. Roesler G M et al. *Proc. SPIE* **2157** 285 (1994)
78. Khusainov M G *Zh. Eksp. Teor. Fiz.* **109** 524 (1996) [*JETP* **82** 278 (1996)]
79. Khusainov M G *Zh. Eksp. Teor. Fiz.* **110** 966 (1996) [*JETP* **83** 533 (1996)]
80. Kochelaev B I, Tagirov L R, Khusainov M G *Zh. Eksp. Teor. Fiz.* **76** 578 (1979) [*Sov. Phys. JETP* **49** 233 (1979)]
81. Hornreich R M, Luban M, Shtrikman S *Phys. Rev. Lett.* **35** 1678 (1975)
82. Abrikosov A A, Gor'kov L P, Dzyaloshinskii I E *Metody Kvantovoi Teorii Polya v Statisticheskoi Fizike* (Quantum Field Theoretical Methods in Statistical Physics) (Moscow: Fizmatgiz, 1962) [Translated into English (Oxford: Pergamon Press, 1965)]
83. Abrikosov A A, Gor'kov L P *Zh. Eksp. Teor. Fiz.* **35** 1158 (1958) [*Sov. Phys. JETP* **8** 1090 (1959)]; **36** 319 (1959) [*Sov. Phys. JETP* **9** 215 (1959)]
84. Kupriyanov M Yu, Lukichev V F *Zh. Eksp. Teor. Fiz.* **94** (6) 139 (1988) [*Sov. Phys. JETP* **67** 1163 (1988)]
85. Radović Z et al. *Phys. Rev. B* **38** 2388 (1988)
86. Gantmakher V F, Levinson I B *Rasseyaniye Nositelei Toka v Metallakh i Poluprovodnikakh* (Carrier Scattering in Metals and Semiconductors) (Moscow: Nauka, 1984) p. 218 [Translated into English (Amsterdam: North-Holland, 1987)]
87. Khusainov M G *Pis'ma Zh. Eksp. Teor. Fiz.* **61** 947 (1995) [*JETP Lett.* **61** 972 (1995)]
88. Khusainov M G, Izyumov Yu A, Proshin Yu N *Pis'ma Zh. Eksp. Teor. Fiz.* **73** 386 (2001) [*JETP Lett.* **73** 344 (2001)]
89. Kittel Ch *Introduction to Solid State Physics* (New York: Wiley, 1976) [Translated into Russian (Moscow: Nauka, 1978)]
90. Buzdin A I, Vedyayev A V, Ryzhanova N V *Europhys. Lett.* **48** 686 (1999)
91. Tagirov L R *Phys. Rev. Lett.* **83** 2058 (1999)
92. Clinton T W, Johnson M *Appl. Phys. Lett.* **70** 1170 (1997)
93. Oh S, Youm D, Beasley M R *Appl. Phys. Lett.* **71** 2376 (1997)
94. Baladié I et al. *Phys. Rev. B* **63** 054518 (2001)
95. McLaughlin A C et al. *Phys. Rev. B* **60** 7512 (1999)
96. Edwards D M et al. *Phys. Rev. Lett.* **67** 493 (1991)
97. Siper O, Gyorffy B L *J. Phys.: Condens. Mat.* **7** 5239 (1995)
98. Sá de Melo C A R *Phys. Rev. B* **62** 12303 (2000)
99. Parkin S S P *Phys. Rev. Lett.* **67** 3598 (1991)
100. Bergeret F S, Efetov K B, Larkin A I *Phys. Rev. B* **62** 11872 (2000)
101. Buzdin A *Phys. Rev. B* **62** 11377 (2000)
102. Koshina E A, Krivoruchko V N *J. Low Temp. Phys.* **26** 115 (2000)
103. Demler E A, Arnold G B, Beasley M R *Phys. Rev. B* **55** 15174 (1997)
104. Oh S et al. *Phys. Rev. B* **63** 052501 (2001)
105. Weber H W et al. *Phys. Rev. B* **44** 7585 (1991)
106. Stearns M B *Phys. Rev. B* **8** 4383 (1973)
107. Yousuf M, Sahu P Ch, Rajan K G *Phys. Rev. B* **34** 8086 (1986)
108. Kasuya T, in *Magnetism* Vol. 2B (Eds G T Rado, H Suhl) (New York: Acad. Press, 1966) p. 215
109. Proshin Yu N, Izyumov Yu A, Khusainov M G *Izv. Ross. Akad. Nauk Ser. Fiz.* **65** 841 (2001)
110. Kuboya K, Takanaka K *Phys. Rev. B* **57** 6022 (1998)
111. Takahashi S, Tachiki M *Phys. Rev. B* **33** 4620 (1986)
112. Lodder A, Koperdraad R T W *Physica C* **212** 81 (1993)
113. de Gennes P G *Phys. Lett.* **23** 10 (1966)
114. Maki K, in *Superconductivity* Vol. 2 (Ed. R D Parks) (New York: M. Dekker, 1969) p. 1035
115. Millis A, Rainer D, Sauls J A *Phys. Rev. B* **38** 4504 (1988)
116. Tokuyasu T, Sauls J A, Rainer D *Phys. Rev. B* **38** 8823 (1988)
117. Kulić M L, Endres M *Phys. Rev. B* **62** 11846 (2000)
118. Buzdin A I, Bulaevskii L N, Panyukov S V *Pis'ma Zh. Eksp. Teor. Fiz.* **35** 147 (1982) [*JETP Lett.* **35** 178 (1982)]
119. Buzdin A I, Kupriyanov M Yu *Pis'ma Zh. Eksp. Teor. Fiz.* **53** 308 (1991) [*JETP Lett.* **53** 321 (1991)]
120. Prokić V, Buzdin A I, Dobrosavljević-Grujić L *Phys. Rev. B* **59** 587 (1999)
121. Andreev A V, Buzdin A I, Osgood R M *Phys. Rev. B* **43** 10124 (1991)
122. Ryazanov V V et al. *Phys. Rev. Lett.* **86** 2427 (2001)
123. Ryazanov V V et al., cond-mat/0103240
124. Ioffe L B et al. *Nature* **398** 679 (1999)
125. Blatter G, Geshkenbein V B, Ioffe L, cond-mat/9912163
126. Kulić M L, Kulić I M *Phys. Rev. B* **63** 104503 (2001)
127. Bulaevskii L N et al. *Phys. Rev. B* **28** 1370 (1983)
128. Bergeret F S, Volkov A F, Efetov K B *Phys. Rev. Lett.* **86** 3140 (2001)
129. Prinz G A *Phys. Today* **48** (4) 58 (1995)
130. Johnson M J *Magn. Magn. Mater.* **156** 321 (1996)
131. Golubov A A *Physica C* **326**–**327** 46 (1999)
132. Golubov A, Tafuri F *Phys. Rev. B* **62** 15200 (2000)
133. Takahashi S, Imamura H, Maekawa S *Phys. Rev. Lett.* **82** 3911 (1999)
134. Zheng Z et al. *Phys. Rev. B* **62** 14326 (2000)
135. Moodera J S et al. *Phys. Rev. Lett.* **74** 3273 (1995)
136. Vas'ko V A et al. *Phys. Rev. Lett.* **78** 1134 (1997)
137. Dong Z W et al. *Appl. Phys. Lett.* **71** 1718 (1997)
138. Yeh N-C et al. *Phys. Rev. B* **60** 10522 (1999)
139. Geers J M E et al., cond-mat/0101138; submitted to *Phys. Rev. B*
140. Abrikosov A A *Osnovy Teorii Metallov* (Fundamentals of the Theory of Metals) (Moscow: Nauka, 1987) [Translated into English (Amsterdam: North-Holland, 1988)]
141. Andreev A F *Zh. Eksp. Teor. Fiz.* **46** 1823 (1964) [*Sov. Phys. JETP* **19** 1228 (1965)]
142. Kashiwaya S et al. *Phys. Rev. B* **60** 3572 (1999)
143. Hu C-R *Phys. Rev. Lett.* **72** 1526 (1994)
144. Zhu J-X, Friedman B, Ting C S *Phys. Rev. B* **59** 9558 (1999)
145. Žutić I, Valls O T *Phys. Rev. B* **61** 1555 (2000)
146. Furusaki A, Tsukada M *Phys. Rev. B* **43** 10164 (1991)
147. Andreev A F *Zh. Eksp. Teor. Fiz.* **49** 655 (1966) [*Sov. Phys. JETP* **22** 455 (1966)]
148. Kuplevakhskii S V, Fal'ko I I *Fiz. Met. Metalloved.* **71** 668 (1991)
149. de Jong M J M, Beenakker C W J *Phys. Rev. Lett.* **74** 1657 (1995)
150. Kuplevakhskii S V, Fal'ko I I *Pis'ma Zh. Eksp. Teor. Fiz.* **52** 957 (1990) [*JETP Lett.* **52** 340 (1990)]
151. Zikić R, Dobrosavljević-Grujić L, Radović Z *Phys. Rev. B* **59** 14644 (1999)
152. Kashiwaya S et al. *Phys. Rev. B* **51** 1350 (1995)
153. Hu C-R *Phys. Rev. B* **57** 1266 (1998)
154. Eschrig M *Phys. Rev. B* **61** 9061 (2000)
155. Fogelström M *Phys. Rev. B* **62** 11812 (2000)
156. Tanaka Y, Kashiwaya S *Physica C* **274** 357 (1997)
157. Veretennikov A V et al. *Physica B* **284**–**288** 495 (2000)
158. Sillanpaa M A et al., cond-mat/0102367; *Europhys. Lett.* **56** 590 (2001)
159. Sonin E B, cond-mat/0102102; submitted to *Phys. Rev. B*
160. Bulaevskii L N et al. *Phys. Rev. B* **63** 012502 (2001)
161. Melin R *Europhys. Lett.* **51** 202 (2000)
162. Roussev R, Millis A J *Phys. Rev. B* **63** 140504 (2001)
163. Blagoev K B, Engelbrecht J R, Bedell K S *Phys. Rev. Lett.* **82** 133 (1999)
164. Karchev N I et al. *Phys. Rev. Lett.* **86** 846 (2001)
165. Saxena S S et al. *Nature* **406** 587 (2000)
166. Houzet M, Buzdin A *Phys. Rev. B* **63** 184521 (2001)
167. Bergeret F S, Volkov A F, Efetov K B *Phys. Rev. Lett.* **86** 4096 (1999)
168. Krivoruchko V N, Koshina E A, cond-mat/0104251
169. Zhu Yu, Sun Qing-feng, Lin Tsung-han, cond-mat/0104103
170. Zikić R, Dobrosavljević-Grujić L, Radović Z *Phys. Rev. B* **64** 012501 (2001)
171. Balestrino G et al. *Phys. Rev. B* **64** 020506(R) (2001)
172. Kim S-K et al. *Phys. Rev. B* **64** 052406 (2001)
173. Aumentado J, Chandrasekhar V *Phys. Rev. B* **64** 054505 (2001)
174. Izquierdo J et al. *Phys. Rev. B* **64** 060404(R) (2001)
175. Geers J M E et al. *Phys. Rev. B* **64** 094506 (2001)
176. Bergeret F S, Volkov A F, Efetov K B *Phys. Rev. B* **64** 134506 (2001)